Proceedings
of the
National Academy of Sciences, India

Section A - Physical Sciences

The National Academy of Sciences, India
(Registered under Act XXI of 1860)
Founded 1930

COUNCIL FOR 2005

President
1.   Prof. Ved Prakash Kamboj, Ph.D., D.Sc., F.N.A., F.N.A.Sc., Lucknow.

Two Past Presidents (including the Immediate Past President)
2.   Prof. Jai Pal Mittal, Ph.D.(Notre Dame,USA), F.N.A., F.A.Sc., F.N.A.Sc., F.T.W.A.S., Navi Mumbai.
3.   Prof. V.P. Sharma, D.Phil.,D.Sc.,F.A.M.S.,F.E.S.I., F.I.S.C.D., F.N.A., F.A.Sc., F.N.A.Sc., F.R.A.S., S.T.P. SEARO (WHO), New Delhi

Vice-Presidents
4.   Prof. Suresh Chandra, D.Phil., Grad.Brit.I.R.E., F.N.A.Sc., Varanasi.
5.   Prof. Ashok Misra, M.S.(Chem.Engg.), M.S.(Polymer Sc.), Ph.D., F.N.A.Sc., Mumbai.

Treasurer
6.   Prof. S.L. Srivastava, D.Phil.,F.I.E.T.E., F.N.A.Sc., Allahabad.

Foreign Secretary
7.   Prof. Vijayalakshmi Ravindranath, Ph.D., F.N.A., F.A.Sc., F.N.A.Sc., F.T.W.A.S., Manesar(Haryana).

General Secretaries
8.   Prof. P.K. Seth, Ph.D., F.N.A., F.N.A.Sc., Lucknow.
9.   Prof. Pramod Tandon, Ph.D.,F.B.S.,F.N.A.Sc.,Shillong.

Members
10.   Prof. Anil K. Bhatnagar, Ph.D. (Maryland), F.N.A., F.N.A.Sc., Pondicherry.
11.   Prof. Virander Singh Chauhan, Ph.D., D.Phil.(Oxford), F.N.A., F.N.A.Sc., New Delhi.
12.   Prof. Kasturi Datta, Ph.D., F.N.A., F.A.Sc., F.N.A.Sc., F.T.W.A.S., New Delhi.
13.   Prof. Sushanta Dattagupta, Ph.D., F.N.A., F.A.Sc., F.N.A.Sc., F.T.W.A.S., Kolkata.
14.   Prof. Amit Ghosh, Ph.D., F.A.Sc., F.N.A.Sc., Chandigarh.
15.   Prof. S.K. Joshi, D.Phil., D.Sc.(h.c.), F.N.A., F.A.Sc., F.N.A.Sc., F.T.W.A.S., New Delhi.
16.   Dr. Anil Kumar, Ph.D., F.A.Sc., F.N.A.Sc., Pune.
17.   Prof. H.S. Mani, Ph.D.(Columbia), F.A.Sc., F.N.A.Sc.,Chennai.
18.   Prof. Kambadur Muralidhar, Ph.D., F.N.A., F.A.Sc., F.N.A.Sc., Delhi.
19.   Prof. Lok Man S. Palni, Ph.D. (Wales), F.N.A.Sc., U.S. Nagar, Uttaranchal.
20.   Prof. Ajay Kumar Sood, Ph.D., F.N.A., F.A.Sc., F.N.A.Sc., F.T.W.A.S., Bangalore.
21.   Prof. C.B.L. Srivastava, D.Phil., D.Sc., F.N.A.Sc., Allahabad.
22.   Prof. Venna Tandon, Ph.D., F.Z.S.I., F.H.S.I., F.N.A.Sc., Shillong.
23.   Prof. Akhilesh Kumar Tyagi, Ph.D., F.N.A., F.N.A.Sc., New Delhi.

Contents

A study of viscosity *B*-coefficients of some organic acids in aqueous solutions of urea at different temperatures

M.L. PARMAR*, O.P. SHARMA and M.K. GULERIA

Department of Chemistry, Himachal Pradesh University, Summer Hill, Shimla-171 005, India.

Abstract

Relative viscosities of three organic acids *viz.* ascorbic acid, citric acid and tartaric acid, at different concentrations have been determined in aqueous solutions of urea (1,2,3,5 and 7 mol kg^{-1} of urea) at 298 K and in 1.0 mol kg^{-1} urea at four equidistant temperatures. The data have been evaluated using Jones-Dole equation and the obtained parameters have been interpreted in terms of solute-solute and solute-solvent interactions. The activation parameters of viscous flow have been obtained which depicts the mechanism of viscous flow. All the three organic acids behave as structure breakers in aqueous solutions of urea.

(Keywords : viscosity *B*-coefficients/ascorbic acid/citric acid/ tartaric acid/aqueous solutions of urea/structure-breaker)

Introduction

The viscosity data provide useful information about various types of interactions occurring in solutions. These studies are of great help in characterizing the structure and properties of solutions. The solution structure is of great importance in understanding the nature of bioactive molecules in the body system. Survey of literature[1-11] shows that although many studies have been carried out for various electrolytic solutions, little attention has been paid to the behaviour of organic acids in aqueous solutions of urea. Such data are expected to high light the role of organic acids in influencing the B-coefficients in aqueous solutions of urea. This consideration prompted us to undertake the present study.

Materials and Method

Ascorbic acid, citric acid, tartaric acid and urea (all of AR grade) were used after drying over P_2O_5 in a desiccator for more than 48 h. The reagents were always placed in the desiccator over P_2O_5 to keep them in dry atmosphere. Freshly distilled conductivity water (sp. cond. ~ 10^{-6} Ohm^{-1}cm^{-1}) was used as standard solvent and for making aqueous solutions of urea.

All the aqueous solutions of urea as well as the solutions of organic acids were made by weight and molalities, *m*, were converted into molarities, *c*, using the standard expression[12] –

$$c = 1000d\,m/(1000 + m\,M_2) \qquad (1)$$

where *d* is the solution density of an organic acid in aqueous solution of urea and M_2 the molecular weight of an organic acid.

The density was measured with a hydrostatic balance similar to that reported by Ward and Millero[13] and described elsewhere[14-16] (accuracy in density measurements, ±1 x 10^{-4} g dm^{-3}). The relative viscosities (accuracy in viscosity ±1 x 10^{-4}cP) were measured at the desired temperature using an Ostwald's suspended level type viscometer with a flow time 381.43s for water at 298K. Runs were repeated until three successive determinations were obtained within ±0.1s. Since all the flow times were

greater than 100 s, the kinetic energy correction was not necessary. The relative viscosities of the solutions (η_{rel}) were calculated by the usual procedure[17,18]. The density and viscosity measurements were carried out in a well stirred water-bath whose temperature was controlled to ±0.01 K.

Results and Discussion

The relative viscosities and densities of the solutions of ascorbic acid, citric acid and tartaric acid in aqueous solution of urea (1,2,3,5 and 7 mol kg⁻¹) were measured at 298K. The experimental results of relative viscosities of the organic acids in aqueous solutions of urea have been analysed by Jones-Dole equation[19]

$$\eta_{rel} = \eta/\eta_0 = 1 + A c^{1/2} + B c \qquad (2)$$

where η and η_0 are the viscosities of the solutions of organic acids and solvent (urea + water) respectively, and c is the molar concentration, A and B are the constants characteristic of solute-solute and solute-solvent interactions respectively. The plots of $(\eta_r - 1)/\sqrt{c}$ versus $\sqrt{c}$ for all the organic acids, were found to be linear, with least scatter. A sample plot for ascorbic acid in different compositions of urea + water at 298 K is shown in Fig. 1. The values of A and B parameters have been calculated using the least square method by fitting the experimental results in the Jones-Dole equation and these values, along with standard errors, obtained in different compositions of urea + water at 298 K, are recorded in Table 1.
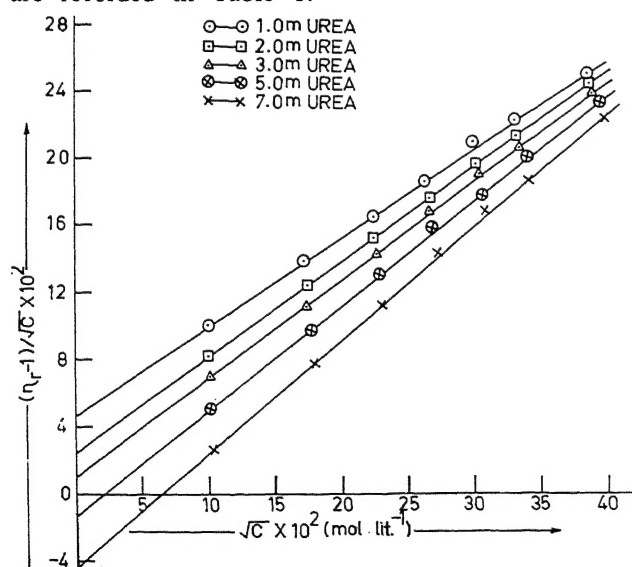

Fig. 1 – Plots of $(\eta_r-1)/\sqrt{c}$ *vs.* $\sqrt{c}$ for ascorbic acid in different compositions of urea + water at 298K.

Table 1 – Values of A and B parameters of Jones-Dole equation for ascorbic acid, citric acid and tartaric acid in different compositions of urea + water at 298K. Standard errors are given in parentheses.

Composition of urea in water (mol kg⁻¹)	A (dm³/²mol⁻¹/²)	B (dm³mol⁻¹)
Ascorbic acid		
0.0 (water)	0.042 (0.002)	0.587 (0.007)
1.0	0.044 (0.003)	0.536 (0.012)
2.0	0.025 (0.001)	0.564 (0.003)
3.0	0.010 (0.002)	0.587 (0.006)
5.0	-0.014 (0.002)	0.628 (0.006)
7.0	-0.044 (0.002)	0.676 (0.005)
Citric acid		
0.0 (water)	0.060 (0.004)	0.630 (0.015)
1.0	0.057 (0.003)	0.548 (0.010)
2.0	0.031 (0.003)	0.576 (0.011)
3.0	0.014 (0.002)	0.581 (0.008)
5.0	-0.008 (0.002)	0.606 (0.005)
7.0	-0.023 (0.001)	0.648 (0.005)
Tartaric acid		
0.0 (water)	0.029 (0.002)	0.566 (0.009)
1.0	0.041 (0.005)	0.409 (0.001)
2.0	0.031 (0.002)	0.473 (0.007)
3.0	0.011 (0.001)	0.500 (0.004)
5.0	-0.010 (0.001)	0.536 (0.005)
7.0	-0.022 (0.002)	0.547 (0.007)

A perusal of Table 1 shows that the value of coefficient A decreases continuously with the increase in composition of urea in water at 298 K, thereby suggesting that the solute-solute interactions, though weak, go on decreasing with the increase of urea content in water. These results indicate that all the three organic acids, mix more ideally with urea + water as compared to water and there is a perfect solvation of all the three organic acids in urea + water solutions thereby resulting in very weak solute-solute interactions.

It is also clear from Table 1 that the values of B-coefficients, for all the three organic acids in water and in aqueous solutions of urea at 298 K, are positive and fairly large suggesting the presence of strong solute-solvent interactions. The value of B-coefficient also increases with the increase in urea composition in water suggesting that the solute-solvent interactions increase with the increase of urea in water at 298 K, for all the three organic acids, which results in the improvement of solute solvation.

The viscosity data have also been analysed on the basis of transition state treatment of relative viscosity as suggested by Feakins et al.[20] The B parameter in terms of this theory is given by

$$B = \frac{\overline{V}_1^0 - \overline{V}_2^0}{1000} + \frac{\overline{V}_1^0}{1000}\left(\frac{\Delta\mu_2^{0*} - \Delta\mu_1^{0*}}{RT}\right) \quad (3)$$

here $\overline{V}_1^0$ is the mean volume of the solvent and $\overline{V}_2^0$ is the partial molar volume of the solute. The free energy of activation per mole of the pure solvent $(\Delta\mu_1^{0*})$, and the free energy of activation per mole of solute $(\Delta\mu_2^{0*})$ were calculated[21] with the help of equations (4) and (5) respectively :

$$\Delta\mu_1^{0*} = RT \ln\left(\eta_0 \overline{V}_1^0 / hN\right) \quad (4)$$

and

$$\Delta\mu_2^{0*} = \Delta\mu_1^{0*} + RT / \overline{V}_1^0\left[1000\,B - \left(\overline{V}_1^0 - \overline{V}_2^0\right)\right] \quad (5)$$

where h is the Planck constant, N the Avogadro number, η_0 the viscosity of solvent, R the gas constant and T is the absolute temperature. The values of $\Delta\mu_1^{0*}$ calculated from equation (4) are given in Table 2. For the mixed solvents, each solvent mixture was treated as pure and the molar volume taken as a mean volume defined as :

$$\overline{V}_1^0 = \left(x_1 M_1 + x_2 M_2\right) / d_1 \quad (6)$$

where x_1, M_1 and x_2, M_2 are the mole fractions, and molecular weights of water and urea respectively, and d_1 is the density of solvent (urea + water). The values of $\Delta\mu_2^{0*}$ and $\overline{V}_1^0$, calculated with the help of relations (5) and (6) respectively, are recorded in Table 2. The values of $\overline{V}_2^0$, the partial molar

volumes at infinite dilution for all the three organic acids, determined from density data, are also recorded in Table 2.

It is evident from the data (Table 2) that $\Delta\mu_1^{0*}$ is practically constant at all solvent compositions implying that $\Delta\mu_2^{0*}$ is dependent mainly on B-coefficient and $(\overline{V}_1^0 - \overline{V}_2^0)$ terms. It is also clear from Table 2 that the values of $\Delta\mu_2^{0*}$ are positive and larger than $\Delta\mu_1^{0*}$ which suggest that the formation of the transition state is less favoured in the presence of these organic acids, meaning thereby

Table 2 – Values of $\overline{V}_1^0$ (dm^{3}mol^{-1}), $\overline{V}_2^0$ (dm^{3}mol^{-1}), $\Delta\mu_1^{0*}$ (kJ mol^{-1}) and $\Delta\mu_2^{0*}$ (kJ mol^{-1}) for ascorbic acid, citric acid, and tartaric acid in different compositions of urea + water at 298 K.

Composition of urea in water (mol kg^{-1})	1.0	2.0	3.0	5.0	7.0
$\overline{V}_1^0$	18.497	18.940	19.376	20.231	21.042
$\Delta\mu_1^{0*}$	9.282	9.424	9.545	9.724	9.893
Ascorbic acid					
$\overline{V}_2^0$	64.214	64.799	65.340	66.044	66.594
$\Delta\mu_2^{0*}$	87.200	89.201	90.481	92.242	94.734
Citric acid					
$\overline{V}_2^0$	93.153	93.410	93.652	93.668	94.284
$\Delta\mu_2^{0*}$	92.683	94.513	93.334	92.933	94.815
Tartaric acid					
$\overline{V}_2^0$	42.754	38.467	39.251	40.568	41.503
$\Delta\mu_2^{0*}$	80.709	73.852	76.020	77.855	76.708

that the formation of transition state is accompanied by the breaking and distortion of the intermolecular bonds between urea and water i.e. solvent.

It has been emphasized by many workers that dB/dT is a better criterion[22] for determining the structure making/breaking nature of any solute rather than simply the B-coefficient. So it means that in order to follow this criterion, the temperature effect must be studied.

Effect of temperature : Since the behaviour of the individual organic acid was found to be linear

and identical in different compositions of urea + water at 298K, only 1.0 mol kg^{-1} urea + water composition was selected for studying the effect of temperature. The plots of $(\eta_r - 1)/\sqrt{c}$ *vs.* $\sqrt{c}$ have been found to be linear at 298, 303, 308, and 313 K in accordance with Jones-Dole equation (equation 2) for individual organic acid. A sample plot is shown in Fig. 2 for citric acid. The values of A and B parameters have been calculated using least square method and these values, along with standard errors, are recorded in Table 3. It is evident from Table 3 that the values of A-coefficient are either positive or negative but very small for all the three organic acids in 1.0 mol kg^{-1} urea + water solution showing the existence of weak solute-solute interactions, which of course are further weakened with the rise in temperature.

The values of B-coefficients are positive and large, as compared to that of A for all the three organic acids in urea + water (1.0 mol kg^{-1}) solution at all temperatures, showing the presence of strong solute-solvent interactions. The value of dB/dT is positive for all the three organic acids in urea + water showing that all the three acids act as structure breakers in aqueous solutions of urea.

The data of viscosity B-coefficients at different temperatures have also been analysed by applying the transition state theory. The values of $\Delta\mu_1^{0*}$ and $\Delta\mu_2^{0*}$ have been calculated from equations (4) and (5) respectively, and are recorded in Table 4.
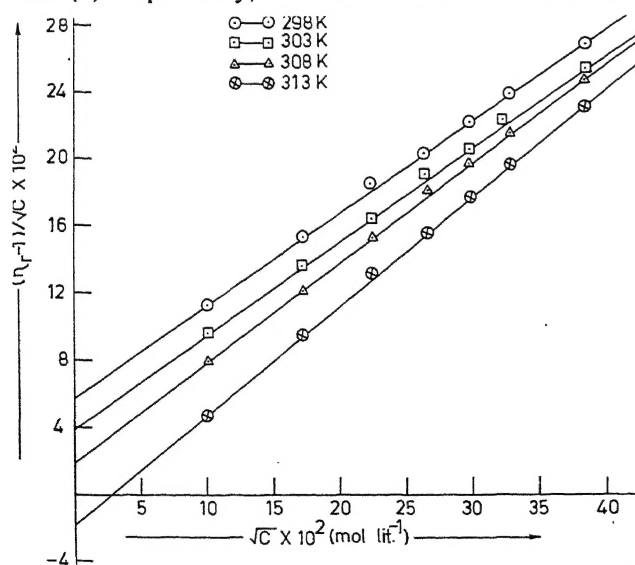
Table 3– Values of parameters A (dm$^{3/2}$mol$^{-\frac{1}{2}}$) and B (dm^{3}mol^{-1}) of Jones-Dole equation for ascorbic acid, citric acid and tartaric acid in urea + water (1.0 mol kg^{-1}) solution at different temperatures. Standard errors are given in parentheses.

Temperature (K)	298	303	308	313
Ascorbic acid				
A	0.44 (0.003)	0.022 (0.002)	0.003 (0.002)	– 0.028 (0.002)
B	0.536 (0.012)	0.573 (0.006)	0.614 (0.009)	0.673 (0.006)
Citric acid				
A	0.057 (0.003)	0.037 (0.004)	0.016 (0.004)	– 0.018 (0.002)
B	0.548 (0.010)	0.571 (0.017)	0.612 (0.015)	0.653 (0.006)
Tartaric acid				
A	0.041 (0.005)	0.020 (0.001)	– 0.001 (0.002)	– 0.025 (0.002)
B	0.509 (0.001)	0.556 (0.005)	0.60 (0.007)	0.650 (0.008)

Table 4 – Values of $\bar{V}_1^0$ (dm^{3}mol^{-1}), $\bar{V}_2^0$ (dm^{3}mol^{-1}), $\Delta\mu_1^{0*}$ (kJ mol^{-1}) and $\Delta\mu_2^{0*}$ (kJ mol^{-1}) for ascorbic acid, citric acid and tartaric acid in urea + water (1.0 mol kg^{-1}) solution at different temperatures.

Temperature (K)	298	303	308	313
$\bar{V}_1^0$	18.497	18.554	18.610	18.661
$\Delta\mu_1^{0*}$	9.282	9.144	8.778	8.550
Ascorbic acid				
$\bar{V}_2^0$	64.214	79.543	95.115	121.353
$\Delta\mu_1^{0*}$	87.199	95.223	103.791	116.720
Citric acid				
$\bar{V}_2^0$	93.153	107.196	128.738	144.510
$\Delta\mu_2^{0*}$	92.683	98.706	108.142	117.160
Tartaric acid				
$\bar{V}_2^0$	42.754	82.499	103.286	106.104
$\Delta\mu_2^{0*}$	80.708	93.316	103.814	111.386

Fig. 2 –   Plots of (η_r-1) $\sqrt{c}$ *vs.*$\sqrt{c}$ for citric acid in 1.0 m urea + water at different temperatures.

The corresponding values of $\overline{V}_1^0$ and $\overline{V}_2^0$ have also been recorded in Table 4. According to Feakins model[20], $\Delta\mu_2^{0*}$ increases with temperature for the solutes having positive values of dB/dT. This is nicely shown by all the three organic acids which act as structure breakers in aqueous solutions of urea.

The activation entropy for all the organic acids has also been calculated from the following relation[20]:

$$d(\Delta\mu_2^{0*})/dT = -\Delta S_2^{0*} \qquad (7)$$

Table 5 – Entropy, $T\Delta S_2^{0*}$ (kJ mol^{-1}) and enthalpy, ΔH_2^{0*} (kJ mol^{-1}), of activation for viscous flow of ascorbic acid, citric acid and tartaric acid in urea + water (1.0 mol kg^{-1}) solution at different temperatures.

Temperature (K)	298	303	308	313
		Ascorbic acid		
$T\Delta S_2^{0*}$	– 576.014	– 588.729	– 598.444	– 608.159
ΔH_2^{0*}	– 491.815	– 493.506	– 494.653	– 491.439
		Citric acid		
$T\Delta S_2^{0*}$	– 493.786	– 502.071	– 510.356	– 518.641
ΔH_2^{0*}	– 401.103	– 403.365	– 402.214	– 401.481
		Tartaric acid		
$T\Delta S_2^{0*}$	– 611.198	– 621.453	– 631.708	– 641.963
ΔH_2^{0*}	– 530.490	– 528.137	– 527.894	– 530.577

The values of ΔS_2^{0*} have been calculated from the slopes of linear plots of $\Delta\mu_2^{0*}$ vs. T. The values of $T\Delta S_2^{0*}$ at different temperatures are listed in Table 5. The activation enthalpy (ΔH_2^{0*}) has been calculated with the help of following relation[20]:

$$\Delta H_2^{0*} = \Delta\mu_2^{0*} + T\Delta S_2^{0*} \qquad (8)$$

and the values are also recorded in Table 5.

It is evident from Table 5 that both enthalpy and entropy of activation are negative for all organic acids, which suggest that the transition state is associated with bond breaking and increase in order. Although a detailed mechanism for this cannot be easily advanced, it may be suggested that the slip-plane is in the disordered state.

References

1. Lawrence, K. G., Sacco, A., Giglio, A. D. & Dell Atti, A. (1989) *J. Chem. Soc. Faraday Trans I* **87** : 23.

2. Parmar, M. L. & Sharma, S. (1990) *J. Ind. Chem. Soc.* **67** : 592.

3. Parmar, M.L., Rao, Ch.V.N. & Bhardwaj, S.K. (1992) *Ind. J. Chem.* **31A** : 716.

4. Parmar, M. L. & Chauhan, M. K. (1995) *Ind. J. Chem.* **34A** : 434.

5. Jauhar, S.P., Markandeya, B. & Kapila, V. P. (1997) *Ind. J. Chem.* **36A** : 898.

6. Parmar, M. L. & Sharma, S. (1998) *Res. J. Chem. Environ.* **2** : 17.

7. Pandey, J. D., Akhtar, Y. & Sharma, A. K. (1998) *Ind. J. Chem.* **37A** : 1094.

8. Parmar, M. L. (1998) *J. Indian Council Chem.* **15** : 10.

9 Mishra, A. P. & Gautam, S. K. (2001) *Ind. J. Chem.* **40A** : 100.

10. Kipkemboi, P. K. & Easteal, A. J. (2002) *Ind. J. Chem.* **41A** : 1139.

11. Nikam, P. S. & Sonawane, V. P. (2003) *Int. J. Chem. Sci.* **1** : 210.

12. Shoemaker, D. P. & Garland, C. W. (1967) *"Experiments in Physical Chemistry"*, McGraw Hill, New York, p. 131.

13. Ward, G. K. & Millero, F. J. (1974) *J. Soln. Chem.* **3** : 417.

14. Parmar, M. L. & Kundra, A. (1983) *Electrochim. Acta.* **28** : 1655.

15. Parmar, M. L. & Sharma, S. (1999) *J. Ind. Chem. Soc.* **76** : 202.

16. Parmar, M. L. & Dhiman, D. K. (2001) *Ind. J. Chem.* **40A** : 1161.

17. Parmar, M. L., Khanna, A. & Gupta, V. K. (1989) *Ind. J. Chem.* **28A** : 565.

18. Parmar, M.L., Dhiman, D.K. & Thakur, R.C. (2002) *Ind. J. Chem.* **41A** : 2032.

19. Jones, G. & Dole, M. (1929) *J. Am. Chem. Soc.* **51** : 2950.

20. Feakins, D., Freemental, J. D. & Lawrence, K. G. (1974) *J. Chem. Soc. Faraday Trans I* **70** : 795.

21. Glasston, S., Laidler, K. & Eyring, H. (1941) *"The theory of rate processes"*, McGraw Hill, New York, p. 477.

22. Sarma, T. S. & Ahluwalia, J. C. (1973) *Rev. Chem. Soc.* **2** : 217.

High-performance liquid chromatographic determination of loratadine

K.BASAVAIAH*, V.S.CHARAN and U.CHANDRASHEKAR

Department of Chemistry, University of Mysore, Manasagangotri, Mysore-570 006, India.

email : basavaiahk@yahoo.co.in; Fax : 91-821-242126, 2516133

Abstract

A rapid and sensitive high performance liquid chromatographic method has been developed for the determination of loratadine in bulk drug and in tablets. The drug was eluted from a 5 μm C_{18} reversed phase column (ODS, 250x4.6mm) with a mobile phase consisting of acetonitrile – 0.1% orthophosphoric acid of pH 3.0 (80:20) and at a flow rate of 1ml/min. with UV-detection at 249 nm. The quantification was achieved by measurement of peak area and the calibration curve revealed a linear response over the concentration range 20-800 μg/mL loratadine. The limit of detection was 2.03 μg/mL and the limit of quantification was 7.00 μg/mL. The intra day co-efficient variation (CV) ranged from 0.11 to 0.55% and the inter-day CV ranged from 0.05 to 0.73%. The method was successfully applied to the determination of loratadine in tablets and the results were consistent with the label claim of the formulation. The method was validated by comparing the results with those of an established reference method by calculating the Student's t-value and F-value and by performing recovery experiment using standard addition technique.

Introduction

Loratadine, chemically, 4 – (8-chloro – 5,6 – dihydro – 11 H – benzo [5,6] cyclohepta [1,2 – b] pyridin – 11 ylidene] – 1 – piperidine carboxylic acid ethyl ester, is a long-acting tricyclic antihistamine with selective peripheral histamine H_1 receptor antagonistic activity[1] . It is used in the treatment of seasonal allergic rhinitis, acute coryz and allergic dermatological disorders either individually or in combination with psuedoephidrine.

Determination of loratadine in pharmaceuticals has previously been achieved by procedures based on several techniques such as visible spectrophotometry[2-4], UV-spectrophotometry[5-6],

derivative UV-spectrophotometry[7], atomic absorption spectrometry and colorimetry[8], spectrofluorimetry[9], proton-NMR spectroscopy[10], polarography[11] and densitometry[12]. High performance liquid chromatography (HPLC) is the most widely used technique for the determination of loratadine in body fluids as well as pharmaceuticals. Vasudevan et al.[13], have reported a reversed phase- HPLC method for the determination of loratadine in a combined dosage form containing pseudoephedrine. The separation was achieved on a spherisorb $RP-C_{18}$ column with a mobile phase consisting of methanol-phosphate buffer of pH 4.5 at a flow rate of 1.0 ml/min with UV-detection at 215 nm. The calibration graph was rectilinear in the range 2.5-7.5 μg mL^{-1}. Loratadine in a binary mixture[14] has also been determined by RP-HPLC consisting of 5μm inertsil C_8 column. The mobile phase was 0.025M sodium dihydrogenphosphate and acetonitrile (40:60) with pH adjusted to 3.5 with a flow rate of 1.0 ml/min. and the UV-detector was set at 265 nm. The method was applicable over the range 2.5–7.5 μg mL^{-1} loratadine.

Estimation of loratadine in single dosage forms has also been carried out by several HPLC methods. A method employing a Symmetry Shield RP18 column (5μm) has been developed by Radhakrishan et al.[15] The mobile phase consisted of 1% triethylamine (pH adjusted to 6 by orthophosphoric acid) and acetonitrile (40:60) with a flow rate of 1.0 mL/min. and UV-detection at 220 nm. The detector response was linear over 107-537μg/mL for the assay of drug. Ruperez et al.,[16] have reported the use of Symmetry Shield RP 8 column for the assay of loratadine. Their mobile phase consisted of methanol and phosphate buffer pH (65:35) with UV detection

at 244 nm. Analysis of tablets for loratadine[17] has also been achieved by HPLC on a Shandon ODS C_{18} column (10µm) using acetonitrile-octasulphonic acid sodium salt, diethylamine and acetic acid buffer (85:15) with UV detection at 232 nm. The method was applicable in the range 10-70 µg/mL. A stability indicating method for the determination of loratadine in the presence of its degradation product has been reported by El-Regehy *et al.*[5]. The procedure employed acetonitrite and orthophosphoric acid (35:65) as the mobile phase and benzophenone as the internal standard, with UV detection at 250 nm. Sensitivity range was 5-50 µg/mL. The method was applied for the assay of loratadine in dosage forms.

The reported HPLC methods for combined dosage forms[13,14] are critically dependent on the composition and polarity of the mobile phase whereas the procedures for single dosage forms[5,15-17] are either less sensitive or have narrow linear dynamic range of applicability. The present paper describes a couple of modifications (in terms of mobile phase composition and internal standard) to the method of El Regeby *et al.*, which allows the determination of loratadine in single dosage forms. The method is characterised by increased sensitivity, and long dynamic linear range of response and absence of internal standard.

Materials and Method

Apparatus : A HPLC system (Agilent 1100 Series) equipped with an in built solvent degasser, quaternary pump, photodiode array detector with variable injector and auto sampler was used. A 250 mm x 4.6 mm ODS Hypersil C_{18} column (reversed phase, particles size 5µm) was used at a flow rate of 1.0 mL/min. Detection was monitored at 249 nm, and the sensitivity was set at 0.2 AUFS.

Reagents and standards : Analytical grade orthophosphoric acid (Qualigens India, Ltd), HPLC grade acetonitrile (Rankem, India) and distilled water filtered through a 0.45µm filter (Millipore) were used. The diluent solution was prepared by mixing acetonitrile and water in the ratio 60 : 40.

Mobile phase : The mobile phase consisted of acetonitrile − 0.1% orthophosphoric acid of pH 3.0 (80:20). The solvents were vacuum filtered through

a 0.45µm filter. Prior to injection the column was stabilised with the eluent mixture at a flow rate of 0.7 mL/min for approximately 1 h.

Standard drug solution : Pharmaceutical grade loratadine was obtained from Morepen Labs Ltd., India, and assayed at 99.28% by non-aqueous titration method. A stock standard solution of loratadine equivalent to 1015µg/mL was prepared by dissolving 101.5mg of pure loratadine in the diluent solution and diluting to 100 ml in a volumetric flask with the diluent.
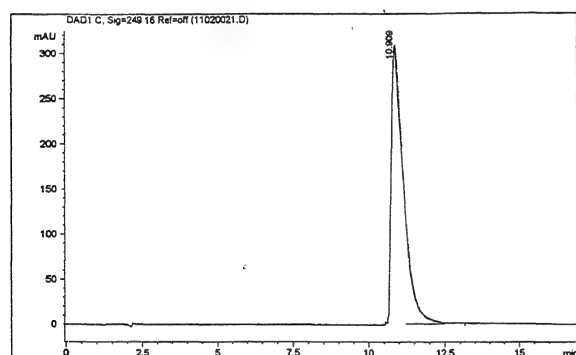
Procedures

Calibration graph : Working standard solutions containing 20.3− 812 µg/mL loratadine were prepared by transferring 1 to 40 ml of stock standard solution (1015µg/mL) into separate 50 mL volumetric flasks and diluting to volume with the diluent solution. A 20µL volume was injected automatically into the chromatograph in duplicate and chromatograms were recorded. Calibration graph was constructed by plotting the mean peak area against loratadine concentration. The six concentrations of the compound were subjected to regression analysis to calculate the calibration equation and correlation coefficient.

For tablets : Pharmaceutical preparations containing loratadine were procured from local commercial sources. Twenty tablets were weighed accurately and ground into a fine powder with agate pestle and mortar. An amount of the powder equivalent to about 50 mg of loratadine was accurately weighed and dissolved in the diluent solution and the resulting mixture was transferred quantitatively into a 50 mL calibrated flask and made up to volume with the diluent solution through thorough mixing. A small portion of this solution (~10 mL) was withdrawn and filtered through a 0.2 µm filter to ensure the absence of particulate matter. This filtrate was appropriately diluted to get the final solution for analysis.

Results and Discussion

Method development : The mobile phase was chosen after several trials with methanol, isopropanol, acetonitrile, water and buffer solutions in various proportions and at different pH values. A mobile

phase consisting of acetonitrile – 0.1% orthophosphoric acid of pH 3.0 (80:20), was selected to achieve maximum separation and sensitivity.

Flow rates between 0.5 and 1.5 mL/min were studied. A flow rate of 1.0 mL/min gave an optimal signal to noise ratio with a reasonable separation time. Using a reversed phase C_{18} column, the retention time was 11 min. Total time of analysis was less than 15 min. The maximum absorption of loratadine was at 249 nm and this vavelength was chosen for analysis. The chromatogram at 249 nm showed complete resolution (Fig. 1).

Fig. 2 – Linearity graph.

Fig.1 – Typical chromatogram of loratadine (203 µg/ mL)

Linearity :   For quantitative determination, a linear calibration graph $Y=135.47+41.72X$; $r=0.9999$, $n=6$ (where Y and X are mean peak area and concentration in µg/mL, respectively) was obtained over the working concentration range of 20.3 – 812 µg/mL (Fig. 2).

Limits of detection and quantification : Limit of detection which was established at a signal-to-noise ratio of 3 was 2.03 µg/mL and the limit of quantification, established at a signal-to-noise ratio of 9 was found to be 7.00 µg/mL.

Method validation

Precision : The precision of the method (within-day variations of replicate determinations) was determined for both peak area and retention time by repeat analysis (seven replicate injections) of the

Table 1 – Evaluation of accuracy and precision.

Loratadine injected (µg/mL)	Loratadine found (µg/mL)	Deviation (%)	RSD, # (%) ($n=7$)	RSD, @ (%) ($n=7$)
40.6	39.37	3.02	0.46	0.36
121.8	122.18	0.31	0.11	0.55
162.4	165.87	2.13	0.10	0.36

RSD : Relative Standard Deviation; # Based on peak area;
@ Based on retention time.

Table 2 – Between-day precision.

Loratadine injected, (µg/mL)	RSD, # (%)	RSD, @ (%)
40	0.46	0.36
160	0.14	0.20
200	0.05	0.73

Based on peak area; @ Based on retention time.

standard solution containing the drug at three different concentration levels. The relative standard deviation (RSD) for retention time ranged from 0.36

Table 3 – Results of analysis of loratadine tablets by the proposed method.

Tablet brand name	Labelled amount (mg)	% found * ± SD		Student's t-value (2.77)	F-value (6.39)
		HPLC method	Reference method		
Claridin [a]	10	101.36 ± 0.36	102.3 ± 0.85	2.24	5.57
Lorfast [b]	10	97.85 ± 0.63	99.12 ± 1.14	2.18	3.27
Loridin [c]	10	98.78 ± 0.43	99.53 ± 0.96	1.60	4.98
Lormeg [d]	10	103.8 ± 0.52	104.26 ± 0.76	1.26	2.13
Roletra [e]	10	97.63 ± 0.65	98.34 ± 0.65	2.24	6.25

* Mean value of five determinations
Marked by : [a] Morepen, [b] Cadila Pharma, [c] Cadila Healthcare, [d] Megacare, [e]Rexcel
Figures in the parantheses are the tabulated values at the tabulated values at the 95% confidence level.

to 0.55% and that for peak area ranged from 0.10 to 0.46% (Table 1). The day-to-day precision was established by performing the analysis over a period of five days on solutions prepared freshly each day. The low RSD values indicate the robustness of the method (Table 2).

Accuracy : Accuracy of the proposed method for the determination of loratadine was established by assaying the solutions of known concentrations as done for determining the within–day precision. The accuracy, defined in terms of % deviation of the calculated concentrations from the actual concentrations is also listed in Table 1.

Application to formulations

On applying the preposed method to the determination of loratadine in several brands of tablets, the results obtained (Table 3) demonstrated the accuracy and precision of the method. The same batch tablets were analysed simultaneously by an established UV spectrophotometric method[18] for comparision. The performance of the proposed method was assessed by calculating the Student's t-value for accuracy and F-value for precision. Since the calculated t- and F-values are less than the tabulated values at the 95% confidence level (Table 3), it can be concluded that there in no significant difference between the proposed and the reference methods with respect to accuracy and precision.

Table 4 – Results of recovery studies by standard-addition method.

Tablet studied	Amount of lorata-dine in the tablet (mg)	Amount of pure drug added (mg)	Total found (mg)	Recovery* of pure drug added (%)
Claridin tablet	5.07	10.00	14.89	98.16
	5.07	20.00	25.34	101.4
	5.07	30.00	35.22	100.5
Loridin tablet	4.90	10.00	15.26	103.6
	4.90	20.00	24.59	98.74
	4.90	30.00	34.64	99.25

* Mean value of three determinations
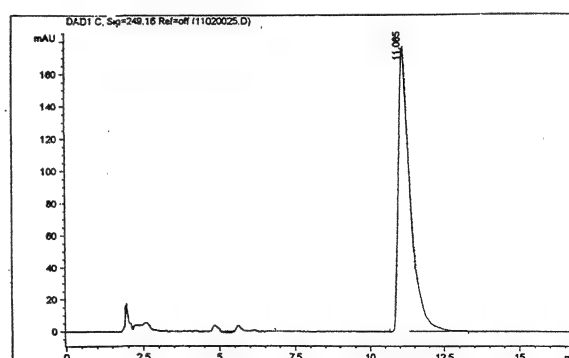
Fig. 3 – Typical chromatogram of tablet extract (118.9 µg/ mL)

The validity and the accuracy of the method were further confirmed by performing recovery studies. To a fixed and known quantity of the pre-analysed tablet powder, pure loratadine (standard) at three different concentration levels was added and the total was found by the proposed method. The experiment at each level was repeated three times. The per cent recoveries of the pure drug added which are compiled in Table 4 indicate that commonly added excipients such as lactose, talc, starch, acacia, alginate, stearate, calcium gluconate, calcium dihydrogen orthophosphate did not interfere in the proposed method. This is amply demonstrated by a single peak due to loratadine in the chromatogram of the sample solution (Fig.3).

Conclusions

A simple method for the determination of loratadiane has been developed and validated. The method does not require extensive sample pre-treatment and involves a HPLC system employing an inexpensive mobile phase. The method is more sensitive than the existing HPLC procedures besides being applicable over long dynamic linear range. The method can be used for the regular determination of loratadine and for checking the stability of its formulations.

References

1. *Physicians' Desk Reference*, (1993) 53rd ed., Medical Economic Company, Inc., Montvlae.

2. Singhvi, I. (2003) *Indian J. Pharm.* Sci. **65** : 291.

3. Rajput, S.J. & Vyas, A.G. (1998) *Indian Drugs* **35** : 352.

4. Seshagiri Rao, J.V.L.N., Srinivasa Rao, Y., Murthy, T.K., Jitendrababu, V.& Chowdary, K.B.R. (2003) *Acta Ciencia Indica Chem.* **29** : 207.

5. El-Ragehy, N.A., Badawey, A.M. & Khateeb, S.Z.(2000) *J.Pharm, Biomed. Anal.* **28** : 1041.

6. Tello, M.E., Daza, J.A. & Rocha, M.(1997). *Rev. Colomb. Cienc.Quim. Farm.* **26** : 43.

7. Onur, F., Yucesoy, C., Dermis, S., Kartal, M. & Mandic, G. (2000) *Talanta* **51** : 269.

8. El-Kousy, N. & Bebawy, L.I. (1999) *J. Pharm. Biomed. Anal.* **90** : 671.

9. El-Khateeb, S.Z., El-Ragehy, N.A. & Badavey, A.M. (1995) *Bull. Fac. Pharm (Cario Univ)* **33** : 7.

10. El-Ragehy, N.A., Bodawy, A.M. & El-Khateeb, S.Z. (1996) *Egyptian J. Pharm. Sci.* **37** : 11.

11. Ghoneim, M.M., Mabrouk, M.M., Hassanein, A.M. & Tawfik, A. (2001) *J. Pharm. Biomed. Anal.* **25** : 933.

12. Indrayanto, G., Darmawan, L., Vidjaja, S. & Noorrizka, G.(1999) *J. Planar Chromatogr. Mod TLC.* **12** : 261.

13. Vasudevan, M., Ravishankar, S., Satyanarayan, A. & Chandan, R.S. (2001) *Indian Drugs* **38** : 276.

14. Kanumala, G.V. & Bhanu, R. (2000) *Indian Drugs* **37** : 574.

15. Radhakrishna, T., Satyanarayana, J. & Satyanarayana, A. (2000) *Indian Drugs* **39** : 342.

16. Ruperez, F.J., Fernandez, H. & Barbar, C. (2002) *J. Pharm. Biomed. Anal.* **29** : 35

17. Chandreshekar, T.G., Patel, P., Vyas, S.K. & Dutt, C. (1995) *East. Pharm.* **36** : 141.

18. Nogowska, M., Zajac, M & Muszlska, I. (2000) *Chem. Anal (Warsaw)* **45** : 60.

Generation of electric current by photogalvanic cell : Use of bromo cresol purple – EDTA system

SWETA CHOWDHARY, SONIYA MADHWANI, RAKSHIT AMETA and PINKI B. PUNJABI

Department of Chemistry, University College of Science, M.L. Sukhadia University, Udaipur-313 002, India.

Abstract

A photogalvanic cell, containing bromo cresol purple as a photosensitizer and EDTA as a reductant, has been used for solar energy conversion. The photocurrent and photopotential generated by this cell were 52 µA and 626 mV, respectively. The fill factor and conversion efficiency of the cell were determined as 0.30 and 0.5878% respectively. Current voltage (i-V) characteristics of the cell was also examined and a tentative mechanism for the generation of photocurrent in the photogalvanic cell has been proposed.

(Keywords : photogalvanic cell/photocurrent/photopotential/ solar energy)

Introduction

Energy is needed to meet the subsistence requirement as well as to meet the demand for economic growth and development of a country. Efforts have been made time to time to generate electricity using various solar cells[1-7].

Materials and Method

A photogalvanic cell containing bromo cresol purple (BCP) as photosensitizer and ethylenediamine tetraacetic acid as a reductant was investigated for solar energy conversion.

The pH of the system was maintained by the addition of sodium hydroxide solution (previously standardized against oxalic acid solution). The pH of the solution was measured by pH meter (Systronics Model 335) after stabilizing the dark potential. The light intensity was measured by a direct reading solar intensity meter (Solarimeter Model 501 CEL) in the units of mWcm^{-2}. The photopotential and photocurrent generated by the system bromo cresol purple/EDTA/ OH$^-$/hv were measured by a conductance digital multimeter (CIE 5605) and micro ammeter (Kew), respectively.

A mixture of solutions of dye, EDTA and NaOH was taken in a H-shaped glass cell. A platinum electrode (1×1 cm^2) was dipped in one limb of the cell and saturated calomel electrode (SCE) in the other. The platinum electrode was exposed to a 200 W tungsten lamp (Sylvania) and the limb containing SCE was kept in the dark. A water filter was used to avoid thermal effects. The current voltage (i–V) characteristics of the cell was studied by using an external load (linear 470 K) in the circuit.

Maximum photocurrent and photopotential generated by this cell were 52 µA and 626 mV, respectively. The effect of the various parameters on the power output of the cell was also studied.

Results and Discussion

Effect of pH on the electrical output of the cell : The effect of the variation of pH on the electrical output of the cell was observed and the results are reported in Table 1. It was observed that

Table 1 – Variation of pH.

[Bromo cresol purple]	=	8.66×10^{-5} M
[EDTA]	=	6.40×10^{-3} M
Intensity	=	25.0 mW cm^{-2}
Temperature	=	303 K

pH	Photopotential (mV)	Photocurrent (µA)
11.5	– 386	42
11.6	– 480	47
11.7	– 521	50
11.8	– 626	52
11.9	– 489	49
12.0	– 452	46
12.1	– 316	40

power output of the photogalvanic cell changes with change in pH. Generally, photopotential and photocurrent of the cell increases with increase in pH, till it reaches the maximum. On further increase in pH, a decrease in output was observed. It was quite interesting to observe that pH for optimum condition for each reductant has a relation with its pKa value i.e. the desired pH is slightly higher than their pKa values. It may be due to the availability of reductant in it anionic form, which is a better electron donor form than its unionized form.

Effect of dye and reductant concentration : Dependence of photopotential and photocurrent on the concentrations of dye and reductant was studied and the results are summarized in Tables 2 and 3, respectively.

Table 2 – Variation of dye concentration.

[EDTA]	=	6.40×10^{-3} M
pH	=	11.8
Temperature	=	303 K
Intensity	=	25.0 mW cm^{-2}

(BCP)x10^{5}M	Photopotential (mV)	Photocurrent (μA)
6.66	– 456	44
7.33	– 524	45
8.00	– 553	48
8.66	– 626	52
9.33	– 591	50
10.0	– 495	44
10.66	– 384	42

Table 3 – Variation of EDTA concentration.

[BCP]	=	8.66×10^{-5} M
pH	=	11.8
Temperature	=	303 K
Intensity	=	25.0 mW cm^{-2}

(EDTA)x10^{5}M	Photopotential (mV)	Photocurrent (μA)
5.60	– 406	43
5.87	– 521	46
6.13	– 604	48
6.40	– 626	52
6.67	– 562	46
6.93	– 494	44
7.20	– 425	41

A small output was obtained for a lower concentration of bromo cresol purple because a small number of dye molecules were available for excitation and consecutive donation of the electrons to the platinum electrode. Large concentration of dye again resulted in a decrease in photopotential as the intensity of light reaching the dye molecules (near the electrode) decrease after the absorption of the major portion of the light by the dye molecules available in the path.

A similar trend was observed for the variation of the concentration of reductant. The decrease in the concentration of EDTA resulted into a fall in power output due to the lower number of reductant molecules available for electron donation to dye molecules, whereas a large concentration of reductant hinders the movement of dye molecules reaching the electrode in the desired time limit.

Effect of diffusion length : H-cell of different dimensions were used to study the effect of the variation of diffusion length on the current parameters of the cell (i_{max}, i_{eq} and rate of initial generation of current). The results are reported in Table 4. It was observed that there is a sharp increase in photocurrent (i_{max}) and then there is a gradual decrease to a stable value of photocurrent. This photocurrent at equilibrium is represented as i_{eq}. This behaviour of the photocurrent indicates an initial rapid reaction, followed by a slow rate determining step at a later stage. On the basis of the effect of the diffusion path length on the current

Table 4 – Variation of diffusion length.

[BCP]	=	8.66×10^{-5} M
[EDTA]	=	6.40×10^{-3} M
pH	=	11.8
Temperature	=	303 K
Intensity	=	25.0 mW cm^{-2}

Diffusion length (cm)	Maximum photocurrent (i_{max})	Equilibrium photocurrent (i_{eq})	Rate of initial generation of current (μA min^{-1})
2.0	44	42	0.92
2.5	47	41	0.94
3.0	49	39	1.00
3.5	52	39	1.04
4.0	54	38	1.08

parameters, it may be concluded that the leuco or semi reduced form of the dye and dye itself are the main electrode active species at the illuminated and dark electrode, respectively. However, the reductants and their oxidized products behave as the electron carriers in the diffusing through the path.

Table 5 – Effect of light intensity.

[BCP]   = 8.66×10^{-5} M
[EDTA]   = 6.40×10^{-3} M
pH   =   11.8
Temperature =   303 K

Light intensity I (mW cm^{-2})	Photo-potential V (mV)	Log V	Photocurrent (μA)
7.0	– 507	2.7050	36.0
12.0	– 538	2.7307	40.0
16.0	– 567	2.7543	44.0
20.0	– 595	2.7745	47.0
25.0	– 626	2.7965	52.0

Effect of light intensity : The effect of variation of light intensity on the electrical output of the cell was also studied. The results are given in Table 5. It was observed that photocurrent showed direct linear relationship with light intensity whereas photopotential increases in a logarithmic manner. The number of photons per unit area, incident power, striking the dye molecules around the platinum electrode, increase with the increase in the light intensity and there is a rise in photopotential and photocurrent.

Current voltage (i-V) characteristics, conversion efficiency and performance of the cell : The open circuit voltage (v_{oc}) and short circuit current (i_{sc}) of the cell were measured from multimeter (keeping the circuit open) and from ammeter (keeping the circuit closed), respectively. The values of current and potential between these two extremes were observed with the help of a carbon pot (linear 470 K) connected in circuit of ammeter (by applying an external load). The data are shown in Fig. 1.

It was observed that the *i-V* curve of the cell deviated from its ideal rectangular shape. A point in the *i-V* curve, called the power point (*pp*) was determined, where the product of potential and current is maximum. The values of potential and

current at power point is respresented as V_{pp} and i_{pp}, respectively. With the help of the *i-V* curve, the fill factor and conversion efficiency of the cell were determined as 0.30 and 0.5878% respectively, using the formula.

$$\text{Fill factor} = \frac{V_{pp} \times i_{pp}}{V_{oc} \times i_{sc}}$$

$$\text{Conversion efficiency} = \frac{V_{pp} \times i_{pp} \times 100}{25\text{mW cm}^{-2}}$$

The performance of the cell was studied by applying the external load necessary to have current and potential at power point, after removing the source of illumination. It was observed that this cell can be used for 32 min. even in the dark at its power point. The photovoltaic cells can not be used in dark for even small time periods whereas photogalvanic cells have an additional advantage of being used in dark, however their conversion efficiencies are relatively low.
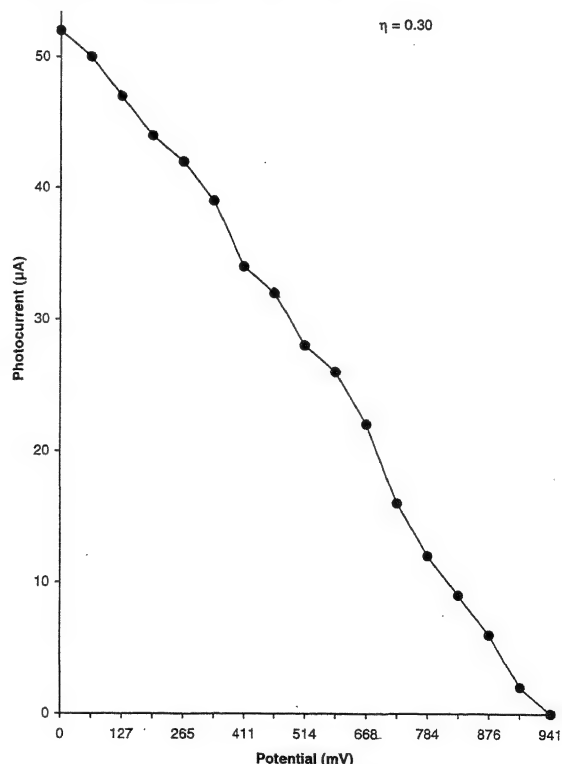

Fig. 1 – Current voltage characteristics of the cell.

Variation of photopotential and photocurrent with time : The variation of potential and current

in the bromo cresol purple–EDTA system with time is given in Fig. 2. A fall in potential was observed with the time of illumination, then it becomes stable and, the direction of the change in potential was reversed (to a small extent only) on removing the source of illumination.
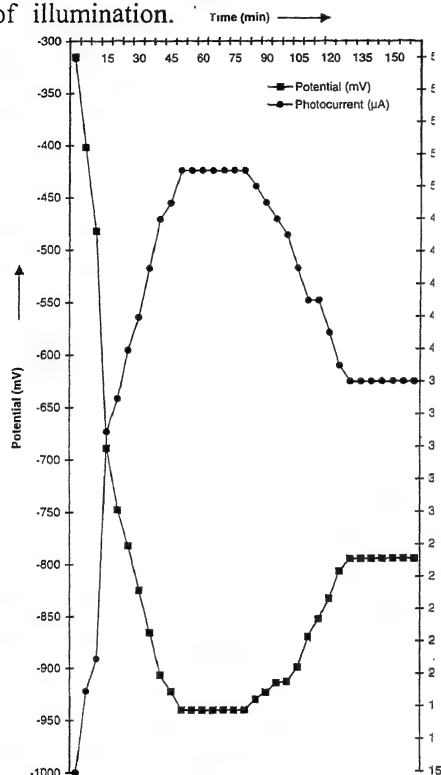

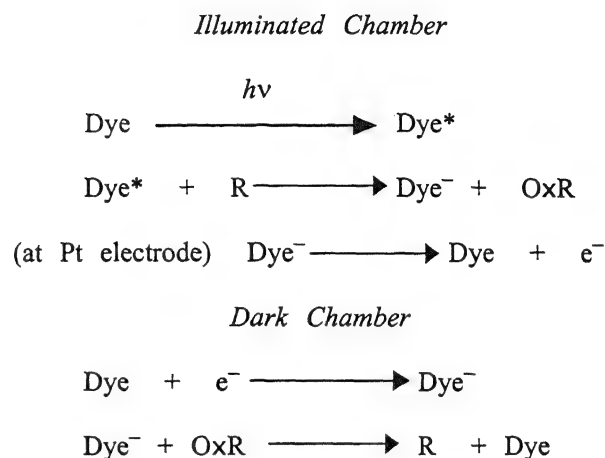Fig. 2 – Variation of potential and photocurrent with time.

It was found that the current increases with the time of illumination, then it becomes constant. After removing the source of illumination, it decreases gradually and finally it becomes constant.

Mechanism

It was observed that there is no reaction between dye and reductant in dark and, therefore, it may be concluded that the redox potential of dyes are much lower than that of reductant. When one of the electrode was exposed to light, potential of the system changes rapidly and became stable after sometime. On removing the source of illumination, the direction of change in potential was slightly reversed thus indicating that the reaction is reversible in nature but to a small extent only. The electrode active species in the cell under investigation is the leuco-form of the dye and the dye itself at the illuminated and dark electrodes, respectively.

The recycling reaction of the oxidation product of the reducing agent and the semi or leuco-dye seems to be the most probable rate determining step for photogeneration of current in photogalvanic cells. On the basis of these observations, a mechanism for the photocurrent generation in photogalvanic cell is represented as

Illuminated Chamber

$$\text{Dye} \xrightarrow{h\nu} \text{Dye}^*$$

$$\text{Dye}^* + \text{R} \longrightarrow \text{Dye}^- + \text{OxR}$$

$$(\text{at Pt electrode}) \quad \text{Dye}^- \longrightarrow \text{Dye} + e^-$$

Dark Chamber

$$\text{Dye} + e^- \longrightarrow \text{Dye}^-$$

$$\text{Dye}^- + \text{OxR} \longrightarrow \text{R} + \text{Dye}$$

When the concentration of reduced dye was increased around the electrode, electrical output of the cell was also found to increase. This may be due to rapid oxidation (irreversible) of reductant into electrochemical inactive material.

References

1. Jana, A.K. & Bhowmik, B.B. (1999) *J. Photochem. Photobiol.* **122A** : 53.

2. Cahen, D., Hodes, G., Gratzel, M., Guillemoles, J.F. & Riess, I. (2000) *J. Phys. Chem.* **104** : 2053.

3. Kalyanasundaram, K. & Gratzel, M. (1997) *Proc. Indian Acad. Sci. (Chem. Sci.)* **109** : 447.

4. Ameta, S.C., Ameta, R., Sharma, D. & Dubey, T.D. (1988) *J. Hung. Ind. Chem.* **16** : 245.

5. Ferber, J. & Luther, J. (2002) *J. Phys. Chem.* **105B** : 4895.

6. Park, N.G., Kang, M.G., Ryu, K.S., Kim, K.M. & Chang, S.H. (2004) *J. Photochem. Photobiol.* **161** : 105.

7. Islam, A., Sugihara, H. & Arakawa, H. (2003) *J. Photochem. Photobiol.* **158** : 131.

Synthesis and biological evaluation of 2-oxo-azetidinone derivatives using 2-mercaptobenzothiazole as the heterocyclic moiety

R. YADAV, S.D. SRIVASTAVA and S.K. SRIVASTAVA

Synthetic Organic Chemistry Laboratory, Department of Chemistry, Dr. H.S. Gour University, Sagar (M.P.), 470 003, India.

Abstract

Twenty new 2-(arylidenylamino)-5-[(2-benzothiazolylthio) methyl] 1,3,4 thiadiazoles 4 and 1-[5-{(2-benzothiazolylthio) methyl}-1',3',4'-thiadiazole-2'-yl]-4-substituted-3-chloro-2-oxo-azetidinone 5 have been synthesized and tested for their biological activity such as antifungal and antibacterial.

(**Keywords** : 2-oxo-azetidinone derivatives/2-mercapto-benzothiazole/heterocyclic moiety/antifungal/antibacterial)

Introduction

1,3,4-thiadiazole, 2-oxo-azetidinone and 2-mercaptobenzothiazoles have been extensively investigated by medicinal chemists due to their close association with various types of biological activities[1-6]. In recent years, sulphur and nitrogen bearing heterocycles have received much attention because of many chemotherapeutic agents[7-9]. Keeping in view the importance of the title heterocyclic compounds in medicinal chemistry, we report herein the synthesis, structural and biological evaluation of 2-(arylidenylamino)-5-[(2-benzothiazolylthio) methyl]-1,3,4-thiadiazoles **(4a-j)** and 1-[5-{(2-benzothiazolylthio) methyl}-1',3',4'-thiadiazole-2'-yl]-4-substituted-3-chloro-2-oxo-azetidinone **(5a-j)**. The synthesised compounds **4a-j** and **5a-j** were screened for their antifungal and antibacterial activity.

Heterocycle bearing nitrogen, sulphur and thiazole moiety constitute the core structure of a number of biologically interesting compounds. 2-Mercaptobenzothiazole and its derivatives are well known pharmacophore. Thiadiazoles show versatile biological interest as pesticides and chemotherapeutic agents. 2-Azetidinones and its derivatives possess variety of therapeutic activities. A large number of antibiotics contain azetidinone moiety. Hence it was thought worthwhile to synthesize compounds 4 and 5 and evaluate their antifungal and antibacterial activities. The structures of the synthesized compounds have been elucidated on the basis of their elemental analysis, IR and ^{1}H-nmr spectral data (Table 1).

Table 1

Compd.	IR, υ_{max} (cm^{-1})	^{1}H-NMR, δppm
4a	3025, 1518, 1108, 1070, 1031, 636 (aromatic ring), 2980, 2885, 1475, 1230, (CH$_2$, 1610 (C=N), 715 (C-S-C), 1600, 1440, 1305, 1172 and 700 cm^{-1} (C=N and thiadiazole nucleus), 1590 (N=CH) and 768 (Ar-Cl)	4.45 (s, 2H, S-CH$_2$); 4.96 (s, 1H, N=CH) and 6.90 −7.95 (m, 7H, ArH)
4d	3015, 1510, 1100, 1075, 1030, 635, 2985, 2880, 1470, 1230, 1605, 1442, 1300, 1155, 690, 1595.	4.40 (s, 2H, S-CH$_2$), 4.85 (s, 1H, N=CH), 6.90 − 7.90 (m, 8H, Ar-H)
4f	3020, 1510, 1115, 1065, 1030, 635; 2990, 2865, 1455, 1230, 1605, 1440, 1315, 1160, 696, 1595.	4.46 (s, 2H, S-CH$_2$); 4.90 (s, 1H, N=CH) and 6.95−7.95 (m, 8H, Ar-H)
4h	3010, 1514, 1115, 1060, 1030, 636, 2990, 2880, 1460, 1230, 1610, 1445, 1305, 1160, 695, 1580 1170 and 2860 (OCH$_3$ group in aromatic ring).	4.48 (s, 2H, S-CH$_2$); 4.80 (s, 1H, N=CH) and 7.10 − 7.96 (m, 7H, Ar-H)
4i	3010, 1515, 1110, 1060, 1030, 635, 2985, 2880, 1465, 1230, 1610, 1440, 1305, 1160, 690, 1580 and 650, 2925.	4.60 (s, 2H, S-CH$_2$); 4.85 (s, 1H, N = CH) and 6.80 − 7.85 (m, 8H, Ar-H)
4j	3020, 1510, 1110, 1070, 1035, 635, 2985, 2880, 1462, 1235, 1620, 1445, 1305, 1160, 690,	4.40, (s, 2H, S-CH$_2$); 4.90 (s, 1H, N=CH)

Compd.	IR, υ_{max} (cm^{-1})	^{1}H-NMR, δppm
	1590, 655, 2920, 1515 and 1345 (Ar-NO$_2$)	and 6.95-7.95 (m, 8H, Ar-H)
5a	3025, 1510, 1100, 1060, 1020 and 630 (aromatic ring) 2982, 2880, 1460 and 1230 (CH$_2$), 1765 (C=O), 1605, 1440, 1305, 1160, 705 (C=N and thiadiazole nucleus) and 760 (C-Cl)	4.15 (d, 1H, J = 5Hz,N-CH), 4.45 (s, 2H, S-CH$_2$), 5.05 (d, 1H, J = 5Hz, CHCl), 7.10-7.90 (m, 7H, ArH)
5d	3028, 1515, 1110, 1065, 1030, 635, 2990, 2880, 1460, 1225, 1760, 1615, 1440, 1305, 1160, 690, 768	4.05 (d, 1H, J = 5Hz, N-CH), 4.62 (s, 2H, S-CH$_2$), 5.01 (d, 1H, J = 5Hz, CHCl) and 6.70 –7.95 (m, 8H, Ar-H)
5f	3020, 1510, 1115, 1060, 1025, 630, 2990, 2885, 1460, 1230, 1762, 1615, 1440, 1305, 1160, 695, 763.	4.00 (d, 1H, J = 5Hz, N-CH), 4.65 (s,2H, S-CH$_2$), 5.05 (d, 1H, J = 5Hz, CHCl) and 6.75 – 7.90 (m, 8H, Ar-H)
5h	3025, 1500, 1100, 1075, 1030, 630, 2990, 1450, 1230, 1765, 1605, 1442, 1305, 1160, 695, 765	4.10 (d, 1H, J = 5Hz, N-CH), 4.55 (s, 2H, S-CH$_2$), 5.15 (d, 1H, J = 5Hz, CHCl), 6.95 7.95 (m, 7H, Ar-H)
5i	3025, 1510, 1105, 1060, 1036, 635, 2980, 2885, 1455, 1245, 1760, 1605, 1440, 1308, 1160, 690 and 665, 2925.	4.15 (d, 1H, J = 5Hz, N-CH), 4.45 (s, 2H, S-CH$_2$), 5.05 (d, 1H, J=5Hz, CHCl) and 6.70 – 7.95 (m, 8H, Ar-H)
5j	3020, 1505, 1100, 1075, 1030, 630, 2990, 1450, 1230, 1765, 1605, 1442, 1305, 1160, 695, 760, 660, 2930, 1475, 1380 (C–CH$_3$), 1510 – 1345, C-NO$_2$ in aromatic ring)	4.10 (d, 1H, J = 5Hz, N-CH), 4.55 (s, 2H, S-CH$_2$), 5.15 (d, 1H, J = 5Hz, CHCl) and 6.75 – 7.95 (m, 8H, Ar-H)

Materials and Method

Melting points were taken in open capillaries and are uncorrected. IR spectra (KBr) were recorded on a Shimadzu 8201 PC FTIR spectrophotometer and ^{1}H-NMR spectra on Brucker DRX 300 at 200 MHz using TMS as an internal standard. Purity of compounds in addition to the elemental analysis was checked by TLC using silica gel. All the compounds showed satisfactory results for C, H and N.
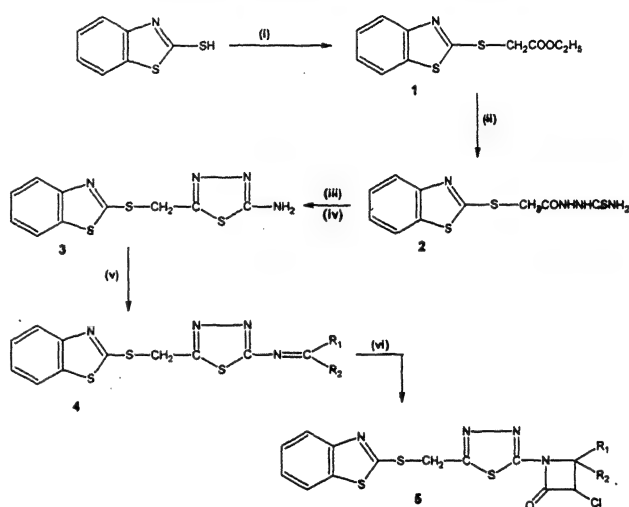
4a, 5a	$R_1 = H$	$R_2 = 2,4–(Cl)_2C_6H_3$
4b, 5b	$R_1 = H$	$R_2 = 2,6–(Cl)_2C_6H_3$
4c, 5c	$R_1 = H$	$R_2 = 2,3–(Cl)_2C_6H_3$
4d, 5d	$R_1 = H$	$R_2 = 2–C_2H_5OC_6H_4$
4e, 5e	$R_1 = H$	$R_2 = 4–C_2H_5OC_6H_4$
4f, 5f	$R_1 = H$	$R_2 = 3–C_2H_5C_6H_4$
4g, 5g	$R_1 = H$	$R_2 = 4–C_2H_5C_6H_4$
4h, 5h	$R_1 = H$	$R_2 = 2,3(CH_3O)_2C_6H_3$
4i, 5i	$R_1 = CH_3$	$R_2 = 4–CH_3C_6H_4$
4j, 5j	$R_1 = CH_3$	$R_2 = 3–NO_2C_6H_4$

Scheme – 1 : REAGENTS

(i) $ClCH_2COOEt$ (ii) $H_2NNHCSNH_2$ (iii) H_2SO_4 r.t. overnight

(iv) Liq. NH_3 (v) R_1COR_2 (vi) $ClCH_2COCl/Et_3N$

Ethyl-2-(benzothiazolylthio) acetate, (1) : A mixture of 2-mercaptobenzothiazole (0.1 mol) and ethyl chloroacetate (0.1 mol) in dry acetone (40 ml) in the presence of anhydrous K_2CO_3 (5g) was refluxed on a waterbath for about 15 h. The solvent was removed *in vacuo* and the residue was recrystallized from chloroform to get brown coloured crystals, yield 79%, m.p. 57 – 58^{0}C; υ_{max} 3025, 1518, 1108, 1075, 1031, 636 (aromatic ring) 1719

Table 2 – Antifungal activity data of compounds (4a-j) and (5a-j)

Comp	A.niger			C. albicans			R. oryzae		
	10 ppm	50 ppm	100 ppm	10 ppm	50 ppm	100 ppm	10 ppm	50 ppm	100 ppm
4a	++	+++	+++	+	++	+++	++	++	++
4c	+++	+++	+++	++	+++	+++	++	++	+++
4j	+	++	+++	++	++	++	+	++	+++
5a	+++	+++	+++	++	+++	+++	++	+++	+++
5c	++	+++	+++	++	++	+++	++	++	+++
5h	+	++	+++	+	++-	+	+	++	+++
5j	++	+++	+++	++	++	+++	++	++	+++
Grisco-fulvin	++	++	++++	+++	+++	++++	+++	+++	+ + + +

Zone of inhibition diameter in mm
+ = 6 – 10 mm; ++ = 10 – 18 mm; +++ = 18 – 23 mm; ++++ = 23 – 28 mm

(C=O of ester); 1610 (C = N), 1220 and 1040 (C-O-C), 715 (C-S-C) and 2912, 2875, 1427 and 710 (CH$_2$ and CH$_3$); δ (CDCl$_3$), 1.20 (3H, t, J=7Hz, COOCH$_2$CH$_3$), 4.15 (2H, q, J=7Hz, COOCH$_2$CH$_3$), 4.40 (2H,s,S-CH$_2$) and 6.72 – 7.94 (4H, m, Ar-H). Found C, 52.00; H, 4.09; N, 5,41; C$_{11}$ H$_{11}$ NO$_2$ S$_2$ required: C, 52.10; H, 4.10, N, 5.43%.

[(2-Benzothiazolythio) acetyle] – thiosemi-carbazide (2) : A mixture of 1 (0.07 mol) and thiosemicarbazide (0.07 mol) in methanol (50 ml) was refluxed on a waterbath for about 8 h. The excess of the solvent was removed under reduced pressure and the product was recrystallised from chloroform, yield 70%, m.p. 181 - 82^{0}C; υ$_{max}$ 3350 (-NHNH$_2$); 1130 (C = S); 1660 (CONH); δ (CDCl$_3$) 4.56 (2H, s, S-CH$_2$), 6.83 – 7.82 (4H, m, Ar-H), and 8.30 (4H, m, NHNHCS-NH$_2$), Found: C, 40.17; H, 3.30; N, 18.69; C$_{10}$ H$_{10}$N$_4$OS$_3$ required : C, 40.19; H, 3.31; N, 18.70 %.

2-Amino-5-[2-benzothiazolylthio)methyl] 1,3,4-thiadiazole(3) : The compound 2 (0.05 mol) mixed with conc. H$_2$SO$_4$ (16 ml) was kept overnight at room temperature. It was then diluted with 100 ml ice cold water and the excess acid was neutralized

with liquid ammonia. The product obtained was recrystallised from chloroform : methanol mixture to get 3, yield 74%, m.p. 209 -11^{0}C; υ$_{max}$ 3355 and 3315 (-NH$_2$), 1600, 1440, 1305, 1172 and 700 (C-N and thiadiazole nucleus); δ (CDCl$_3$); 4.20 (2H, s, -NH$_2$), 4.45 (2H, s, S-CH$_2$) and 6.75 – 7.93 (4H, m, Ar-H). Found : C, 40.17; H, 3.30; N; 18.69; C$_{10}$H$_8$N$_4$S$_3$ required : C, 40.19, H, 3.31; N, 18.75%.

2-(Arylidenylamino)-5-[(2-benzothiazolylthio) methyl]-1,3,4-thidiazoles, 4(a) : The compound 3 (25 m mol), 2,4-dichloro benzaldehyde (25m mol) in glacial acid were refluxed in ethanol (50 ml) for about 8 h. Ethanol was removed under reduced pressure, and the solid thus obtained was dried and recrystallised from methanol : chloroform mixture as dark brown crystals, yield 73%, m.p. 222-23^{0}C; Found: C, 46.59; H, 2.21; N. 12.76%; C$_{17}$H$_{10}$N$_4$S$_3$Cl$_2$ required : C,46.68; H, 2.28; N, 12.81. Other compounds 4b-j were synthesised in a similar way using various carbonyls. Their spectral data are given in Table 1.4b yield 75%, m.p. 213 – 15^{0}C, Found: C, 46.65; H, 2.22; N, 12.74; C$_{17}$H$_{10}$N$_4$S$_3$Cl$_2$ required : C, 46.68; H 2.28; N, 12.81%. 4c (74%), m.p. 229-30^{0}C, Found: C. 46.58; H, 2.20; N, 12.70 C$_{17}$H$_{10}$N$_4$S$_3$Cl$_2$ required; C, 46.68; H, 2.28; N,

12.81%, 4d, (61%), m.p.- 201-02^{0}C, Found: C, 55.23; H, 3.84; N, 13.51 $C_{19}H_{16}N_4S_3O$ required : C, 55.33; H, 3.88; N, 13.59% 4e, (69%), m.p. 219 – 23^{0}C, Found : C, 55.25 : H, 3.80; N, 13.52 C_{19} H_{16} N_4S_3O required : C, 55.33; H, 3.88 N, 13.59%. 4f, (60%), m.p. 211-13^{0}C, Found; C, 57.48; H, 3-91; N, 14.10 $C_{19}H_{16}N_4S_3$ required; C, 57.57; H, 4.04; N, 14-14. 4g, (58%), m.p. 200-02^{0}C, Found: C, 57.49; H, 3.90; N, 14.10 $C_{19}H_{16}N_4S_3$ required : C, 57.57; H, 4.04; N, 14.14%, 4h (65%), m.p.- 189-91^{0}C, Found : C, 53.21; H, 3.66; N, 12.93; $C_{19}H_{16}N_4S_3O_2$ required : C, 53.27; H, 3.73; N, 13.08%, 4i,(68%), m.p. 230- 32^{0}C, Found: C, 57.50; H, 3.95; N, 14.11; $C_{19}H_{16}N_4S_3$ required : C, 57.57; H, 4.04; N, 14.14%, 4j-(65%), m.p. 240- 03^{0}C, Found: C, 50.51; H, 2.92; N, 16.30; $C_{18}H_{13}N_5S_3O_2$ required : C, 50.58; H, 3.04; N, 16.39%.

1-5'-{(2-Benzothiazolylthio)methyl}-1',3',4'-thiadiazol-2'-yl]-4-(2,4-dichloro-benzaldehyde) -3-chloro-2-oxo-azetidinone (5a) : Compound 4a (5.0 m mol) and Et_3N (10.0 m mol) were mixed with dioxane (50 ml) and stirred well. To this solution chloroacetyl chloride (10.0 m mol) was added dropwise at 0 – 5^{0}C. The reaction mixture was stirred for about 5h. and the separated amine hydrochloride was filtered off. The filtrate was refluxed and the solid product thus obtained was

recrystallized from methanol, yield 76 %, m.p. 239 – 40^0. Found : C, 45.37; H, 2.16; N, 11.20; $C_{19}H_{11}N_4S_3OCl_3$ required : C, 45.40; H, 2.14; N, 10.90%. The compounds 5b-j were synthesized from 4b-j in a similar way. Spectral data are presented in Table 1. 5b, (72 %), m.p. 220 – 01^{0}C, Found : C, 45.79; H, 2.13; N, 1$^-$.19; $C_{19}H_{11}N_4S_3OCl_3$ required; C, 45.40; H, 2.14; N, 10.90%, 5c, (76 %), m.p. 244-01^{0}C, Found : C, 45.27; H, 2.18; N; 11.19%, $C_{19}H_{11}N_4S_3OCl_3$ required : C, 45.40; H, 2.14; N, 10.90 %. 5d, (59 %) m.p. 208 – 09^{0}C, Found : C, 51.49; H, 3.41; N, 11.44; $C_{21}H_{17}N_4S_3O_2Cl$ required : C, 51.58; H, 3.48; N, 11.46 %. 5e, (70 %) m.p. 239-40^{0}C, Found : 51.44; H, 3.40; N, 11.43; $C_{21}H_{17}N_4S_3O_2Cl$ required : C, 51.58; H, 3.48; N, 11.46%. 5f, (62 %), m.p. 230-35^{0}C, Found : C, 53.26; H, 3.52; N, 11.80; $C_{21}H_{17}N_4S_3OCl$ required : C, 53.33; H, 3.59; N, 11.85 %. 5g, (55 %); 225-6^{0}C, Found : C, 53.31; H, 3.50; N, 11.81; $C_{21}H_{17}N_4S_3OCl$ required : C, 53.33; H, 3.59; N, 11.85 %. 5h, (66 %), m.p. 253-55^{0}C, Found : C, 49.88; H, 3.31; N, 11.03; $C_{21}H_{17}N_4S_3O_3Cl$ required : C, 49.95; H, 3.36; N, 11.10 %. 5i, (72 %), m.p. 268-69^{0}C, Found : C, 53.25; H, 3.51; N, 11.81; $C_{21}H_{17}N_4S_3OCl$ required : C, 53.33; H, 3.59; N, 11.85 %. 5j, (63 %), m.p. 272-75 ^{0}C, Found : C, 47.58; H, 2.71; N, 13.85; $C_{20}H_{14}N_5S_3O_3Cl$ required : C, 47.66; H, 2.78; N, 13.90 %.

Results and Discussions

Compounds 4 and 5 were screened for their antifungal activity against *Aspergillus niger*, *Candida albicans* and *Rizopus oryzae* at 10, 50 and 100 ppm concentrations. The antibacterial activity was assayed against the bacteria *Escherchia coli*, *Shigella dysentriae* and *Streptococcus aureus* at 50 and 100 ppm concentration by filter paper disc technique[10]. Griseofulvin and streptomycin were used as standard. The results of active compounds are given in Tables (2 and 3) respectively.

Acknowledgement

Table 3 - Antibacterial activity data of compounds (**4a-j**) and (**5a-j**).

Comp	E. coli		S. dysentriae		S. aureus	
	50 ppm	100 ppm	50 ppm	100 ppm	50 ppm	100 ppm
4a	+	++	++	++	++	++
4c	++	+++	++	+++	++	++
4j	++	++	++	++	++	+++
5a	+++	+++	++	+++	++	+++
5b	+	++	++	+++	+	++
5c	++	++	++	+++	++	+++
5h	++	++	++	++	++	+++
5j	++	++	++	+++	++	++
Stepto-mycin	+++	++++	+++	++++	+++	++++

Zone of inhibition diameter in mm
+ = 4 – 8mm; ++ = 8 – 19 mm; +++ = 19 – 25 mm; ++++ = 25 – 32 mm

References

1. Guru, N. & Srivastava, S.D. (2001) *J. Sci. Ind. Res.* **60** : 601.

2. Chande, M.S. & Jathar, K.S. (1995) *Indian J. Chem.* **38** : 654.

3. Yadav, R., Srivastava, S., Srivastava, S.K. & Srivastava, S.D. (2003) *Chem: An Indian Journal* **1** : 95.

4. Srivastava, S.K., Yadav, R. & Srivastava, S.D. (2004) *J. Ind. Chem. Soc.* **81** : 342.

5. Rawat, T.R. & Srivastava, S.D. (1999) *Indian J. Chem.* **8B** : 183.

6. Radha, R.B., Bhalerao, U.T. & Rahman, M.F. (1990) *Indian J. Chem.* **29B** : 995.

7. Jaish, L. & Srivastava, S.K. (2001) *J. Sc. Indus. Res.* **60** : 331.

8. Desai, P.S. & Desai, K.R. (1994) *J. Indian Chem. Soc.* **71** : 155.

9. Sawhney, S.N., Sharma, P.K. & Gupta, A. (1993) *Indian J. Chem.* **32B** : 1190.

10. Vincent, J.G. & Vincent, H.W. (1995) *Proc. Soc. Exp. Biol. Med.* **55** : 112.

Studies on some unsymmetrical bis(hydroxyaryl) tellurium(IV) dichlorides

K.K. VERMA* and SUNIL VERMA

Department of Chemistry, M.D. University, Rohtak-124001, India

E-mail : vermakk123@yahoo.com

Abstract

The preparation and properties of some unsymmetrical bis(hydroxyaryl)tellurium(IV) dichlorides, $RR'TeCl_2$ (where R and R' are different hydroxyaryl groups as 4-hydroxyphenyl; 2,4-dihydroxyphenyl; 2-methyl-4-hydroxyphenyl; 3-methyl-4-hydroxyphenyl and 3-methyl-6-hydroxyphenyl) are reported for the first time. Cryoscopic measurements, in general, are consistent with conductivity measurements, and reflect the molecular nature of these dichlorides. The infrared, far infrared and proton magnetic resonance spectral studies suggest the linkage of tellurium to the ring carbon atoms *para* to the OH groups unless otherwise occupied. A pseudo trigonal bipyramidal structure having two chlorine atoms transe to each other, has been suggested for these diaryltellurium dichlorides.

(**Keywords:** IR/PMR/hydroxyphenyl / methyl hydroxyphenyl /tellurium)

Introduction

Although a number of symmetrical bis-(hydroxyaryl)tellurium(IV) dihalides are reported in the literature, there appears to be no report on the unsymmetrical bis-(hydroxyaryl) tellurium(IV) derivatives. Rust[1] reported the formation of bis(2,4-dihydroxyphenyl)tellurium dichloride by the reaction of $TeCl_4$ with resorcinol. Morgan and Burgess[2] investigated the reaction of 'tellurium oxychloride' with isomeric cresols and isolated R_2TeCl_2 type compounds. Several workers[3-5] carried a systematic study on the reactions of $TeCl_4$ with a number of hydroxybenzenes. They reported the formation of bis-(hydroxyaryl)tellurium(IV) dichlorides with phenol, *o*-, *m*- and *p*-cresols, resorcinol and catechol. In addition to these symmetrical bis-(hydroxyaryl) tellurium(IV) dichlorides, a few diaryltellurium(IV) compounds where one of the aryl groups is a hydroxyaryl group, are also reported. Petragnani[6]

prepared such diaryltellurium(IV) dichlorides by reacting aryl-tellurium trichlorides with resorcinol. Malik *et al.*[7] synthesized aryl (trans-2-chloro/ethoxy-1-cycloalkyl) tellurium (IV) dichlorides by reacting 3,5-dimethyl-4-hydroxyphenyltellurium trichloride with cyclo-alkenes. No bis(hydroxyaryl) tellurium (IV) compound having different types of hydroxyaryl groups appears to have been synthesized. In this paper, we report for the first time the preparation and characterization of some unsymmetrical bis-(hydroxyaryl) tellurium(IV) dichlorides, $RR'TeCl_2$.

Materials and Method

Tellurium tetrachloride and phenol used were of E. Merck and BDH (Anal R) quality, respectively. Resorcinol, mercuric acetate and sodium chloride were of Loba Chemie. *o*-Cresol was obtained from Ranbaxy Laboratories Ltd. and *m*- and *p*-cresols from SISCO research laboratories. Solvents were purified and dried by conventional method.

Conductance measurements were performed under dry conditions in nitrobenzene, acetone and acetonitrile solutions at $35 \pm 1^\circ C$ using a highly sensitive Systronics conductivity bridge Type 305 (which can read up to $\pm 0.1 \times 10^{-6}$ mhos) and a dip type cell with smooth platinum electrodes with a cell constant of 0.50 cm^{-1}. Molecular weights were determined cryoscopically in nitrobenzene up to the saturation point.

IR and far IR spectra were recorded using KBr pellet and polyethylene pellet technique on a BRUKER IFS 66 v FT-IR spectrophotometer at RSIC, IIT Chennai. ^1H NMR spectra were recorded in $CDCl_3$ or DMSO-d_6 using tetramethylsilane as

an internal reference at RSIC, IIT Mumbai on a BRUKER DPX-300 NMR spectrophotometer. Carbon and hydrogen analysis were obtained from RSIC, Panjab University Chandigarh.

All the preparations were carried out under dry nitrogen atmosphere. The unsymmetrical bis-(hydroxyaryl) tellurium(IV) dichlorides, $RR'TeCl_2$ have been prepared by reactions of $RTeCl_3$ (R = 4-hydroxyphenyl or 3-methyl-4-hydroxyphenyl) with hydroxybenzene (R'-H = phenol, resorcinol)- Method A or with R'HgCl (R'-H = m-and p-cresols)- Method B, the mercuration method[8]. The reaction conditions are given in Table 1.

The 4-hydroxyphenyl- and 3-methyl-4-hydroxy-phenyltellurium trichlorides in turn were obtained by reaction of $TeCl_4$ with phenol and o-cresol respectively[3-5]. The organyl mercuric chlorides, R'HgCl, were prepared by reported method[9].

Results and Discussion

The formation of hydroxyaryltellurium trichloride by the reaction of $TeCl_4$ with phenol and o-cresol involves the electrophillic substitution of the ring by $TeCl_3^+$ at a position para to the hydroxyl group.

$$R–H + TeCl_4 \longrightarrow RTeCl_3 + HCl$$
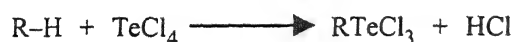
This $RTeCl_3$ when reacted with other hydroxy-benzene (phenol, resorcinol) or with organylmercuric chloride, R'HgCl (R'-H = m- and p-cresol), yields the unsymmetrical bis-(hydroxyaryl)tellurium(IV) dichlorides :

$$RTeCl_3 + R'\text{-H} \longrightarrow RR'TeCl_2 + HCl \text{ (Method A)}$$

$$RTeCl_3 + R'HgCl \xrightarrow{\text{dioxane}} RR'TeCl_2 + HgCl_2.\text{dioxane.}$$
$$\text{(Method B)}$$

These unsymmetrical bis-(hydroxyaryl) tellurium (IV) dichlorides are air stable, crystalline solids which are soluble in polar organic solvents. The analytical data, preparative conditions and some physical properties are compiled in Table 1.

Conductance and Cryoscopic Studies : The molar conductance data in nitrobenzene, acetone and acetonitrile (Table 2) reflect the non-electrolyte type behaviour of these dichlorides. The Λ_M values in all the three solvents are much less than those reported for 1:1 electrolytes[10]. The cryoscopic measurements in nitrobenzene (Table 2) also predict their molecular nature in solution and thus, support the results of conductance studies.

IR and Far IR Spectra : The important IR and far IR frequencies for the unsymmetrical

Table 1 – Preparative, physical characteristics and analytical data for unsymmetrical bis(hydroxyaryl) tellurium (IV) dichlorides, $RR'TeCl_2$.

Comp. No.	$RR'TeCl_2$ (Parent hydroxybenzene)	Method (Reaction conditions)	Yield (%)	Colour	M.P. (°C)	Analysis found (Calculated)			
						Te	Cl	C	H
I.	R = 3-methyl-4-hydroxyphenyl-; (o-cresol) R' = 4-hydroxyphenyl-; (phenol)	A (110°C, 20 h)	60	Light brown	190-193	31.63 (32.01)	16.67 (17.81)	39.37 (39.14)	2.61 (3.01)
II.	R= 4-hydroxyphenyl-; (phenol) R' = 2-methyl-4-hydroxyphenyl-; (m-cresol)	B (dioxane, reflux, 12 h)	75	White	95-97	31.60 (32.01)	17.22 (17.81)	38.42 (39.14)	2.75 (3.01)
III.	R= 4-hydroxyphenyl-;(phenol) R' = 3-methyl-6-hydroxyphenyl-; (p-cresol)	B (dioxane, reflux, 12 h)	70	White	90-93	31.55 (32.01)	17.38 (17.81)	38.40 (39.14)	2.75 (3.01)
IV.	R= 4-hydroxyphenyl-; (phenol) R' = 2,4-dihydroxyphenyl-; (resorcinol)	A (methanol, room temp., 24 h)	63	Light brown	140-142*	31.33 (31.85)	17.19 (17.72)	35.19 (35.95)	2.05 (2.50)
V.	R = 3-methyl-4-hydroxyphenyl-; (o-cresol) R' = 2-methyl-4-hydroxyphenyl-; (m-cresol)	B (dioxane, reflux, 12 h)	58	White	132-135	30.35 (30.93)	16.67 (17.21)	40.10 (40.72)	3.06 (3.40)
VI.	R = 3-methyl-4-hydroxyphenyl-; (o-cresol) R' = 3-methyl-6-hydroxyphenyl-; (p-cresol)	B (dioxane, reflux, 12 h)	55	White	150-155	30.08 (30.93)	16.81 (17.21)	39.82 (40.72)	3.12 (3.40)

* melt with decomposition; yields with respect to $RTeCl_3$.

Table 2 – Molar conductance and cryoscopic data for unsymmetrical bis(Hydroxyaryl)tellurium(IV) dichlorides.

Compound No.	Λ_M at ca $.10^{-3}$ M (ohm^{-1} cm^2 mol^{-1})			Molecular weight data		
	Nitrobenzene	Acetone	Acetonitrile	Formula weight	Conc. range mmoles/litre of nitrobenzene	Average molecular weight found
I.	0.24	5.40	7.20	398.6	2.8-9.0	389.4
II.	1.86	9.00	15.60	398.6	2.7-12.2	384.2
III.	2.40	12.00	18.00	398.6	2.5-12.5	375.8
IV.	1.71	22.20	36.00	400.6	6.2-14.0	378.9
V.	4.80	8.40	17.40	412.6	2.4-12.0	375.3
VI.	3.00	9.60	18.00	412.6	5.2-12.0	388.1

* Values reported[10] for 1:1 electrolytes,   nitrobenzene = 20-30,   acetone = 100-140,   acetonitrile = 120-160.

Table 3 – Important IR and far IR data (cm^{-1}) for unsymmetrical bis(hydroxyaryl)tellurium(IV) dichlorides.

Compound No.	ν_{O-H}	$\nu_{(C-O)}$	$\nu_{C=C}$	ν_{Te-Ph}	$\nu_{s\ Te-Cl}$	$\nu_{as\ Te-Cl}$
I.	3298 sb	1265 s	1578 vs	232 w 222 m	277 m	250 s
II.	3331 sb	1277 m	1574 vs	236 m	293 w	262 w
III.	3346 mb	1269 w	1572 m	238 m	313 m	275 w 260 w
IV.	3243 sb	1316 w 1263 sh	1580 vs	230 s	290 w	273 m
V.	3400 mb	1277 m	1610 vs 1578 m	250 m 235 vs 215 m	280 m	265 m
VI.	3388 mb	1268 w	1612 vs	239 w	283 m	267 m

s = strong, m = medium, w = weak, b = broad, vs = very strong, sh = shoulder.

bis(hydroxyaryl) tellurium(IV) dichlorides are presented in Table 3. The presence of a broad band ~3500-3300 cm^{-1} corresponding to O-H stretching frequency rules out the involvement of this group in bonding with tellurium. The vibration pertaining to C-O stretching, which appears normally at 1260-1180 cm^{-1} in hydroxybenzenes, is shifted to high frequency suggesting an increase in C-O bond order due to the substitution of tellurium at the *para* or *ortho* position to the OH group. All these compounds show a strong band around 1600-1580 cm^{-1}, which suggests the *para* substitution (unless it is otherwise occupied) of benzene ring by electron withdrawing

TeCl$_2$ group. The high intensity of this band is due to dipole moment change provided by groups of different nature. The linkage of tellurium to a phenyl carbon atom is confirmed by presence of bands around 250-215 cm^{-1} due to ν_{Te-C} or ν_{Te-Ph} as reported for other diaryltellurium (IV) compounds[3-5,11,12]. The symmetric and asymmetric tellurium-chlorine bands appear at 277-313 and 275-250 cm^{-1}, respectively, which suggest[3-5,11,13,14] the monomeric nature of these compounds in solid state having a pseudo trigonal bipyramidal structure with the two chlorine atoms trans to each other.

Table 4 - Proton magnatic resonance data (δ ppm) for unsymmetrical bis(hydroxyaryl)tellurium(IV) dichlorides.

Comp. No.	RTe(Cl$_2$)R'	Solvent	Aryl protons of R	Aryl protons of R'	CH$_3$	OH
I.	R = 3-methyl-4-hydroxyphenyl- R' = 4-hydroxyphenyl-	CDCl$_3$	7.24-7.42, 7.96-8.25 (m, 5H)	6.97 (d, J = 9 Hz, 2H, *ortho* to OH); 7.94 (d, J = 9 Hz, 2H, *ortho* to TeCl$_2$)	2.29 (s, 3H)	Mixed with aryl of R
II.	R= 4-hydroxyphenyl- R' = 2-methyl-4-hydroxyphenyl-	DMSO-d$_6$	6.74-8.1 (m, 7H)	Mixed with R	2.28 (s, 3H)	10.24 (s, b, 2H)
III.	R= 4-hydroxyphenyl- R' = 3-methyl-6-hydroxyphenyl-	DMSO-d$_6$	6.93 (d, J=9 Hz, 2H, *ortho* to OH); 8.02 (d, J = 9 Hz, 2H, *ortho* to TeCl$_2$)	7.75 (s, 1H, *ortho* to TeCl$_2$ and Me); 7.05 (d, J = 8.7 Hz, 1H, *ortho* to OH); 7.19 (d, J = 8.4 Hz, 1H, *ortho* to Me)	2.13 (s, 3H)	9.60 (s, 2H)
IV.	R= 4-hydroxyphenyl- R' = 2,4-dihydroxyphenyl-	DMSO-d$_6$	7.02 (d, J = 8.4 Hz, 2H, *ortho* to OH); 7.99 (d, J = 8.4 Hz, 2H, *ortho* to TeCl$_2$)	7.40 (d, J = 7.2 Hz, 1H, *ortho* to TeCl$_2$); 6.95 (d, J = 8.4 Hz, 1H, *ortho* to OH); 6.53 (s, 1H, *ortho* to both OH)	——	10.35, 11.40 (b, 3H)
V.	R = 3-methyl-4-hydroxyphenyl- R' = 2-methyl-4-hydroxyphenyl-	DMSO-d$_6$	6.90-7.88 (m, 6H)	Mixed with R	2.12 (s, 3H) 2.21 (s, 3H)	11.01 (b,2H)

Spectrum of compound no. VI not well resolved due to poor solubility.
s = singlet, d = doublet, m = multiplet, b = broad

Proton Magnetic Resonance Spectra : The ^{1}H NMR chemical shift data for these dichlorides are compiled in Table 4. Since these compounds contain identical organic moieties (both hydroxyaryl), the aryl proton chemical shifts are expected to show a lot of mixing or overlapping. Thus, the assignments of aryl protons have been made by comparison of the spectra of these compounds with those of already reported symmetrical hydroxyaryl tellurium(IV) derivatives[3-5,12].

Methyl protons in the compounds derived from isomeric cresols having only one such group appear at δ 2.12-2.29 ppm as sharp singlet whereas two separate singlets at 2.12 and 2.21 are observed for compound containing *o*-cresol and *p*-cresol moieties indicating two different types of methyl groups. Presence of δ OH between 7.96-11.4 ppm reveals the non-participation of this group in bonding with tellurium. The NMR patterns for aryl protons suggest the linkage of TeCl$_2$ group at phenyl carbon atoms which are *para* to the OH group (*ortho* in *p*-cresol derivatives).

The ^{1}H NMR spectrum of *p*-hydroxyphenyl (2,4-dihydroxyphenyl) tellurium(IV) dichloride show the four protons of *p*-hydroxyphenyl group resonating at 7.02 and 7.99 ppm as two separate doublets. The single proton of resorcinol moiety, which is *ortho* to both OH groups is most shielded and resonate at 6.53 ppm as sharp singlet. The proton *ortho* to tellurium is most deshielded and appear at 7.40 ppm as a doublet with J = 7.2 Hz. The third proton, *ortho* to OH show a separate doublet at 6.95 with a J value of 8.4 Hz. The three hydroxyl protons show two separate broad signals at d 10.35 and 11.45 ppm.

Thus, the proton magnetic resonance spectral studies support the predictions of IR and far IR studies that tellurium is bonded to ring carbon atoms at positions *para* to the OH groups, unless otherwise occupied.

References

1. Rust, E. (1897) *Ber.* **30** : 2829.

2. Morgan, G. T. & Burgess, H. (1929) *J. Chem. Soc.* 2214.

3. Kumar, K. (1981) *Ph.D. Thesis,* IIT Delhi, New Delhi.

4. Khandelwal, B. L., Kumar, K. & Berry, F. J. (1981) *Inorg. Chim. Acta* **47** : 135.

5. Khandelwal, B. L., Kumar, K. & Raina, K. (1981) *Synth. React. Inorg. Met.-Org. Chem.* **11** : 65.

6. Petragnani, N. (1961) *Tetrahedron* **12** : 219.

7. Malik, M. A., Ali, M. E. S., Berry, F. J., Kaur, J., Rowshani, M. & Smith, B. C. (1991) *Inorg. Chim. Acta* **180** : 251.

8. Petragnani, N. (1994) *Tellurium in Organic Synthesis,* Academic Press, London, p. 65.

9. Thomas, S. (1991) *Ph.D. Thesis,* IIT Delhi, New Delhi.

10. Geary, W. J. (1971) *Coord. Chem. Rev.* **7** : 81.

11. McWhinnie, W. R. & Patel, M. G. (1972) *J. Chem. Soc. Dalton* 199.

12. Khandelwal, B. L., Singh, A. K., Mehta, R. & Kumar, K. (1984) *Synth. React. Inorg. Met.-Org. Chem.* **14** : 921.

13. Verma, K. K. & Garg, S. (1994) *Synth. React. Inorg. Met.-Org. Chem.* **24** : 647.

14. Verma, K. K. & Garg, S. (1994) *Synth. React. Inorg. Met.-Org. Chem.* **24** : 1631.

Kinetic, mechanistic and spectral investigation of oxidation of 4-hydroxy coumarin by diperiodatocuprate (III) in aqueous alkaline medium

MANJUNATH B. BELLAKKI, MAHESH T. RAMADURGA and SHARANAPPA T. NANDIBEWOOR*

Post Graduate Department of Studies in Chemistry, Karnatak University, Dharwad-580 003, India.

Corresponding author : E-mail : stnandibewoor@yahoo.com

Abstract

The kinetics of oxidation of 4-hydroxy coumarin(HDC) by alkaline diperiodatocuprate (III) (DPC) at a constant ionic strength has been studied spectrophotometrically. The reaction is first order with respect to [DPC] and is an apparent less than unit order, each in [4-hydroxy coumarin] and [alkali] under the experimental conditions. Potassium periodate has a retarding effect on the rate of reaction. A mechanism involving the monoperiodatocuprate (III) (MPC) as the reactive oxidant species has been proposed. The main products were identified by the spot test, I.R. and N.M.R. spectroscopy. The reaction constants involved in the mechanism were evaluated. There is a good agreement between the observed and calculated rate constants under varying experimental conditions. The activation parameters with respect to the slow step of scheme were evaluated and discussed.

(Keywords:kinetics/spectral study/oxidation/4-hydroxycoumarin/ diperiodatocuprate(III)(DPC))

Introduction

The periodate and tellurate complexes of copper in its trivalent state have been extensively used in the analysis of several organic compounds[1]. The kinetics of self decomposition of these complexes were studied in some detail[2]. Diperiodatocuprate (III) (DPC) is a versatile one-electron oxidant for various organic compounds in alkaline medium and its use as an analytical reagent is now well recognized and also used in the estimation of amino acids[3]. Movius[4] reported the reactivity of some alcohols with DPC. Copper (III) is shown to be an intermediate in the copper (II) catalysed oxidation of amino acids by peroxydisulphate[5]. Moreover, when the copper (III) periodate complex is oxidant, since multiple equilibria[6] between the different copper (III) species are involved,

it needs to be known which of species is the active oxidant.

4-hydroxy coumarin(4-hydroxy-2H-1-benzopyran-2-one) (HDC) is used in the synthesis of pharmaceuticals especially for anticoagulants. It is used in manufacturing fluorescent dyes and rodenticides. The literature survey reveals that there are no reports on the oxidative mechanism of 4-hydroxycoumarin by any oxidant. Hence the title reaction is undertaken.

Materials and Method

All chemicals used were of A.R grade and double distilled water was used throughout. The solution of 4-hydroxy coumarin (M/s. S.S. Antibiotics Pvt. Ltd, Aurangabad, India) was prepared by dissolving known amount of the sample in distilled water. The purity of the sample was checked by TLC and its m.p. 212°C. The copper(III) periodate complex was prepared by standard procedure[7]. The purity of the complex was checked by its spectra, which showed broad absorption band at 415 nm. The aqueous solution of copper(III) was standardized by back titration method[7].

The copper(II) solution was made by dissolving the known amount of copper sulphate (BDH) in distilled water. Periodate solution was prepared by weighing the required amount of sample in hot water. Its concentration was ascertained iodometrically[8] at neutral pH by phosphate buffer. Since periodate is present in excess in DPC, the possibility of oxidation of 4-hydroxy coumarin by periodate in alkaline

medium at 25 °C was tested. The progress of the reaction was followed iodometrically. However, it was found that there was no significant reaction under the experimental conditions employed compared to the DPC oxidation of 4-hydroxy coumarin. Potassium hydroxide and potassium nitrate (BDH, Analar) were employed to maintain the required alkalinity and ionic strength respectively in reaction solutions.

Kinetic measurements : The oxidation of 4-hydroxy coumarin by DPC was followed under pseudo-first order conditions where [HDC] was excess over [DPC] at $25\pm0.1^\circ C$ unless otherwise stated. The reaction was initiated by mixing the required quantities of previously thermostatted solution of 4-hydroxy coumarin and DPC, which also contained known quantities of KOH, KNO_3 and IO_4^- to maintain the required alkalinity, ionic strength and periodate. The total $[OH^-]$ was calculated considering the KOH in DPC as well as the KOH additionally added. Similarly, the total metaperiodate concentration was calculated by considering metaperiodate present in solution of DPC and additionally added. The progress of reaction was followed by measuring the absorbance of unreacted DPC in the reaction mixture in 1 cm quartz cell located in the thermostatted compartment of a Peltier Accessory (temperature control) attached Varian CARY 50 spectrophotometer at 415 nm as a function of time. Earlier it was verified that there is negligible interference from other species present in the reaction mixture at this wavelength. The obedience of Beer's law by DPC at 415 nm was verified earlier and the molar absorbance coefficient, ε was found to be 6213 ± 250 $dm^3\ mol^{-1}\ cm^{-1}$ at this wavelength. The reaction was followed to more than 80% completion. The first order rate constants, k_{obs} were obtained from the plots of log (Abs) *vs.* time. The rate constants were reproducible within $\pm5\%$.

Stoichiometry and product analysis : Different sets of reaction mixtures containing excess DPC over 4-hydroxy coumarin with constant concentration of OH^-, IO_4^- and KNO_3 were kept for 6 h in a closed vessel under nitrogen atmosphere. The remaining concentration of DPC was estimated spectrophotometrically at 415 nm. The results indicate 1:6 stoichiometry as given in equation (1).

(1)
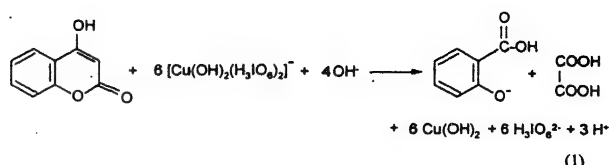
The reaction product was extracted with ether and recrystallised from aqueous alcohol and the purity was checked by HPLC. This is identified as salicylic acid by its I.R. spectrum (KBr), which showed a band at (δ) 1701 cm^{-1} due to C=O stretching of acid, a broad band at 2920 cm^{-1} due to O-H stretching of acids and 3392 cm^{-1} due to phenolic OH. Salicylic acid was further characterised by ^1H NMR spectrum ($CDCl_3$ + $DMSO-d_6$/TMS) δ, 5.74 (s, 1H, phenolic OH, disappeared on D_2O exchange), 7.27 to 7.82 (m, 4H, 4 aromatic protons), 11.5 (s, 1H, acidic OH, vanished on D_2O exchange). The other product oxalic acid, which is highly soluble in water, was identified by spot test[9] and copper(II) sulphate was identified by spot test[10] and spectral study. It was observed that the salicylic acid and oxalic acid do not undergo further oxidation under the present kinetic conditions.

Results and Discussion

The reaction orders were determined from the slope of log k_{obs} *vs.* log [Reactant] by varying the concentrations of reductant, alkali and periodate in each while keeping all other concentrations and conditions constant.

The oxidant DPC concentration was varied in the range of 2.0×10^{-5} to 2.0×10^{-4} mol dm^{-3} and the fairly constant k_{obs} values indicate that order with respect to [DPC] was one as given in Table 1. This was also confirmed by linearity of the plots of log (Abs) *vs.* time ($r > 0.9963$, $S \leq 0.0162$) upto about 80% completion of the reaction. The substrate, 4-hydroxy coumarin was varied in the range of 5.0×10^{-4} to 5.0×10^{-3} mol dm^{-3} at 25°C. The k_{obs} values increased with increase in concentration of 4-hydroxy coumarin. The order with respective [HDC] was found to be an apparent less than unit order (Table 1). The effect of alkali on the reaction was studied at constant concentrations of 4-hydroxy coumarin, DPC, IO_4^- and at a constant ionic strength of 1.0 mol dm^{-3} at 25°C. The rate constants (k_{obs}) increased with increase in [alkali] (Table 1) with less than unit order. The effect of $[IO_4^-]$ was observed by varying the concentration

Table 1 – Effect of variation of [DPC], [4-hydroxy coumarin], [OH⁻] and [IO₄⁻] on oxidation of 4-hydroxy coumarin by alkaline diperiodatocuprate (III) complex at 25°C, I = 1.0/mol dm⁻³.

[DPC]×10⁴/ (mol dm⁻³)	[HDC]×10³/ (mol dm⁻³)	[OH⁻]/ (mol dm⁻³)	[IO₄⁻] (mol dm⁻³)	k_{obs}×10³/ (s⁻¹)
0.2	1.0	0.2	1.0	3.33
0.4	1.0	0.2	1.0	3.34
0.8	1.0	0.2	1.0	3.36
1.0	1.0	0.2	1.0	3.35
2.0	1.0	0.2	1.0	3.34
1.0	0.5	0.2	1.0	2.22
1.0	1.0	0.2	1.0	3.35
1.0	2.0	0.2	1.0	5.10
1.0	4.0	0.2	1.0	6.65
1.0	5.0	0.2	1.0	7.14
1.0	1.0	0.05	1.0	1.23
1.0	1.0	0.1	1.0	2.17
1.0	1.0	0.2	1.0	3.35
1.0	1.0	0.4	1.0	4.78
1.0	1.0	0.5	1.0	5.26
1.0	1.0	0.2	1.0	3.35
1.0	1.0	0.2	2.0	2.36
1.0	1.0	0.2	4.0	1.58
1.0	1.0	0.2	8.0	0.91
1.0	1.0	0.2	10.0	0.72

from 1.0×10^{-5} to 10×10^{-5} mol dm⁻³ keeping all other reactants concentration constant. It was found that the added periodate retarded the rate and order in periodate was inverse fractional.

Effect of ionic strength and solvent polarity : The effect of ionic strength was studied by varying the potassium nitrate concentration from 0.2 to 2 mol dm⁻³ at constant concentrations of diperiodatocuprate (III) (DPC), 4-hydroxy coumarin, periodate and alkali. It was found that the rate constant increased with increase in the concentration of KNO₃

and the plot of log k_{obs} vs. $I^{1/2}$ was linear with (r>0.9897, S<0.0119) positive slope.

The effect of relative permitivity ($\in_T$) was studied by varying the t-butanol-water content in the reaction mixture with all other conditions being maintained constant. Attempts to measure the relative permittivities were not successful. However, they were computed from the values of pure liquids[11]. The solvent did not react with the oxidant under the experimental conditions. The rate constants, k_{obs} decreased with decrease in dielectric constant of the medium. The plot of log k_{obs} vs. $1/\in_T$ was linear (r>0.9974, S<0.0139) with negative slope.

Effect of initially added products : Addition of the products, salicylic acid, copper sulphate and oxalic acid did not have any significant effect on the rate of the reaction.

Polymerization study : The reaction mixture was mixed with acrylonitrile monomer and kept for 2h in an inert atmosphere at 25°C. On diluting with methanol a white precipitate was formed, indicating the intervention of free radicals in the reaction. The blank experiments of either DPC or 4-hydroxy coumarin alone with acrylonitrile did not induce any polymerization under the same condition as those induced for the reaction mixture. Added acrylonitrile decreases the rate of reaction indicating free radical intervention, which is the case in earlier work[12].

Effect of temperature : The kinetics were studied at four different temperatures under varying concentration of 4-hydroxy coumarin, keeping other conditions constant. The rate constants were found to increase with increase in temperature. The rate constant k, of the slow step of Scheme 1 were obtained from the intercept of $1/k_{obs}$ vs. $1/[HDC]$ (r>0.9965, S≤0.0315) plot at four different temperatures and were used to calculate the activation parameters. The values of $k \times 10^3$ s⁻¹ were, 9.08±0.20, and 9.89±0.30, 10.91±0.40, 12.03±0.60 at 25, 30, 35, and 40°C, respectively. From the Arrhenius plot of log k vs. $1/T$ (r>0.9898, S≤0.0162) with least square analysis, the activation parameters, E_a, $\Delta H^{\#}$, $\Delta S^{\#}$ and $\Delta G^{\#}$ are calculated as 14.6±0.7 k J mol⁻¹, 12.1±0.6 kJmol⁻¹, -243 ± 15 JK⁻¹mol⁻¹ and 86±3 kJmol⁻¹ respectively.

The water soluble Cu(III) periodate complex is reported[13] to be $[Cu(HIO_6)_2(OH)_2]^{7-}$. However, in an aqueous alkaline medium and at a high pH range as employed in the study, periodate is unlikely to exist as HIO_6^{4-} (as present in the complex) as is evident from its involvement in the multiple equilibria[14] (2)-(4) depending on the pH of the solution.

$$H_5IO_6 \rightleftharpoons H_4IO_6^- + H^+ \qquad K_1 = 5.0 \times 10^{-4} \quad (2)$$

$$H_4IO_6^- \rightleftharpoons H_3IO_6^{2-} + H^+ \quad K_2 = 4.9 \times 10^{-9} \quad (3)$$

$$H_3IO_6^{2-} \rightleftharpoons H_2IO_6^{3-} + H^+ \quad K_3 = 2.5 \times 10^{-12} \quad (4)$$
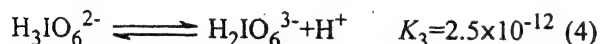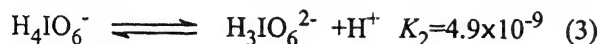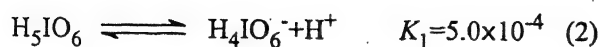
Periodic acid (H_5IO_6) exists in acid medium and also as $H_4IO^-_6$ at pH 7. Thus, under alkaline conditions, the main species are expected to be $H_3IO_6^{2-}$ and $H_2IO_6^{3-}$. At higher concentrations, periodate also tends to dimerise[15]. Hence, at the pH employed in this study, the soluble copper (III) periodate complex exists as diperiodatocuprate (III), $[Cu(H_3IO_6)_2 (OH)_2]^{3-}$ in aqueous alkaline medium, a conclusion also supported by earlier work[6].

The reaction between the diperiodatocuprate(III) complex and 4-hydroxy coumarin in alkaline medium has the stoichiometry 6:1 with a first order dependence on [DPC], apparent less than unit order in [alkali] and [4-hydroxy coumarin] and inverse fractional order in $[IO_4^-]$. In view of the negative less than unit order in periodate on rate of reaction, monoperiodate copper(III) complex is considered to be the active species of copper(III) complex. Here the 4-hydroxycoumarin reacts with alkali in a prior-equilibrium step to form an anionic form of (2z)-3-hydroxy-3-(2-hydroxy phenyl) acrylic acid which reacts with monoperiodatocuprate (III) (MPC) species to form a complex (C). Then, this complex(C) decomposes in a slow step to form an intermediate free radical species of (2z)-3-hydroxy-3-(2-hydroxy phenyl) acrylic acid. Polymerisation of added acrylonitrile also supports the intervention of free radicals in the reaction. This intermediate free radical species then reacts with another five more equivalent of MPC species in a fast step to yield the products. All the results indicate a mechanism as given in Scheme 1.

Scheme 1
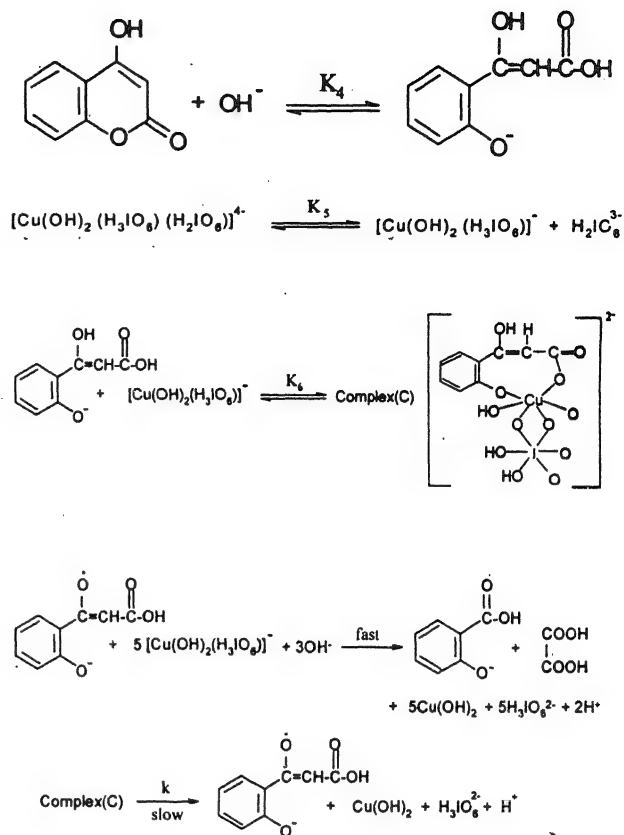
Spectral evidence for complex(C) formation between oxidant and substrate was obtained from spectra of oxidant and mixture of oxidant and substrate. A bathochromic shift, λ_{max}, of ca 6 nm from 308 to 314 nm was observed, together with hyperchromicity at λ_{max} 314 nm. Analogous effects upon complex formation between a substrate and an oxidant have been observed in other studies[16]. Furthermore, the formation of the complex is proved kinetically by the non zero intercept of the plot of $1/k_{obs}$ vs. 1/[HDC] (Michaelis-Menten) (r>0.9965, $S \leq 0.0315$) (Fig. 1). Since Scheme 1 is in accordance with the generally well accepted principle of non-complementary oxidations taking place in sequences of one-electron steps, the reaction between the substrate and oxidant afford a radical intermediate. A free radical scavenging experiment revealed such a possibility (vide infra). This type of radical intermediate has also been observed in earlier work[17].

Scheme 1 leads to the rate law as follows.

$$\text{rate} = -\frac{d[\text{DPC}]}{dt}$$

$$= \frac{kK_4K_5K_6[\text{HDC}][\text{DPC}][\text{OH}^-][\text{H}_2\text{IO}_6^{3-}]}{\left([\text{H}_2\text{IO}_6^{3-}]\right)\left([\text{H}_2\text{IO}_6^{3-}]+K_5+K_4K_5K_6[\text{HDC}][\text{OH}^-]\right)}$$

$$= \frac{kK_4K_5K_6[\text{HDC}][\text{DPC}][\text{OH}^-]}{[\text{H}_2\text{IO}_6^{3-}]+K_5+K_4K_5K_6[\text{HDC}][\text{OH}^-]} \quad (5)$$

$$\frac{\text{rate}}{[\text{DPC}]} = k_{\text{obs}}$$

$$= \frac{kK_4K_5K_6[\text{HDC}][\text{DPC}][\text{OH}^-]}{[\text{H}_2\text{IO}_6^{3-}]+K_5+K_4K_5K_6[\text{HDC}][\text{OH}^-]} \quad (6)$$

The rate law (6) may be verified by rearranging it in the form of equation (7)

$$\frac{1}{k_{\text{obs}}} = \frac{[\text{H}_2\text{IO}_6^{3-}]}{kK_4K_5K_6[\text{HDC}][\text{OH}^-]}$$

$$+ \frac{1}{kK_4K_6[\text{HDC}][\text{OH}^-]} + \frac{1}{k} \quad (7)$$
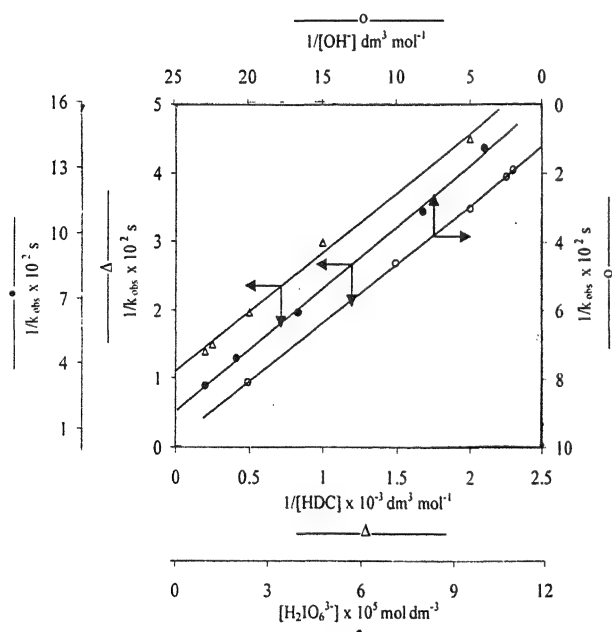
Fig. 1 − Verification of rate law (6); Plot of $1/k_{\text{obs}}$ vs. $1/[\text{HDC}]$, $1/k_{\text{obs}}$ vs. $[\text{H}_2\text{IO}_6^{3-}]$ and $1/k_{\text{obs}}$ vs. $1/[\text{OH}^-]$ (Conditions as in Table 1).

According to equation (7), other conditions being constant, the plots of $1/k_{\text{obs}}$ vs. $1/[\text{HDC}]$ ($r>0.9965$, $S\leq0.0315$), $1/k_{\text{obs}}$ vs. $1/[\text{OH}^-]$ ($r>0.8974$ $S\leq0.0194$) and $1/k_{\text{obs}}$ vs. $[\text{H}_2\text{IO}_6^{3-}]$ ($r>0.9982$, $S\leq0.0189$) should be linear (Fig. 1). From the slopes and intercepts, the values of $K_4 K_6$, K_5 and k could be derived as $(8.70\pm0.30)\times10^3$, $(5.31\pm0.20)\times10^{-6}$ mol dm^{-3} and $(9.08\pm0.10)\times10^{-3}$ s^{-1} respectively.

The increase in the rate with increasing ionic strength qualitatively explains the reaction between two negatively charged species of reactants (Scheme 1). The effect of solvent on reaction rate is described elsewhere[18]. The plot of log k_{obs} vs. $1/\varepsilon_T$ gives a straight line with negative slope for a negative ion, whereas positive slope results for a positive ion and a neutral molecule. In the present study, a plot of log k_{obs} vs. $1/\varepsilon_T$ ($r>0.9974$, $s<0.0139$) is linear with a negative slope which supports the involvement of negative ions as given in Scheme 1.

The values of $\Delta H^{\#}$ and $\Delta S^{\#}$ were both favourable for electron transfer processes. The more negative value of $\Delta S^{\#}$ indicates that the complex (C) is more ordered than the reactants[19].

Conclusions

Among various species of DPC in alkaline medium, monoperiodatocuprate (III)(MPC) is considered as active species for the title reaction. The result demonstrates that the role of pH in the reaction medium is crucial. Rate constant of slow step and other equilibrium constants involved in the mechanism are evaluated and activation parameters with respect to slow step of reaction were computed. The overall mechanistic sequence described here is consistent with product, mechanistic and kinetic studies.

References

1. Shan, J.H., Liu, B.S., Zhang, H.L. & Shan, S.G. (1999) *Hebeisheng Kexueyuan Xuebao* 16 : 6 (Ch.) (CA: 132, 69865x); Niu, W., Zhu, Y., Hu, K., Tong, C. & Yang, H. (1996) *Int. J. Chem. Kinet.* 28 : 899.

2. Rozovoskii, G.I., Misyavichyus, A.K. & Prokopchik, A.Yu. (1975) *Kinetikai kataliz* 16(2) : 402; Eng Translation (1975) *Kinetics and Catalysis* 16 : 337

3. Beck, G. (1951) *Mikrochim* Acta. 38 : 1 (*Chem. Abst.* 1951, 45 : 6539d); Kovatas, Z. (1960) *Acta Chim. Hung.* 22, 373.

4. Movius, W.G. (1973) *Inorg. Chem.* **12** : 31.

5. Ram Reddy, M.G., Sethuram, B. & Navaneeth Rao, T. (1978) *Indian J. Chem.* **16A** : 31.

6. Bal Reddy, K., Sethuram, B. & Navaneeth Rao, T. (1981) *Indian J. Chem.* **20A** : 395; Padmavati, J. & Yusiff, K. (2001) *Transition Met. Chem.* **6** : 315; Bal Reddy, K., Sethuram, B. & Navaneeth Rao, T. (1984) *Indian J. Chem.* **23A** : 593.

7. Jaiswal, P.K. & Yadava, K.L. (1973) *Indian J. Chem.* **11** : 837; Murthy, C.P., Bal Reddy, K., Sethuram, B. & Navaneeth Rao, T. (1981) *Z. Phys. Chem.* **262** : 336

8. Panigrahi, G.P. & Misro, P.K. (1978) *Indian J. Chem.* **16A** : 201.

9. Feigl, F. (1975) *Spot Tests in Organic Analysis*, Elsevier Publishing Company, Amsterdam, p. 106.

10. Svehla, G. (1998) A.I. Vogel's *Qualitative Inorganic Analysis*, 7th edn, Longman Ltd., London, p. 85.

11. Lide, D.R. (1993) *CRC Hand Book of Chemistry and Physics*, 73rd edn, CRC Press, London, p. 8-51.

12. Kolthoff, I.M., Meehan, E.J. & Carr, E.M. (1953) *J. Am. Chem. Soc.* **75**: 1439; Frost, A.A. & Pearson, R.G. (1970) *Kinetics and Mechanism*, Wiley Eastern Private Ltd. New Delhi, p. 367.

13. Bal Reddy, K., Sethuram, B. & Navaneeth Rao, T. (1987) *Z. Phys. Chem.* **268** : 706.

14. Bailar, J.C., Emeleus, H. J., Sir Donald Nyholm. & Trotman-Dikenson, A.F. (1975) *Comprehensive Inorganic Chemistry*, Vol. 2, Edited by Pergamon Press, Oxford, p.1456.

15. Sethuram, B. (2003) *Some Aspects of Electron Transfer Reactions Involving Organic Molecules*, Allied Publishers (P) Ltd., New Delhi, p. 77.

16. Devi, J., Kotahari, S. & Banerje, K.K. (1995) *Indian J. Chem.* **34A** : 16; Halligudi, N.N., Desai, S.M., Mavalangi, S.K. & Nandibewoor, S.T. (2000) *Mona. Fur. Chem.* **131** : 321.

17. Halligudi, N.N., Desai, S.M. & Nandibewoor, S.T. (1999) *Int. J. Chem. Kinet.* **31** : 789; Jaky, M., Szeverenyi, Z. & Simindi, L.I. (1991) *Inorg. Chem.* Acta. **186** : 33; Lott, K.A.K. & Symons, M.C.R. (1960) *Discuss Faraday Soc.* **29** : 205.

18. Amis, E.S. (1966) *Solvent Effects on Reaction Rates and Mechanism*, Academic Press, New York, p.183.

19. Lewis, E.S. (1974) *Investigation of Rates and Mechanism of Reactions in Techniques of Chemistry*, Wiley (Eds), Interscience Publication, New York, p. 421.

Studies on the radical polymerization of methylacrylate initiated by stibonium ylide

SUMITA SRIVASTAVA and A.K. SRIVASTAVA*

Department of Chemistry, H.B. Technological Institute, Kanpur-208 002, India.

e:mail-akspolym@rediffmail.com

Abstract

1,2,3,4-tetraphenylcyclopentadiene triphenylstibonium ylide initiates radical polymerization of methylacrylate (MA) upto 31% conversion without gelation due to autoacceleration. The reaction has been carried out at $70 \pm 0.2°C$ for 60 min. under nitrogen atmosphere. The values of the initiator and the monomer exponent were computed as 0.5 ± 0.01 and 1.5 ± 0.04, respectively. The overall activation energy and the value of k_p^2/k_t have been calculated as 25 ± 0.08 kJ/mol and $8.8 \times 10^{-2} \pm 0.03$ $1\ mol^{-1}s^{-1}$, respectively. The ylide dissociates to generate phenyl radical which initiates the radical polymerization of MA. The DSC technique shows glass transition temperature (T_g) of polymer as 40°C. The NMR spectrum shows a triplet at 1.9-2.1δ which is a characteristic of a syndiotactic PMA.

(**Keywords :** polymerization/kinetics/mechanism/methylacrylate/ylide).

Introduction

Despite the large amount of data available for polymerization of vinyl monomers, limited quantitative kinetic information is available on the homopolymerization of methylacrylate (MA)[1-7]. It is well known[8-11] that bulk polymerization of MA shows a large auto-acceleration of the overall rate of polymerization, referred to as Trommosdorff, or gel effect (G-E). Mahadevan and Santhappa[12] reported a maximum conversion of 10% with BPO. Recently, nitrogen[13-15] and sulphur[16] ylides ($>\overset{\ominus}{C}-\overset{\oplus}{X}$ where X = N, P, As, Sb, Bi, S, Te) have been used as· radical initiator to obtain 19.5%, 14.8%, 33%, 23% conversion respectively, without gelation, which fascinated us to investigate stibonium ylide as noval initiator for the synthesis and characterization of polymethylacrylate with a view to solve the problem of autoacceleration by obtaining high % conversion (31%) without gelation.

Materials and Method

Methylacrylate (Merck) and other solvents were purified according to procedure reported in literature[17,18]. 1,2,3,4-tetraphenylcyclopentadiene (Aldrich : 0.8721 ky), p-toluene sulphonyl hydrazide (Fluka : AG-210899), triphenyl antimony (Merck-Schuchardt Art. 821199), Cu catalyst (Merck) were used. The stibonium ylide was prepared by the following method of Glidewell and Lloyd[19].

Synthesis of triphenyl stibonium ylide

$$(2.19 \times 10^{-4} \text{ moles})$$
1,2,3,4-tetraphenyl-
cyclopentadiene
Aldrich (0.8721ky)

$$(7.46 \times 10^{-4} \text{ moles})$$
p-toluene
sulphonylhydrazide
Fluka (AG-210899)

diethyl amine solvent
10 days at 0°C

diazo compound (yellow crystals)

$(C_6H_5)_3$ Sb
triphenyl antimony,
Cu(II) bishexafluoro-
acetyl acetanato catalyst
refluxed for 2 hours in
benzene.

1,2,3,4-tetraphenylcyclopentadiene triphenyl
stibonium ylide
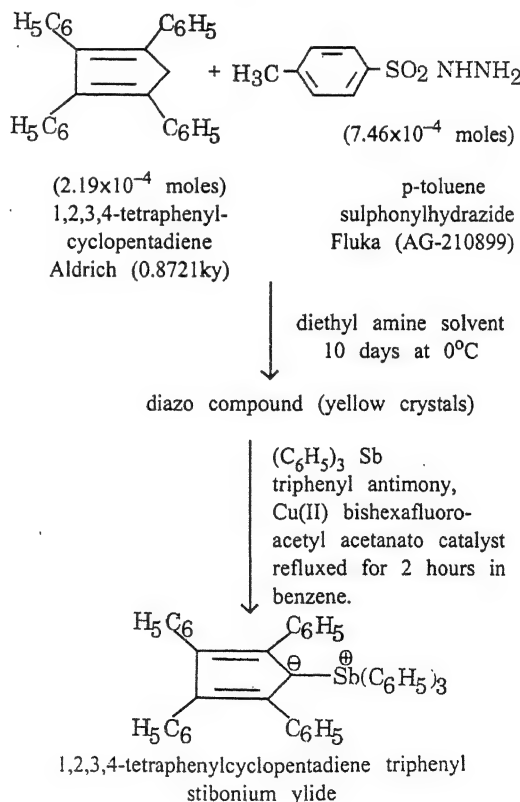
The solution polymerization runs were performed for 60 min. at $70 \pm 0.2°C$ under nitrogen atmosphere. The polymer(s), precipitated with acidified methanol, were dried to constant weight. The rate of polymerization (R_p) was calucalated from the slope(s) of the linear plot of percent conversion vs. the time plots.

The intrinsic viscosity (η) of the polymer(s), determined in benzene at $25 \pm 0.1°C$ using an Ubbelohde viscometer, were used to calculate average degree of polymerization $\left(\overline{P}_n\right)$ using the equation[20].

$$\overline{P}_n = 11.2 \left([\eta] \times 100\right)^{1.22}$$

Characterization :

The FTIR and ^{1}H-NMR spectra were recorded with the help of Perkin-Elmer 599B and varian 100 HA spectrometer respectively using $CDCl_3$ as solvent and tetramethyl silane as internal reference. The elemental analysis of the polymers were carried out in Perkin Elmer 240 'C' element analyzer The TGA runs were carried out using a V5.1A Dupont 2100 analyzer, sample weight ~10mg. The measurements were carried out at a heating rate of 20°C per min. The DSC runs were carried out using VA.0B Dupont 2100 analyzer, sample weight 5.3 mg, at a heating rate of 10°C/min.

Results and Discussion

The ylide initiates the polymerization of MA without gelation upto 31% conversion and the resulting polymers have a high average degree of polymerization (165.4).

The results of kinetic investigations of the polymerization of methylacrylate at $70 \pm 0.2°C$, initiated by stibonium ylide in 1,4-dioxan for 60 min. are summarized in Tables (1-2) and Fig. (1-6).

1. *Effect of the initiator concentration* : The effect of [ylide] on the rate of polymerization has been studied by varying its concentration from 3.08 to 27.68×10^{-6} mol l^{-1} for fixed monomer concentration (1.233 mol l^{-1}). The Rate of

Table 1 – Effect of [ylide] on the rate of polymerization (R_p) of methylacrylate initiated by 1,2,3,4-tetraphenyl cyclopentadiene triphenyl stibonium ylide.

Sample No.	$[Ylide] \times 10^6$ (mol l^{-1})	$R_p \times 10^6$ (mol $l^{-1}s^{-1}$)	$\overline{P}_n$
1	3.08	2.80	434.7
2	9.23	5.87	234.9
3	15.38	6.42	199.5
4	21.53	7.70	165.4
5	27.68	10.27	132.4

[MA] = 1.233 mol l^{-1}, Polymerization temp. = $70 \pm 0.2°C$, Polymerization time = 60 min.

Table 2 –Effect of [MA] on the rate of polymerization (R_p) of methylacrylate initiated by 1,2,3,4-tetraphenyl cyclopentadiene triphenyl stibonium ylide.

Sample No.	[MA] (mol l^{-1})	% conversion	$R_p \times 10^6$ (mol $l^{-1}s^{-1}$)
6	0.246	6.5	0.47
7	0.493	11.5	1.64
8	0.703	16.5	3.41
9	1.233	19	6.42
10	1.727	31	14.39

[Ylide] = 15.38×10^{-6} mol l^{-1}, Polymerization temp. = $70 \pm 0.2°C$, Polymerization time = 60 min.

polymerization (R_p) increases as the ylide concentration is increased (Fig. 1 and Table 1). The initiator exponent calculated from the slope of the linear plot of log R_p vs. log [ylide], is 0.5 ± 0.01 (Fig. 2).

The value of $\overline{P}_n$ of various polymers decreases as [ylide] increases. The value of k_p^2/k_t was determined from the slope of a linear plot of $1/\overline{P}_n$ vs. $R_p/[M]^2$ is $8.8 \times 10^{-2} \pm 0.03$ l $mol^{-1}s^{-1}$ (Fig. 3) which is in accordance with the literature[15] value.
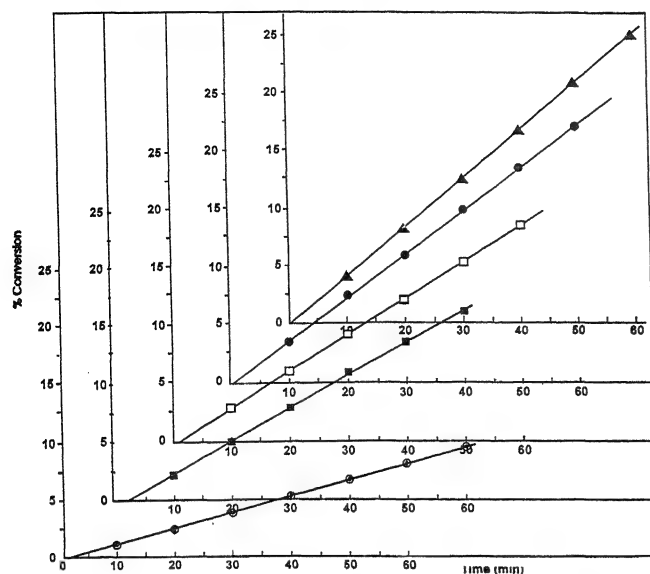
Fig. 1 – Percentage conversion vs. time plots for homopoly-
merization of methylacrylate [MA].

[Ylide] = 3.08 to 27.68x10^{-6} mol l^{-1}
[MA]   = 1.233 mol l^{-1}
Temp.   = 70 ± 0.2°C
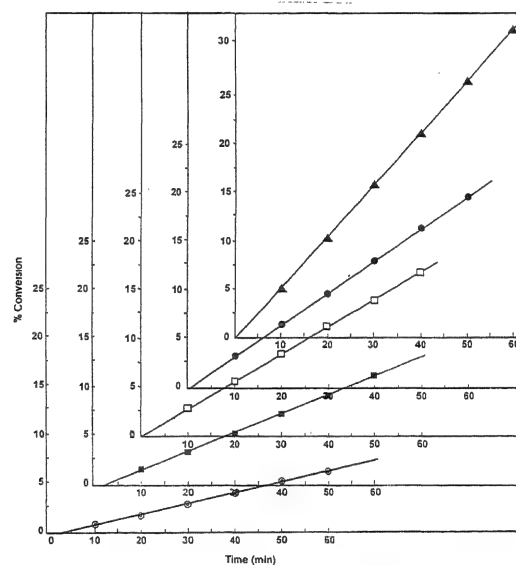Solvent = Dioxan
Time   = 60 min.
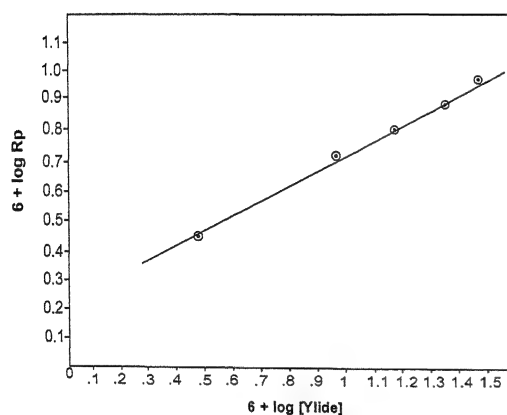
Fig. 2 – Relationship between log R_p and log [ylide] and log R_p
for the homopolymerization of methylacrylate [MA].

[Ylide] = 3.08 to 27.68x10^{-6} mol l^{-1}
[MA]   = 1.233 mol l^{-1}
Temp.   = 70 ± 0.2°C
Solvent = Dioxan
Time   = 60 min.

2. *Effect of the monomer concentration* : The
effect of [MA] on the R_p was studied by varying
the [MA] from 0.246 to 1.727 mol l^{-1} for fixed
[ylide] as 15.38x10^{-6} mol l^{-1} as shown in Table 2
and Fig. 4. The monomer exponent value, calculated
from the slope of a linear plot of log R_p vs. log [MA],
is 1.5 ± 0.04 (Fig. 5).
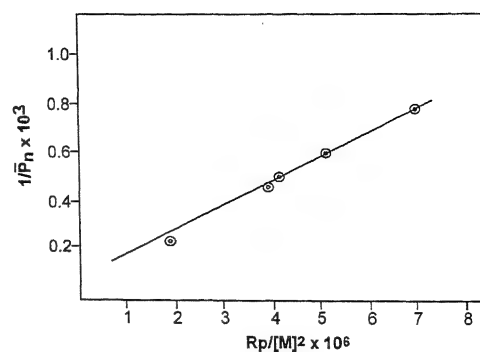
Fig. 3 – Relationship between $1/P_n$ and $R_p/[M]^2$ for the
homopoly-merization of methylacrylate [MA].

[Ylide] = 3.08 to 27.68x10^{-6} mol l^{-1}
[MA]   = 1.233 mol l^{-1}
Temp.   = 70 ± 0.2°C
Solvent = Dioxan
Time   = 60 min.

Fig. 4 – Percentage conversion vs. time plots for homopoly-
merization of methylacrylate [MA].

[Ylide] = 15.38x10^{-6} mol l^{-1}
[MA]   = 0.246 to 1.727 mol l^{-1}
Temp.   = 70 ± 0.2°C
Solvent = Dioxan
Time   = 60 min.

3. *Effect of temperature* : The rate of polymeri-
zation was also measured at four different temperatures
at a fixed monomer concentration (1.233 mol l^{-1})
and initiator concentration (15.38x10^{-6} mol l^{-1}). It
increases with the temperature and the overall
activation energy (ΔE), calculated from the
corresponding slope of the Arrhenius plot of log R_p

vs. 1/*T* (using LSM), is 25 ± 0.08 kJ/mol. (Fig. 6), which is in accordance with the values given in the literature[3] for α-picolinium-p-chloro-phenacylide.
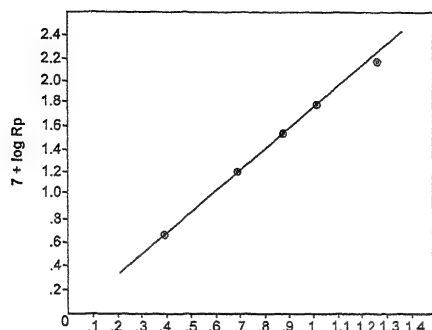
Fig. 5   Relationship between log [MA] and log R_p homopoly-merization of methylacrylate [MA].

[Ylide]   = 15.38×10^{-6} mol l^{-1}
[MA]   =   0.246 to 1.727 mol l^{-1}
Temp.   = $70 \pm 0.2°C$
Solvent   =   Dioxan
Time   =   60 min.
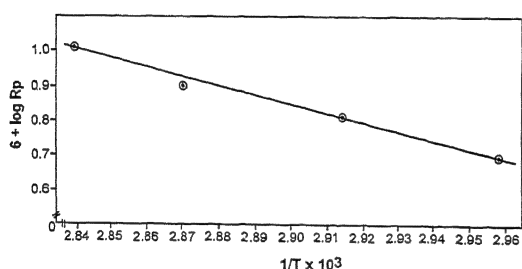
Fig. 6 - Plot of log *Rp* *vs.* polymerization temperature (Arrhenius plot).

[Ylide]   = 15.38×10^{-6} moll^{-1}
[MA]   =   1.233 mol l^{-1}
Temp.   =   60, 70, 75, $80 \pm 0.2°C$
Solvent   =   Dioxan
Time   =   60 min.

Spectral Analysis :

(1) *Fourier Transform Infrared Spectroscopy :* The FTIR spectrum of the (PMA) (Fig. 7) shows the following bands at : 2956 cm^{-1} (C-H st.), 739-896 cm^{-1} (ben.), 1378-1444 cm^{-1} (C-H ben. for CH_2 and CH_3 group) and 1736 cm^{-1} due to acrylate group of the polymer.
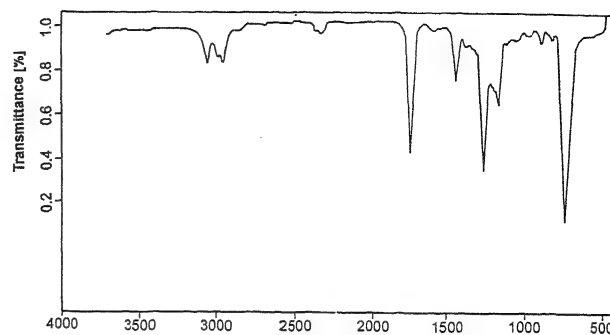
Fig. 7 – FTIR spectrum of poly methylacrylate (Sample 3).
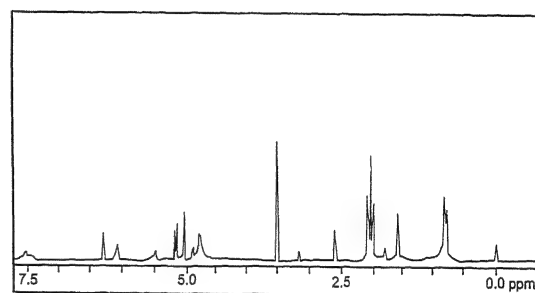
Fig. 8 – ^{1}H-NMR spectrum of poly methylacrylate (Sample 3).
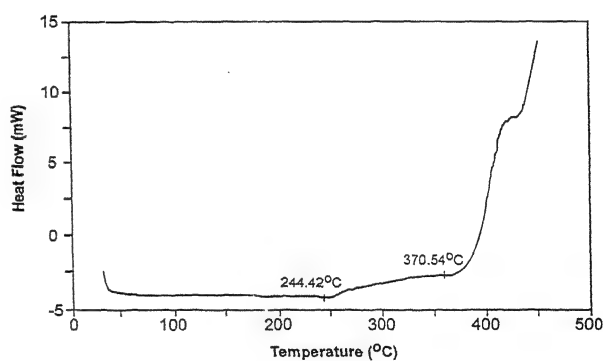
Fig. 9 – DSC curve of poly methylacrylate (Sample 3).
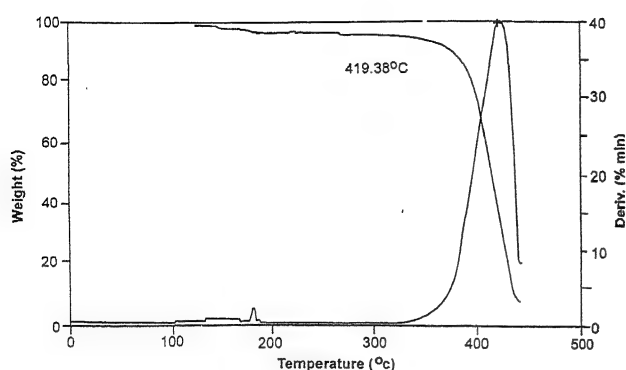
Fig. 10 – TGA curve of poly methylacrylate (Sample 3).

(2) *¹H-Nuclear Magnetic Resonance Spectroscopy* : The ¹H-NMR spectrum (Fig. 8) of the polymer shows a triplet at 1.9-2.1δ due to CH_2 protons, thereby, indicating syndiotactic[21] nature of the polymer. The methoxy protons appear as triplet at 3.5δ.

Elemental Analysis :

The polymer does not give any black precipitate or brown stain on spot analysis[22] which shows that antimony is not incorporated in the polymer.

Found : C = 55%, H = 6.38, O = 38.62%

Calculated : C = 55.81%, H = 6.9%, O = 37.22%

The above data further confirms that antimony has not been incorporated in the polymer.

Thermal Analysis :

(1) *Differential Scanning Calorimetry* : The T_g value of PMA determined from DSC (Fig. 9) is 40°C where as the literature[23] value is 10°C. The high T_g value of polymer may be attributed to syndiotactic nature of PMA because the T_g changes with tacticity[24], molecular weight[25], polarity in the main chain[26]. The temperature for maximum rate of crystallization T_{max} is calculated by following equation[27].

$$T_{max} = T_g + (2/3)(T_m - T_g)$$

T_{max} for PMA is 260.36°C

(2) *Thermogravimetric Analysis* : The TGA curve (Fig. 10) for PMA exhibits weight-loss with

temperature[28-29]. The thermal behaviour data are as follows :

1. Weight loss at different stages of temperature are as follows :

(i) 100-200°C = 3%

(ii) 250-400°C = 30%

2. The voltalization temperature is 419.38°C.

Mechanism

1,2,3,4-tetraphenylcyclopentadiene triphenyl stibonium ylide undergoes bond fission[30] between the heteroatom and the phenyl group to yield phenyl free radical, which is responsible for the initiation of the polymerization reaction. he mechanism is as follows.

Initiation :
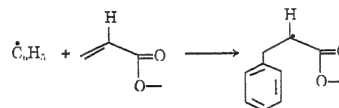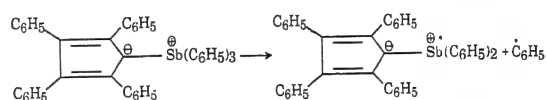
Propagation and termination :
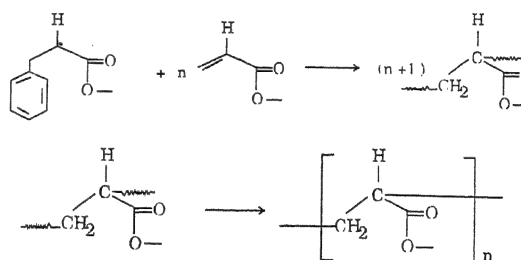
Conclusion

On the basis of above evidences it may be concluded that 1,2,3,4-tetraphenylcyclopentadiene

triphenyl stibonium ylide initiates polymerization of methylacrylate without gelation upto high % conversion of 31%.

Acknowledgements

References

1. Czajlik, I., FOldes-Berezsnich, T., Tudos, F. & Vertes, E. (1981) *Eur. Polym. J.* **17** : 131.

2. Kaszas, G., FOldes-Berezsnich, T. & Tudos, F. (1983) *Eur. Polym. J.* **19** : 469.

3. Buback, M., Kurz, C.H. & Schmaltz, C. (1998) *Macromol. Chem. Phys.* **199** : 1721.

4. Perrier, S., Barner-Kowollik, C., Quinn, J.F., Vana, P. & Davis, T.P. (2002) *Macromolecules,* **35** : 8300.

5. Bagdasarayan, K.S. (1948) *J. Phys. Chem. Moskow* **22** : 1181.

6. Rizzardo, E. & Solomon, D.H. (1979) *Polym. Bull. (Berlin)* **1(8)** : 529.

7. Rubio, S., Serre, B., Sledz, J., Schue, F. & Chapelet-Letourneux, G. (1981) *Polymer* **22(4)** : 519.

8. Allen, P.W., Merrett, F.M. & Scanlan, J. (1984) *Trans. Faraday Soc.* **50** : 756.

9. Ferington, T. & Tobolsky, A.V. (1958) *J. Am. Chem. Soc.* **80** : 2315.

10. Harward, R.N. & Simpson, W. (1951) *Trans. Faraday Soc.* **47** : 212.

11. Trommsdorff, E., Kohle, H. & Lagally, R. (1948) *Macromol. Chem.* **1** : 169.

12. Mahadevan, V. & Santhappa, M. (1955) *Macromol. Chem.* **16** : 119.

13. Shukla, A.K., Saini, S., Kumar, P. & Srivastava, A.K. (1985) *Ind. J. Chem.* **A24** : 1054.

14. Saini, S., Shukla, A.K., Kumar, P. & Srivastava, A.K. (1986) *J. Macromol. Sci. Chem.* **A23(9)** : 1107.

15. Srivastava, A.K., Saini, S., Nigam, S.K. & Rai, J.S.P. (1987) *Eur. Polym. J.* **23(11)** : 931.

16. Vasishtha, R. & Srivastava, A.K. (1997) *Ind. J. Chem. Tech.* **4** : 13.

17. Overberger, C.G. & Yamamoto, N.J. (1966) *J. Polym. Sci.* **4** : 3101.

18. Vogel, A.I. (1994) *"A Text Book of Practical Organic Chemistry",* 5th Edn., Longman, London, p. 395.

19. Glidewell, C. & Lloyd, D. (1988) *Synthesis,* p. 319.

20. Furman, N. & Mesrobian, R.B. (1954) *J. Am. Chem. Soc.* **76** : 3281.

21. Slonim, I. Ya & Lyubimov, A.N. (1970) *"The NMR of Polymers",* Plenum Press, New York, p. 208-210.

22. Fiegel & Anger (1972) *"Spot Test in Inorganic Analysis",* 6th Ed. Elsevier, Amsterdam, London, New York, p. 134.

23. Slade, P.E. & Jenkins, L.T. (1970) *"Thermal characterization techniques",* Marcel Dekker, Inc. New York, **2** : 178.

24. Ibid, p. 182.

25. Ibid, p. 181.

26. Ibid, p. 175.

27. Mark, J.E., Allcock, H.R. & West, R. (1992) *"Inorganic Polymers",* Prentice-Hall International, Inc., New Jersey, p. 46.

28. Gronowski, A. & Wojtczak, Z. (1985) *Macromol. Chem.* **140** : 206.

29. Wojtczak, Z. & Gronowski, A. (1985) *Macromol. Chem.* **186** : 139.

30. Bovey, F.A. & Kolthoff, I.M. (1948) *Chem. Rev.* **42** : 491.

Synthesis and characterisation of metal complexes of Cu(II), Ni(II) and Co(II) with some new macrocyclic compounds

R.C. SHARMA*, DEVENDRA KUMAR and PANKAJ MITTAL

Department of Chemistry, Institute of Basic Sciences, Dr. B.R. Ambedkar University, Khandari Road, Agra-282 002, India.

Abstract

Some new macrocyclic complexes of Cu(II), Ni(II) and Co(II) with {(5,6,11,12 - Bzo$_2$ - 1- pyridonyl - [15] - 1,3,5,11,13 - pentaene - 1,3,14 - N$_3$ - 7,10 - O$_2$)} ([15] pentaene, N$_3$O$_2$), {5,6,12,13 - Bzo$_2$ - 1 - pyridonyl - [16] - 1,3,5,12,14 - pentaene - 1,3,15 - N$_3$ - 7,11 - O$_2$)} ([16] pentaene, N$_3$O$_2$) and {(5,6,13,14 - Bzo$_2$ - 1 - pyridonyl - [17] - 1,3,5, 13,15 - pentaene - 1,3,16 - N$_3$ - 7,12 - O$_2$)} ([17] pentaene, N$_3$O$_2$) have been synthesized by the template synthesis. All the synthesized compounds have been characterized by their elemental analyses, I.R., ^{1}H N.M.R. spectral, molar conductance and magnetic susceptibility studies.

(Keywords : metal complexes/macrocyclic/template/I.R./ N.M.R.)

Introduction

The macrocyclic compounds are well known for their biocidal activities[1-5]. In continuation[6-8] of our previous work, we have synthesized some more new macrocyclic complexes to get a better understanding in this field. The present work deals with the synthesis and characterization of three dioxodibenzaldehydes (2,2' - ethylene dioxodibenzaldehyde, 2,2' - propylene dioxodibenzaldehyde and 2,2' - butylene dioxodibenzaldehyde) and their Cu(II), Ni(II) and Co(II) macrocyclic complexes of the schiff bases obtained by condensing them with 2,6 - diamino pyridine in dry methanol on refluxation.

Materials and Method

1. *Synthesis of dioxodibenzaldehydes* : 15 ml ethanolic solution of salicylaldehyde (0.02 M) with an aqueous solution of sodium bicarbonate (0.02 M) was refluxed for an hour under the atmosphere of nitrogen and cooled at room temperature. 10 ml ethanolic solution of 1,2 -dibromoethane / 1,3 – dibromo propane / 1,4 – dibromobutane (0.01 M)

was then added slowly with constant stirring. The contents were again refluxed for about 3 to 4 h over a water bath using water condenser. The obtained solution was concentrated to half of its original volume on water bath. On cooling this concentrated solution in refrigerator over night, creamish white/ dirty white / white crystalline product was obtained. It was filtered, washed with little water, alcohol followed by ether and recrystallized from ethanol. It was dried under reduced pressure in a desiccator over anhydrous CaCl$_2$.

2. *Synthesis of macrocyclic complexes* : The macrocyclic complexes were synthesized by template reaction taking 15 ml methanolic solution of (0.001 M) copper acetate (H$_2$O) / nickel acetate (4H$_2$O)/ cobalt acetate (4H$_2$O) with 15 ml warm methanolic solution of 2,6 - diamino pyridine (0.001 M) [heated for about 20 min.] and 20 ml methanolic solution of the synthesized 2,2' - ethylene dioxodibenzaldehyde (EDODB)/2,2' - propylene dioxodibenzaldehyde (PDODB)/2,2' - butylene dioxodibenzaldehyde (BDODB). The contents were refluxed for about 3 to 5 h. The resulting solid product was cooled at room temperature, filtered, washed with ethanol followed by ether and recrystallized from DMF. It was dried under reduced pressure in a desiccator over anhydrous CaCl$_2$.

Physical and analytical measurements : The purity of all the synthesized compounds was checked by running their TLC for single spot on silica gel-G plate and by their repeated melting point determination of the recrystallised samples in open capillary tube and thus uncorrected.

Carbon, hydrogen and nitrogen analyses were carried out in the Microanalytical Laboratory,

Edinburgh University, U.K. Cu(II), Ni(II) and Co(II) metals were estimated by decomposing the complexes with 1:1 mixture of conc. HNO_3 and conc. H_2SO_4 and then precipitating them as their pyridine complex[9]. I.R. spectra were recorded on JASCO Spectro - photometer – 0087 in KBr pellets. NMR spectra were recorded on NMR spectrometer (DMSO-d_6) on a varion instrument (270 Hz) using TMS as an internal standard. The molar conductance was determined by using Systronics conductivity meter 306. The magnetic susceptibility was measured by Gouy's method at room temperature.

Results and Discussion

The physical and analytical data of dioxodibenzaldehydes and their M(II) macrocyclic complexes are given Table 1. All the complexes were found coloured and stable at room temperature. In the IR spectra of dioxodibenzaldehydes, the weak bands in the region of 2990-2975 cm^{-1} indicate vC-H of – CH_2 group[10]. The medium bands in the region of 1940-1930 cm^{-1} indicate vC-H of aromatic ring[11]. The sharp bands around 1260 cm^{-1} were observed due to C-O stretching vibrations. The bands observed

Table 1 – Physical and analytical data of dioxodibenzaldehydes and their M (II) macrocyclic complexes.

S.No.	Compound	Molecular formula	Colour	M.P./D.P. (°C)± 1°C	% Analysis Found/ (Calculated)			
					C	H	N	M
1.	EDODB	$C_{16}H_{14}O_4$	Creamish white	114	73.00 (71.11)	5.31 (5.18)	–	–
2.	PDODB	$C_{17}H_{16}O_4$	Dirty white	90	72.69 (71.83)	5.54 (5.63)	–	–
3.	BDODB	$C_{18}H_{18}O_4$	White	80	73.00 (72.48)	5.88 (6.04)	–	–
4.	Cu(II) {[15] pentaene, N_3O_2Ac}Ac	Cu(II)[{$C_{21}H_{17}$ N_3O_2}Ac]Ac	Brown	320	58.10 (57.20)	4.95 (4.39)	7.80 (8.01)	11.95 (12.11)
5.	Cu(II) {[16] pentaene, N_3O_2Ac}Ac	Cu(II)[{$C_{22}H_{19}$ N_3O_2}Ac]Ac	Black	360	58.40 (57.94)	5.20 (4.64)	7.55 (7.80)	11.60 (11.79)
6.	Cu(II) {[17] pentaene, N_3O_2Ac}Ac	Cu(II)[{$C_{23}H_{21}$ N_3O_2}Ac]Ac	Brownish black	350	59.50 (58.64)	5.35 (4.89)	7.42 (7.60)	11.32 (11.49)
7.	Ni(II) {[15] pentaene, N_3O_2Ac}Ac	Ni(II)[{$C_{21}H_{17}$ N_3O_2}Ac]Ac	Green	250	58.70 (57.73)	5.25 (4.43)	7.90 (8.08)	11.15 (11.29)
8.	Ni(II) {[16] pentaene, N_3O_2Ac}Ac	Ni(II)[{$C_{22}H_{19}$ N_3O_2}Ac]Ac	Green	270	59.70 (58.46)	5.55 (4.68)	7.50 (7.87)	10.80 (10.99)
9.	Ni(II) {[17] pentaene, N_3O_2Ac}Ac	Ni(II)[{$C_{23}H_{21}$ N_3O_2}Ac]Ac	Light green	310	60.25 (59.37)	5.31 (4.95)	7.52 (7.70)	10.65 (10.76)
10.	Co(II) {[15] pentaene, N_3O_2Ac}Ac	Co(II)[{$C_{21}H_{17}$ N_3O_2}Ac]Ac	Yellowish green	286	58.50 (57.70)	5.28 (4.42)	7.85 (8.08)	11.21 (11.33)
11.	Co(II) {[16] pentaene, N_3O_2Ac}Ac	Co(II)[{$C_{22}H_{19}$ N_3O_2}Ac]Ac	Green	300	59.60 (58.44)	5.35 (4.68)	7.65 (7.87)	10.90 (11.03)
12.	Co(II) {[17] pentaene, N_3O_2Ac}Ac	Co(II)[{$C_{23}H_{21}$ N_3O_2}Ac]Ac	Dark green	315	60.72 (59.35)	5.60 (4.95)	7.45 (7.70)	10.60 (10.79)

in the region 1200-1060 cm^{-1} and 800-600 cm^{-1} may be assigned to C-H deform vibrations in plane and out of plane[12] respectively.

A comparative study of the IR spectra of the ligands and their metal complexes reveals that a sharp and strong band observed in the region of 1680 - 1660 cm^{-1} in dioxodibenzaldehydes was due to the presence of carbonyl stretching vibrations[13], the band of carbonyl group was absent in the IR spectra of macrocyclic complexes which shows the reaction of carbonyl group with primary amino groups of pyridinediamine resulting in the formation of azomethine (- C = N) group[14], which is further confirmed by a strong band observed around 1595 cm^{-1} due to –C=N bond[15]. Besides the above, the resulting complexes have exhibited some prominent bands around 2990 cm^{-1} due to νCH_2 group and around 1290 cm^{-1} due to $-O-(CH_2)_n$ group[16]. Few bands of medium intensity were observed in the region of 1940–1910 cm^{-1} due to aromatic C–H stretching vibrations. Some absorption bands observed in the region 1200–1060 cm^{-1} and 800–600 cm^{-1} may be assigned to C–H deform vibrations in plane and out of plane respectively. I.R. spectra of all the macrocyclic complexes exhibit two bands in the region 1700-1680 cm^{-1} and 1390-1370 cm^{-1} due to asymmetric and symmetric vibrations of COO$^-$ group of acetate ion suggesting coordinated acetate ion in the coordination sphere[17]. New intense peaks around 555–530 cm^{-1} and 460–440 cm^{-1} in the IR spectra of macrocyclic complexes indicate the formation of M-O and M–N bonds respectively[18,19], which have developed on complexation.

The ^1H NMR spectra of the dioxodibenzaldehydes obtained in DMSO d_6 solution with TMS as an internal standard show the signals δ9.1-9.4 (s, 2H, - CHO), 7.6 - 8.7 (m, 8H, Ar - H) and 2.4-2.9 (m, 2H, - CH$_2$) ppm.

The proton NMR spectra of the complexes obtained in DMSO d_6 solution with TMS as an internal standard show the signals δ8.4-8.8 (s, 2H, -N = CH$^-$), 7.8 - 8.8 (m, 8H, Ar - H), 7.62 - 7.70 (m, 3 H, pyridyl - H), 2.4-2.9 (m, 2 H, CH$_2$ methylene) and 2.6 -2.7 (m, 6H, CH$_3$COO$^-$) ppm.

The molar conductance of 10^{-3} M solution of the macrocyclic complexes in DMF (205-230 ohm^{-1} cm^{-1}mol^{-1}) indicate their electrolytic[20] nature. The

magnetic susceptibilities of the macrocyclic complexes of Cu (II) (1.72-1.79 BM), Ni (II) (2.88-2.98 BM) and Co (II) (3.82-3.94 BM) suggest their octahedral geometry and paramagnetic nature.

On the basis of IR, ^1H NMR, molar conductance, magnetic susceptibility and analytical data, it seems reasonable to assume that the M(II) complexes have the following structures :
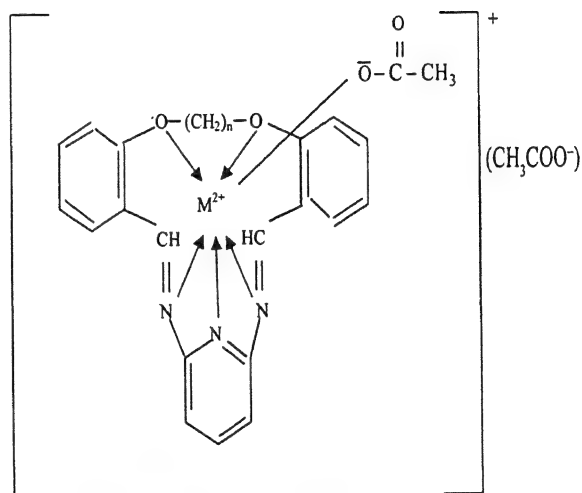
where {n = 2,3 and 4} {M (II) = Cu (II), Ni (II) and Co (II)}
Probable structure of macrocyclic complexes.

References

1. Boucher, L. J. & Coe, C.G. (1975) *Inorg. Chem.* **14** : 1289.

2. Gould, R.F. (1971) *Bio - Inorganic Chemistry,* A.C.S. Manograph N. 200, Am. Chem. Soc., Washington D.C.

3. Skycs, A.G. & Well, J.A. (1970) *Prog. Inorg. Chem.* **13** : 1.

4. Halfpenny, J. & Sloman, Z.S. (2000) *J.Chem. Soc. Perkin Trans.* **1** : 1877.

5. Dong, W., Yang, R. & Yam L. (2001) *Indian J. Chem.* **40A** : 202.

6. Sharma, R.C. & Ambwani, Jitendra (1995) *J. Indian Chem. Soc.* **72** : 507.

7. Sharma, R.C., Khar, V.K. & Sharma, R.S. (1996) *J. Inst. of Chem. (India)* **68 IV** : 109.

8. Sharma, R.C. & Khar, V.K. (1998) *Asian Jour. of Chem.* **10 (3)** : 467.

9. Vogel, A. I. (1968) *A Text Book of Quantitative Inorganic Analysis,* 3rd Ed. Longman's, London.

10. Boobyer, (1967) *Spectrochim. Acta* **23A** : 321.

11. Fox & Martin (1940) *Proc. Roy. Soc.* **175A** : 208.

12. Bellamy, L.J. (1958) *The I.R. Spectra of Complex Molecules*, IInd Ed. John Wiley and Sons, Inc. N.Y.

13. Mathis, F. (1953) *Bull. Soc. Chem.* **9D** : 22.

14. Clougherty, Sousa & Wyman (1957) *J. Org. Chem.* **22** : 462.

15. Welsh W.A., Reynold G.T. & Henry, P.M. (1977) *Inorg. Chem.* **16** : 2558.

16. Armstrong, L.G., Lindoy, L.F. & Tasker, P.A. (1977) *Inorg. Chem.* **16** : 1665.

17. Straughan, B.P., Moore, W. & Mc Loughlin, R.Mc (1986) *Spectrochim Acta* **42A** : 451.

18. Nakamoto, N. K. (1988) *Spectroscopy and Structure of Metal Chelate Compounds,* Wiley, New York.

19. Ferraro, J. R. (1971) *Low Frequency Vibrations of Inorganic and Coordination Compounds,* Plenum Press, New York.

20. Sharma H.K., Chandra S. & Gupta S. (1997), *Synth. React. Inorg. Metal Org. Chem.* **27** : 695.

Probability inequalities of the multivariate t distribution

SARALEES NADARAJAH[1] and SAMUEL KOTZ[2]

[1]*Department of Statistics, University of Nebraska, Lincoln, NE 68583.*

[2]*Department of Engineering Management and Systems Engineering, The George Washington University, Washington, D.C. 20052.*

Abstract

Results on probability inequalities of the multivariate t distribution are reviewed. We believe that this review will serve as an important reference and encourage further research activities in the area.

(**Keywords :** multivariate normal ditribution/multivariate t distribution/probability inequalities)

Introduction

A p-dimensinal random vector $\mathbf{X} = (X_1, ..., X_p)^T$ is said to have the p-variate t distribution with degrees of freedom v, means vector μ, and correlation matrix $\mathbf{R}$ and (with Σ denoting the corresponding covariance matrix) if its joint probability density function (pdf) is given by

$$f(x) = \frac{\Gamma\left((v+p)/2\right)}{(\pi v)^{p/2}\,\Gamma(v/2)\,|\mathbf{R}|^{1/2}} \cdot$$

$$\cdot \left[1 + \frac{1}{v}(\mathbf{x}-\mu)^T \mathbf{R}^{-1}(\mathbf{x}-\mu)\right]^{-(v+p)/2} \tag{1}$$

The degrees of freedom parameter v is also referred to as the shape parameter, as the peakedness of (1) may be diminished, preserved or increased by varying v (Jensen[1]). The distribution is said to be central if $\mu=0$. Note that if $p=1$, $\mu=0$ and $\mathbf{R}=1$ then (1) reduces to the univariate Student's t distribution with degrees of freedom v. If $p=2$, then (1) is a slight modification of the bivariate surface of Pearson[2]. If $v=1$, then (1) is the p-variate Cauchy distribution. If $(v+p)/2=m$, an integer, then (1) is the p-variate Pearson type VII ditribution. The limiting form of (1) as $v \rightarrow \infty$ is the joint pdf of the p-

variate normal distribution with mean vector μ and covariance matrix $\mathbf{R}$. The particular case of (1) for $\mu=0$ and $\mathbf{R}=\mathbf{I}_p$ is a mixture of the normal density with zero means and covariance matrix $\upsilon \mathbf{I}_p$ – in the scale parameter υ.

Multivariate t distributions are of increasing importance in classical as well as in Bayesian statistical modeling; however, relatively little is known by means of mathematical properties or statistical methods. These distributions have been perhaps unjustly overshadowed by the multi-variate normal distribution. Both the multivariate t and the multivariae normal are members of the general family of elliptically symmetric distributions. However, we feel that it is desirable to focus on these distributions separately for several reasons :

- Mutivariate t distributions are generalizations of the classical univariate Student t distribution, which is of central importance in statistical inference. The possible structures are numerous, and each one possesses special characteristics as far as potential and current applications are concerned.

- Application of multivariate t distributions is a very promising approach in multivariate analysis. Classical multivariate analysis is soundly and rigidly tilted toward the multivariate normal distribution while multivariate t distributions offer a more viable alternative with respect to real-world data, particularly because its tails are more realistic. We have seen recently some unexpeced applications in novel areas such as cluster analysis, discriminant analysis, multiple regression, robust projection indices, and missing data imputation.

- Multivariate t distributions for the past 20 to 30 years have played a crucial role in Bayesian analysis of multivariate data. They serve by now as the most popular prior distribution (because elicitation of prior information in various physical, engineering, and financial phenomena is closely associated with multivariate t distributions) and generate meaningful posterior distributions.

This paper concerns probability inequalities involving multivariate t distributions. Probability inequalities on Pr ($Y_1 \leq y_1, Y_2 \leq y_2, ... Y_p \leq y_p$) for multivariate distributions have been a popular topic of investigation since the 1950s. It is well known[3-6] that, for arbitrary positive numbers $y_1, y_2, ..., y_p$, the inequality

$$\Pr\left(|Y_1| \leq y_1, |Y_2| \leq y_2, ..., |Y_p| \leq y_p\right) \geq \prod_{k=1}^{p} \Pr\left(|Y_k| \leq y_k\right)$$

holds for any random vector $\mathbf{Y}^T = (Y_1, Y_2, ..., Y_p)$ having the multivariate normal distribution with zero means and an arbitrary correlation matrix. A question then arises as to whether there is an analog of this for multivariate t distributions. Here, we provide a comprehensive review of known results on this topic. We believe that this review will serve as an important reference and encourage further research activities in the area.

Dunnett and Sobel's Probability Inequalities

Dunnett and Sobel[7] obtained bounds for the probability integral

$$P = \Pr\left(X_1 \leq x_1, X_2 \leq x_2, ..., X_p \leq x_p\right)$$

$x_1 \geq 0$, $x_2 \geq 0$, ..., $x_p \geq 0$, when $(X_1, X_2, ..., X_p)$ follows the central p-variate t distribution with degrees of freedom v and the correlation matrix $\mathbf{R}$ taking the special structure $r_{ij} = b_i b_j$ for all $i \neq j$. Using the definition that $\mathbf{X}$ can be represented as $(Z_1/S, Z_2/S, ..., Z_p/S)$, where $\mathbf{Z}$ is a p-variate normal random vector with correlation matrix $\mathbf{R}$ and vS^2/σ^2 is an independent chi-squared random variable with degrees of freedom v, one can rewrite P as

$$P = \Pr\left\{\frac{Z_1}{S} \leq x_1, \frac{Z_2}{S} \leq x_2, ..., \frac{Z_p}{S} \leq x_p\right\}$$

$$= \int_0^{\infty} G\left(x_1 s, x_2 s, ..., x_p s,\right) h(s) ds, \qquad (2)$$

where G is the joint cdf of $\mathbf{Z}$ and h is the pdf of S. If Y_0, Y_1, Y_2, ..., Y_p are independent standard normal random variables, then one can represent $Z_j = \sqrt{1 - b_j^2} Y_j - b_j Y_0$ for $j = 1, 2, ..., p$. Using this result, one can rewrite G as

$$G\left(x_1 s, x_2 s, ..., x_p s,\right) =$$

$$\Pr\left\{\sqrt{1 - b_j^2} Y_j - b_j Y_0 < x_j s, j = 1, 2, ..., p\right\}$$

$$= \int_{-\infty}^{\infty} \prod_{j=1}^{p} \Phi\left(\frac{x_j s + b_j z}{\sqrt{1 - b_j^2}}\right) \phi(z) dz \qquad (3)$$

$$= E\left\{\prod_{j=1}^{p} \Phi\left(\frac{x_j s + b_j Z}{\sqrt{1 - b_j^2}}\right)\right\},$$

where ϕ and Φ are, respectivley, the pdf and the cdf of the standard normal distribution. Using the well known inequality

$$E\left\{\prod_{j=1}^{p} F_j(X)\right\} \geq \prod_{j=1}^{p} E\left\{F_j(X)\right\} \qquad (4)$$

(where F_j denotes a cdf), one can now bound G by

$$G\left(x_1 s, x_2 s, ..., x_p s,\right) \geq \prod_{j=1}^{p} E\left\{\Phi\left(\frac{x_j s + b_j Z}{\sqrt{1 - b_j^2}}\right)\right\}$$

$$= \prod_{j=1}^{p} \Pr\left\{\sqrt{1 - b_j^2} Y_j - b_j Y_0 < x_j s\right\}$$

$$= \prod_{j=1}^{p} \Phi\left(x_j s\right)$$

Substituting this result into (2) and applying (4) once more, one obtains the lower bound for P given by Dunnett and Sobel[7] as

$$P \geq \int_0^\infty \prod_{j=1}^p \Phi\left(x_j s\right) h\left(s\right) ds$$

$$\geq \prod_{j=1}^p \int_0^\infty \Phi\left(x_j s\right) h\left(s\right) ds$$

$$= \prod_{j=1}^p \Pr\left\{Z_j < x_j\right\}$$

$$= \prod_{j=1}^p \Pr\left\{X_j < x_j\right\} \tag{5}$$

This lower bound for P holds more generally for any correlation matrix $\mathbf{R}$ with $r_{ij} \geq 0$ and any arbitrarily fixed $(x_1, ..., x_p)$. This is a consequence of the fact that P is an increasing function of each r_{ij} for all $i \neq j$, while other correlations are held fixed. It can be shown further that

$$\Pr\left(X_1 > x_1,...,X_p > x_p\right) \geq \prod_{j=1}^p \Pr\left(X_j > x_j\right)$$

and

$$\Pr\left(|X_1| > x_1,...,|X_p| > x_p\right) \geq \prod_{j=1}^p \Pr\left(|X_j| > x_j\right)$$

Since the bound (5) does not depend on r_{ij}, it can be calculated easily from a table of the cdf of the univariate Student's t distribution. Dunnett and Sobel[7] also obtained two sharper bounds by slight modifications of the above arguments : For even $p \geq 2$,

$$P \geq \prod_{j=1}^{p/2} \Pr\left\{X_{2j-1} < x_{2j-1}, X_{2j} < x_{2j}\right\}, \tag{6}$$

and for odd $p \geq 3$,

$$P \geq \Pr\left\{X_1 < x_1\right\}.$$

$$\prod_{j=1}^{(p-1)/2} \Pr\left\{X_{2j} < x_{2j}, X_{2j+1} < x_{2j+1}\right\}, \tag{7}$$

In the case where $r_{ij} = \rho$ for all $i \neq j$ and $x_j = x$ for all j, inequalities that are sharper than (6) and (7) can be obtained. Let

$$\beta_1(p) = \Pr\left(X_1 \leq d, X_2 \leq d, ..., X_p \leq d\right)$$

and

$$\beta_2(p) = \Pr\left(|X_1| \leq d, |X_2| \leq d, ..., |X_p| \leq d\right).$$

It is well known that $\beta_k(p)$, $k=1,2$ are monotonically increasing in $r_{ij}(i \neq j)$ and, if $r_{ij} \geq 0$, then

$$\beta_k(p) \geq \beta_1^k(1), \qquad\qquad k = 1, 2. \tag{8}$$

Tong[8] provided the following sharper bounds for β_k

$$\beta_k(p) \geq \left\{\beta_k(m)\right\}^{p/m} \geq \beta_k^p(1) + \left\{\beta_k(2) - \beta_k^2(1)\right\}^{p/2}, \tag{9}$$

where $p \geq m \geq 2$. These inequalities certainly improve on (8), but neither of them are very sharp when p is large. Also observe that the first inequality in (9) depends on p and m only through their ratio p/m. Hence, for fairly large p and m as long as p/m is close to 1 (even if the difference $p-m$ is not small), the first inequality is quite adequate. If $\rho=0$, then a necessary and sufficient condition for $\beta_k(p) \rightarrow \beta_k^p(1)$ for every fixed p is that $\nu \rightarrow \infty$.

Recently Seneta[9] pointed out that the "sub-Markov" inequality

$$\beta_1(p) \geq \left[\Pr\{X_1 \leq x, X_2 \leq x\}\right]^{p-1} \Big/ \left[\Pr\{X_1 \leq x\}\right]^{p-2} \tag{10}$$

is sharper than the corresponding inequality

$$\beta_1(p) \geq \left[\Pr\{X_1 \leq x, X_2 \leq x\}\right]^{p/2} \tag{11}$$

as given by (9). This fact is illustrated in the following table, which is taken from Seneta[9].

Comparison of the bounds (11) and (10) for P. x chosen such that the true value of P=0.95.

	v	x	Bound (11)	Bound (10)
	10	2.34	0.945	0.946
p=3	15	2.24	0.946	0.947
	20	2.19	0.945	0.946
	60	2.10	0.944	0.945
	10	2.81	0.921	0.921
p=9	15	2.67	0.924·	0.924
	20	2.60	0.926	0.927
	60	2.48	0.934	0.936

Actually, (10) is a particular case of the following inequalities

$$\beta_1(p) \geq \Pr\left(X_j \leq x; j = 1,...,m-1\right)$$

$$\times\left\{\Pr\left(X_m \leq x \mid X_j \leq x; j = 1,..., m-1\right)\right\}^{p-m+1} \quad (12)$$

and

$$\beta_2(p) \geq \Pr\left(|X_j| \leq x; j = 1,...,m-1\right)$$

$$\times \left\{\Pr\left(|X_m| \leq x \mid |X_j| \leq x; j = 1,..., m-1\right)\right\}^{p-m+1}$$

given by Glaz and Johnson[10], who also provided a formal proof of the fact that (12) is sharper than (9).

Dunnett[11] wrote a *Fortran* programs for evaluating the integral (3). It uses Simpson's rule to compute an approximation to (3) in such a way that a prescribed accuracy is achieved. To approximate the integral of a function $\alpha(z)$, say, over an interval $[a,b]$ using Simpson's rule, the value of the function is computed at the two end points and at the midpoint of the interval; then the approximate value of the integral is given by

$$\left\{\alpha(a) + 4\alpha\left(\frac{a+b}{2}\right) + \alpha(b)\right\}\frac{b-a}{6},$$

with its error bounded by $\alpha_4(a,b)$ $(b-a)^5/2880$, where $\alpha_4(a,b)$ is a bound on the absolute value of the

fourth derivative of $\alpha(z)$ over the interval (see, for example, page 66 in Shampine and Allen[12]). The central processor unit time (on a VAX 8600 computer using single-precision arithmetic) taken to compute (3) ranges from 0.01 to 2.37 seconds for cases of equal correlation ($r_{ij} = \rho$) and identical ranges of integration ($x_j=x$). Slightly longer computing times are required for unequal correlations or different limits of integration. Dunnett[11] suggested that his program can be used along with an appropriate numerical integration routine, such as the Integral Mathematical and Statistical Libraries[13] (Volume 1, Chapter 4) *QDAGI*, to evaluate the multivariate t probability integral (2).

Dunn's Probability Inequalities

The univariate Student's t distribution has the property that the probability evaluated from $-x$ to $+x$ is an increasing function of the degrees of freedom v– this also applies to the probability from $-\infty$ to $+x$ (see, for example, Ghosh[14] for details). Dunn[15] pointed out that this monotonicity does not generalize to p dimensions in the usual multivariate t distribution. Specifically, let **X** have the central p-variate t distribution with degrees of freedom v and correlation matrix **R**. If $F(x)$ is defined by

$$F(x) = \Pr\left\{\cap_{k=1}^{p} - x < X_k < x\right\},$$

then $F(x)$ equals the probability mass in the multivariate t distribution evaluated over a p-dimensional hypercube centered at the origin of the half side x and $F(x)$ in the distribution of the maximum of the absolute values of the p X variables. Similarly, if $G(x)$ is defined by

$$G(x) = \Pr\left\{\cap_{k=1}^{p} - \infty < X_k < x\right\},$$

then $G(x)$ equals the probability mass evaluated from $-\infty$ to x in each direction and $G(x)$ is the distribution function of the maximum of the p X variables. Dunn showed that, for any given x>0 and degrees of freedom $v_1 > v_2$, there exists an integer K such that, for all $p \geq K$,

$$F_{p,v_1}(x) < F_{p,v_2}(x)$$

and

$$G_{p,v_1}(x) < G_{p,v_2}(x).$$

Here, $F_{p,v}$ and $G_{p,v}$ are F and G as defined above, with dimension p and degrees of freedom v. This result covers the case of all correlations equal to 0. When all correlations are equal to 1, the distribution is the same as the univariate Student's t distribution, so that, for all dimensions, $F(x)$ and $G(x)$ are monotonically increasing functions of v. Other correlation matrices may be considered in some sense to lie between these two extremes. In various unpublished tables of $F(x)$, the change is found to occur at a dimension where $F(x)$ is approximately 0.25 or 0.30.

Halperin's Probability Inequalities

Halperin[16] extended the inequality (5) for generalized bivariate t distributions as follows. Let (Y_{i1}, Y_{i2}), $i = 0,1,2,...,r$, $r \geq 1$ be independent samples from a bivariate normal distribution with zero means, variances σ_1^2, σ_2^2, and covariances $\sigma_1\sigma_2\rho_i$, $|\rho_i| \leq 1$. Let Y_{i1}, $i = r + 1,...., r+n$ and Y_{i2}, $i = r + 1,..., r+m$ be independent normal samples with zero means and variances σ_1^2 and σ_2^2, respectively, and independent of (Y_{i1}, Y_{i2}), $i = 0,1,2,..., r$. Define

$$(X_1, X_2) = \left(\frac{Y_{01}}{S_1}, \frac{Y_{02}}{S_2} \right),$$

where

$$S_1 = \frac{1}{r+n} \sum_{i=1}^{r+n} Y_{i1}^2$$

and

$$S_2 = \frac{1}{r+m} \sum_{i=1}^{r+m} Y_{i2}^2$$

Halperin[16] then showed that the probability integral of (X_1, X_2) satisfies the inequality

$$\Pr(|X_1| \leq x_1, |X_2| \leq x_2) \geq \Pr(|X_1| \leq x_1) \Pr(|X_2| \leq x_2)$$

for all real numbers x_1 and x_2.

Sidak's Probability Inequalities

In the bivariate case considered above, it is assumed that the correlation between Y_{i1} and Y_{i2} may be different for different i's. For a general p, but for a special correlation structure of Y's, Sidak[6] established the following result. Let $\mathbf{Y}^T = (Y_1, Y_2, ..., Y_p)$ have a p-variate normal distribution with zero means and an arbitrary correlation matrix. Let $\mathbf{Z}_i^T = (Z_{i1}, Z_{i2}, ..., Z_{ip})$, $i = 1, ..., n$ be a p-variate normal random sample, which is mutually independent and independent of $\mathbf{Y}$, each of which has zero means, unit variances, and the decomposable correlation structure given by

$$Corr\ (Z_{ki}, Z_{kj}) = b_i b_j$$

for $i, j = 1, ..., p$, $i \neq j$; $k = 1, ..., n$ with $0 \leq b_j \leq 1$, $i = 1, ..., p$. Then

$$\Pr\left(\frac{|Y_1|}{\sqrt{Z_{11}^2+....+Z_{n1}^2}} \leq x_1,...., \frac{|Y_p|}{\sqrt{Z_{1p}^2+....+Z_{np}^2}} \leq x_p \right)$$

$$\geq \prod_{i=1}^{p} \Pr\left(\frac{|Y_i|}{\sqrt{Z_{1i}^2+....+Z_{ni}^2}} \leq x_i \right). \tag{13}$$

Essentially the same result, assuming more generally only $|b_i| \leq 1$, followed by an easy specialization of Corollary 8 is given in Khatri[3].

A general proof of the inequality (13) under the assumption that $\mathbf{Y}$ and all $\mathbf{Z}_i$'s have the same normal distribution with zero means and an arbitrary covariance matrix was provided by Scott[4]. Unfortunately, this proof is correct only for $p=2$, and Sidak[17] produced a counterexample showing its incorrectness for $p>2$. Sidak[17] went on to show that, if

$$Corr\ (Y_i, Y_j) = c_i c_j r_{ij}$$

for $i, j = 1, 2, ..., p$, $i \neq j$ with $|c_j| \leq 1$ $(j = 1, 2, ..., k)$ and $\{r_{ij}\}$ any fixed correlation matrix, and if

$$Corr\ (Z_{li}, Z_{lj}) = b_{li} b_{lj}$$

for $i,j = 1,2,...., p$; $i \neq j$; $l = 1,2,...., n$ with $|b_{li}| < 1$ ($i=1,2,...., p$, $l = 1,2,..., n$), then the left-hand side probability in (13) as a function of c_j is nonincreasing for $-1 \leq c_j < 0$ and nondecreasing for $0 < c_j \leq 1$, so that it has a minimum for $c_j = 0$ and, as a function of b_{li}, is nonincreasing for $-1 < b_{li} < 0$ and nondecreasing for $0 < b_{li} < 1$, so that it has a minimum for $b_{li} = 0$. Hence, (13) is also true for this more general correlation structure.

Sidak[18] obtained an inequality using exchangeability when $\mathbf{X}$ is a central p-variate t random vector with the equicorrelation structure $r_{ij} = \rho$, $i \neq j$. He showed that

$$\Pr \ (b \leq X_1 \leq a,...., \ b \leq X_p \leq a)$$

$$> \ \{\Pr \ (b \leq X_1 \leq a,...., \ b \leq X_r \leq a)\}^{p/r}$$

$$> \ \{\Pr \ (b \leq X_i \leq a)\}^p$$

for all $p > r \geq 2$ and $a > b$. In an earlier paper, Tong[8] obtained similar results for a much larger class of random vectors.

Tong's Probability Inequalities

The multivariate t density is Schur-concave in the particular case $r_{ij} = \rho$, $i \neq j$. Tong[9] used this property to derive certain probability inequalities. He showed that if $f: \mathfrak{R}^P \to [0, \infty]$ is Borel-measureable and Schur-concave, then, provided that the integral exists, $\int_{A(x)} f(\mathbf{y}) \, d\mathbf{y}$ is also a Schur-concave function of $(x_1,...,x_p)$, where $A(\mathbf{x})$ denotes the rectangular set

$$A(\mathbf{x}) = \left\{ \mathbf{y} \middle| \mathbf{y} \in \mathfrak{R}^P, \ |y_j| \leq x_j, \ j = 1,....,p \right\}.$$

Taking f to be the pdf of the multivariate t, it follows that

$$\Pr\left(|X_j| \leq x_j, j = 1,....,p\right) \leq \Pr\left(|X_j| \leq \bar{x}, j = 1,...,p\right),$$

where $\bar{x} = \left(x_1 + ... + x_p\right) / p$.

References

1. Jensen, D.R. (1994) *Statistics and Prob. Lett.* **20** : 307.

2. Pearson, K. (19233) *Biometrika* **15** : 231.

3. Khatri, C.G. (1967) *Annals of Math. Stats.* **38** : 1853.

4. Scott, A. (1967) *Annals of Math. Stats.* **38** : 278.

5. Sidak, Z. (1965) *Bull. of the Instit. Intnl. Stats.* **41** : 380.

6. Sidak, Z. (1967) *Jour. of the Amer. Statist. Assoc.* **62** : 626.

7. Dunnett, C.W. & Sobel, M. (1955) *Biometrika* **42** : 258.

8. Tong, Y.L. (1970) *Jour. of the Amer. Statist. Assoc.* **65** : 1243.

9. Seneta, E. (1993) in *Multiple Comparisons, Selection, and Applications in Biometry*, Marcel Dekker, New York, p. 29.

10. Glaz, J. & Johnson, B.McK. (1984) *Jour. of the Amer. Statis. Assoc.* **79** : 435.

11. Dunnett, C.W. (1989) *Appld. Stats.* **38** : 564.

12. Shampine, L.F. & Allen, R.C. (1973) *Numerical Computing : An Introduction*, Saunders, Philadelphia.

13. International Mathematical and Statistical Libraries (1987) *MATH/Library, Fortran Subroutines for Mathematical Applications*, International Mathematical and Statistical Libraries, Houston.

14. Ghosh, B.K. (1973) *Jour. of the Royal Statist. Soc.* **B35** : 480-492.

15. Dunn, O.J. (1965) *Annals of Mathematical Stats.* **36** : 712.

16. Halperin, M. (1967) *Jour. of Amer. Statist. Assoc.* **62** : 603.

17. Sidak, Z. (1971) *Annals of Mathematical Stats.* **42** : 169.

18. Sidak, Z. (1973) *Applications of Mathematics* **18** : 110.

19. Tong, Y.L. (1982) *Annals of Stats.* **10** : 637.

Triple coincidence among R_2 numbers

M.A. GOPALAN*, MANJU SOMANATH and N. VANITHA

*Department of Mathematics, National College, Trichy, India.

Department of Mathematics, Cauvery College for Women, Trichy, India.

Abstract

An elegant formulation to construct triple coincidence among R_2 numbers is presented together with generation of quadruple coincidences.

(Keywords : R_2 numbers/triple coincidence/quadruple coincidences)

Introduction

The numbers that can be expressed as the sum of the squares of two numbers in two different ways are called second order Ramanujan numbers (R_2 numbers). It is observed[1] that to construct a triple coincidence we have to follow its basic definition. It follows from literature[2] that if any prime of the form $n = 4p + 1$ happens to be the hypotenuse of a primitive Pythagorean triangle, then $(n^k)^2$ can be used for multiple coincidences among R_2 numbers of order k (k=1, 2, 3 ...). Now a challenging task strikes our mind to obtain an elegant alternative formulation to construct triple coincidences among R_2–numbers and to generate quadruple coincidences among them which are the main thrusts of this paper.

Construction of Triple Coincidence Among R_2 Numbers

Let u, v, w be three non-zero distinct integers such that u^2, w^2, v^2 are in arithmetic progression, which is represented as

$$u^2 + v^2 = 2w^2 \qquad (1)$$

which is satisfied by

$$u = 2r^2 + s^2 + 4rs$$

$$v = 2r^2 - s^2 \qquad (2)$$

$$w = 2r^2 + s^2 + 2rs$$

Now, let a, b be two non-zero distinct numbers such that

$$a = A + B$$

$$b = A - B \qquad (3)$$

from which we have

$$a^2 + b^2 = 2(A^2 + B^2) \qquad (4)$$

Multiplication of (2) with (4) leads to

$$(au + bv)^2 + (av - bu)^2 = (au - bv)^2 +$$

$$(av + bu)^2 = (2Aw)^2 + (2Bw)^2$$

Employing (2) and (3), the triple coincidences among R_2 numbers is represented by

$$[2A\,(r^2 \pm rs) + B(s^2 \pm 2rs)]^2 + [-A(s^2 \pm 2rs)$$

$$+ 2B\,(r^2 \pm rs)]^2 = (A^2 \pm B^2)w^2$$

Some examples are given below :

1. $30^2 + (-10)^2 = 26^2 + 18^2 = 30^2 + 10^2$

2. $82^2 + (-6)^2 = 54^2 + 62^2 = 78^2 + 26^2$

3. $158^2 + 6^2 = 90^2 + 130^2 = 150^2 + 50^2$

4. $328^2 + (-24)^2 = 216^2 + 248^2 = 312^2 + 104^2$

5. $212^2 + (-36)^2 = 156^2 + 148^2 = 204^2 + 68^2$

Suppose we want two R_2 numbers M and N denoted by

$$M : a^2 + b^2 = A^2 + B^2$$

$$N : e^2 + f^2 = E^2 + F^2$$

It is verified that the following represents quadruple coincidences among R_2 numbers.

$$(ae+bf)^2 + (af-be)^2 = (aE-bF)^2 + (aF+bE)^2$$

$$= (aE+bF)^2 + (aF-bE)^2 = (AE-BF)^2 + (AF+BE)^2$$

A few illustrations are given below.

1. $12920^2 + 1440^2 = 5000^2 + 12000^2 = 10400^2$
$$+ 7800^2 = (- 3200)^2 + 12600^2$$

2. $70400^2 + 6720^2 = 33280^2 + 62400^2 = 56576^2$
$$+ 42432^2 = (- 3008)^2 + 70656^2$$

3. $17600^2 + (- 1680)^2 = 6800^2 + 16320^2 = 14144^2$
$$+ 10608^2 = (- 752)^2 + 17664^2$$

In a similar manner, knowing two triple coincidences among R_2 numbers, one may generate coincidences of higher order among R_2 numbers.

References

1. Meyyappan, M. (1996) *Ramanujan Numbers,* S. Chand & Co., Delhi, Ist Ed.

2. Pattabhi Ramacharyulu N. Ch. (2003) *Pythagoras Theorem : A Mine of Gold, The Mathematics Teacher* **39** : Issues 3-4.

Neutron induced reaction cross-sections of ^{45}Sc, ^{46}Ti, ^{51}V and ^{54}Fe

SNEH LATA GOYAL and R.K. MOHINDRA*

Department of Applied Physics, Guru Jambheshwar University, Hisar-125 001, India.

*Physics Department, Kurukshetra University, Kurukshetra-132 119, India.

Abstract

Neutron induced reaction cross-sections of ^{45}Sc, ^{46}Ti, ^{51}V and ^{54}Fe for $(n,2n)$, (n,p), (n,α), (n,d), (n,t) and $(n, {}^{3}\text{He})$ reactions have been evaluated in the energy range of 1-20 MeV. Computer codes ALICE-91, SC2N3N, NX-1 and NX-2 have been used for the computations. The computations are based on evaporation model considering the pre-equilibrium emission mechanism under some approximations. The excitation functions of different isotopes have been shown alongwith the available experimental data. The results are in fairly good agreement with earlier results.

(**Keywords** : neutron induced reactions/excitation functions/ pre-equilibrium emission/evaporation model/exciton model)

Introduction

Charged particle production data of neutron induced reactions are of great importance from the viewpoint of fusion reactor technology, particularly for the calculations of nuclear transmutation rate, nuclear heating and radiation damage due to gas formation.

Multineutron emission[1] assumes a great deal of significance in the MeV region since the charged particle emission becomes more and more prohibitive due to the coulomb barrier and radiative neutron capture, is insignificantly small. Cross-sections for $(n,2n)$ reaction play an important role in fast neutron multiplying media and fusion-fission hybrid systems. Using the computer codes ALICE-91 |2, 3|, SC2N3N |4, 5|, NX-1 and NX-2 |6, 7| the excitation functions of different isotopes have been computed and compared with the available measured cross-sections. The pairing correction and shell correction were applied with the use of the ALICE code.

Calculations

An analysis has been carried out of $(n,2n)$ and $(n,$ charged particle$)$ reaction cross-sections of ^{45}Sc, ^{46}Ti, ^{51}V and ^{54}Fe in the energy range of 1-20 MeV. The computation of excitation functions of $(n,2n)$, (n,p) and (n,α) reactions for 1-20 MeV neutrons have been carried out at the steps of 1 MeV using the computer code ALICE-91 developed by Blann[2,3]. This code accounts for compound/statistical calculations in general framework of the Weisskopf-Ewing evaporation model and hybrid/geometry dependent hybrid model for precompound decay. These cross-sections were also computed after applying pairing energy correction and shell correction with backshifted pairing. The Fermi gas level density used is of the form

$$\rho(U) \propto (U - \delta)^{-5/4} \exp 2 \sqrt{a(U - \delta)} \qquad (1)$$

The level density parameter $a = A/9$, which is default option of the code and the pairing correction is defined by $\delta = 11/A^{1/2}$.

The hybrid model for precompound decay may be formulated as

$$\frac{d\sigma}{d\varepsilon} = \sigma_R P_b(\varepsilon) \qquad (2)$$

$$\frac{d\sigma}{d\varepsilon} = \sigma_R \sum_{n=n_0}^{\bar{n}} \left[\frac{X_U \rho_{n-1}(U)}{\rho_n(E)} \right] \left[\frac{\lambda_c(\varepsilon)}{\lambda_c(\varepsilon) + \lambda_+(\varepsilon)} \right] D_n d\varepsilon \qquad (3)$$

where the term in the first set of the brackets uses terms similar to the Ericson partial state densities

to calculate the number of excitons of type X_υ (υ = neutron or proton) which are available for emission in the energy range ε to $\varepsilon + d\varepsilon$ and $U = E - B_\upsilon - \varepsilon$, where B_υ is the binding energy of particle type υ. The term λ_c (ε) is the rate of nucleon emission into the continuum and λ_+ (ε) is the competing rate of two body collissions for the nucleons at energy ε. The factor D_n is a depletion factor which represents the fraction of the population surviving to the n exciton term in the summation over exciton number.

According to GDH model the nucleus has a density distribution which can affect pre-equilibrium decay in two ways. First, the nucleon mean free path (λ) is expected to be longer (on average about a factor of two) in the diffuse nuclear surface. Secondly, in a local density approximation, there is a limit to the hole depth; this will be expected to modify the Ericson state densities. These two changes were incorporated into the GDH model. To consider both surface effects (λ and hole depth limit), the equation (2) was reformulated replacing σ_R' by

$$\pi\lambda^2 \sum_{l=0}^{\infty} (2l+1) \, T_l$$

Hence, the differential emission spectrum is given in the GDH model as

$$\frac{d\sigma}{d\varepsilon} = \pi\lambda^2 \sum_{l=0}^{\infty} (2l+1) T_l P_\upsilon(l,\varepsilon) \qquad (4)$$

where l is the entrance channel orbital angular momentum, T_l is the transmission coefficient and P_υ (l, ε) is the decay probability at exit channel energy ε. When the approach is used for incident nucleons, the T_l are provided by an optical model subroutine. The optical model potential is defined as follows :

$$U(r) = V_c - Vf(r) - i\left[-4Wg(r) + W_v f(r)\right] +$$

$$\left(\frac{h}{m_\pi c}\right)^2 (\overline{l}.\overline{s}) \, V_{so} h(r) \qquad (5)$$

where

$$V_c = \begin{cases} zz'e^2 / r, & \text{if } r \geq R_c \\[2mm] \dfrac{zz'e^2}{2R_c}\left(3 - \dfrac{r^2}{R_c^2}\right) & \text{if } r < R_c \end{cases} \qquad (6)$$

where z and z' are the charges of the incident particle and the target nucleus. The imaginary absorptive potential is pure surface so $W \neq 0$ and $W_v = 0$, which have a derivative Woods-Saxon shape and

$$f(r) = \left[1 + \exp(r - R)/a_v\right]^{-1} \qquad (7)$$

$$g(r) = \exp\left[(r - R)/a_w\right]\left[1 + \exp(r - R)/a_w\right]^{-2} \qquad (8)$$

and $\quad h(r) = \dfrac{1}{r}\dfrac{d}{dr} f(r) \qquad (9)$

are the Woods-Saxon, derivative Woods-Saxon (surface peaked) and spin-orbit form factors with appropriate radius and diffusivity parameters $R = r_0 A^{1/3}$ is the nuclear radius and a is the surface diffuseness parameter.

$$\left(\frac{h}{m_\pi c}\right)^2 = 2 \ (fm)^2$$

Table 1 – Optical model parameters for neutrons.

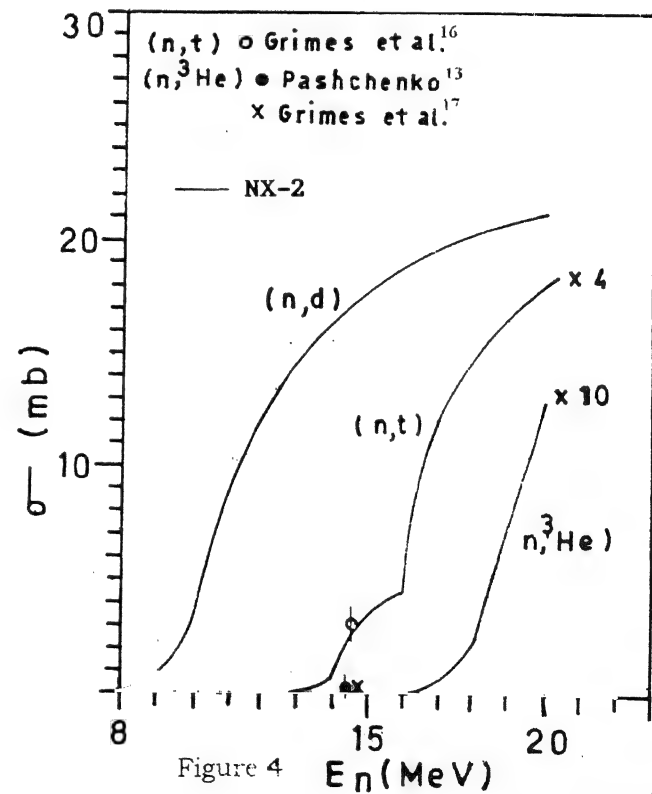| Parameter		Neutrons
Real Potential V (MeV)		48 (Woods-Saxon)
Imaginary W (MeV)		9.0
Form of W		Pure Surface
Spin Orbit (MeV)		7.0
Radius	R_v (f_m)	= $(1.322 - 7.6 \times 10^{-4}A + 4 \times 10^{-6}A^2 - 8 \times 10^{-9}A^3) \times A^{1/3}$
	R_w (f_m)	= $(1.266 - 3.7 \times 10^{-4}A + 2 \times 10^{-6}A^2 - 4 \times 10^{-9}A^3) \times A^{1/3}$
	R_{so} (f_m)	= R_w
	Rcoulomb	= $1.25 \ A^{1/3}$
Diffusivity	a_v (f_m)	0.66
	a_w	0.48
	a_{so}	0.48
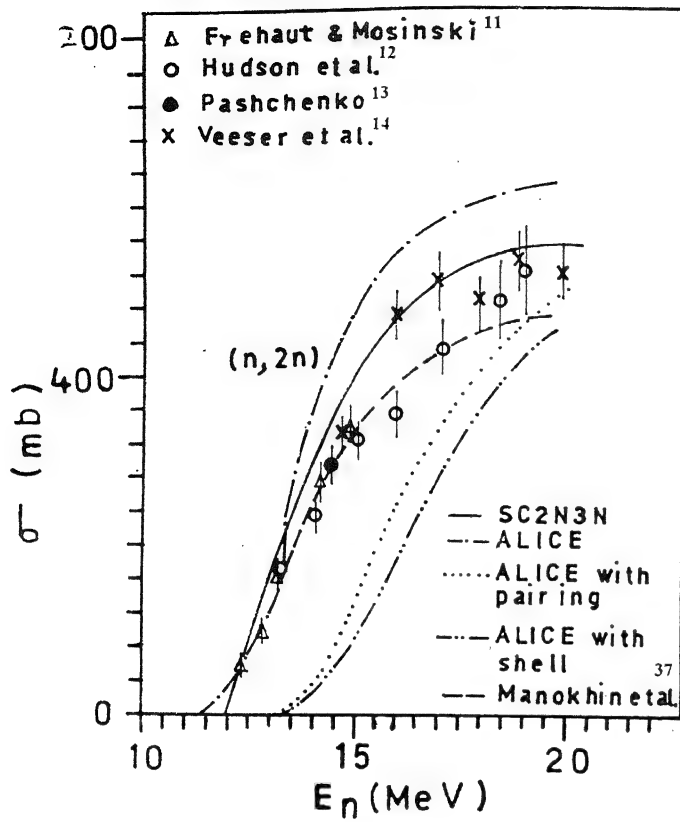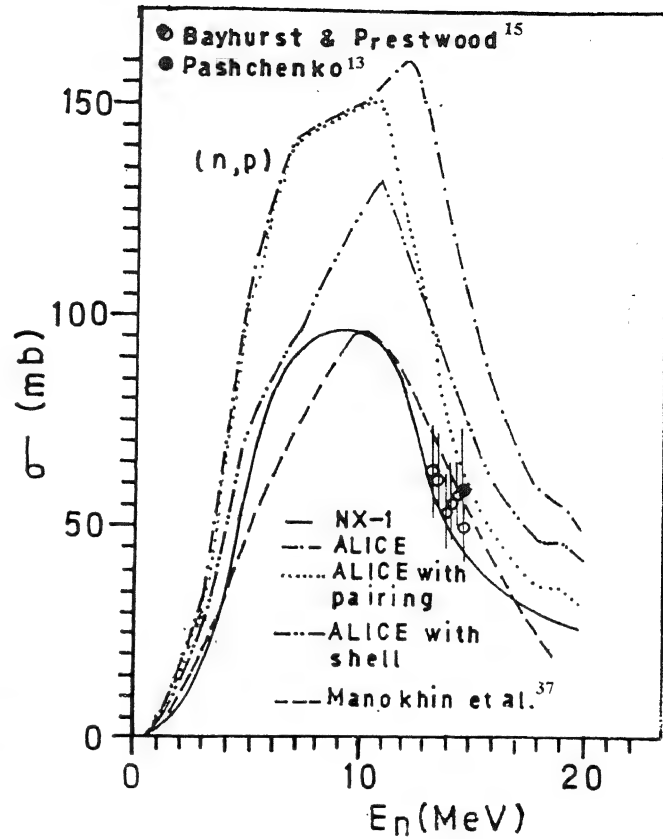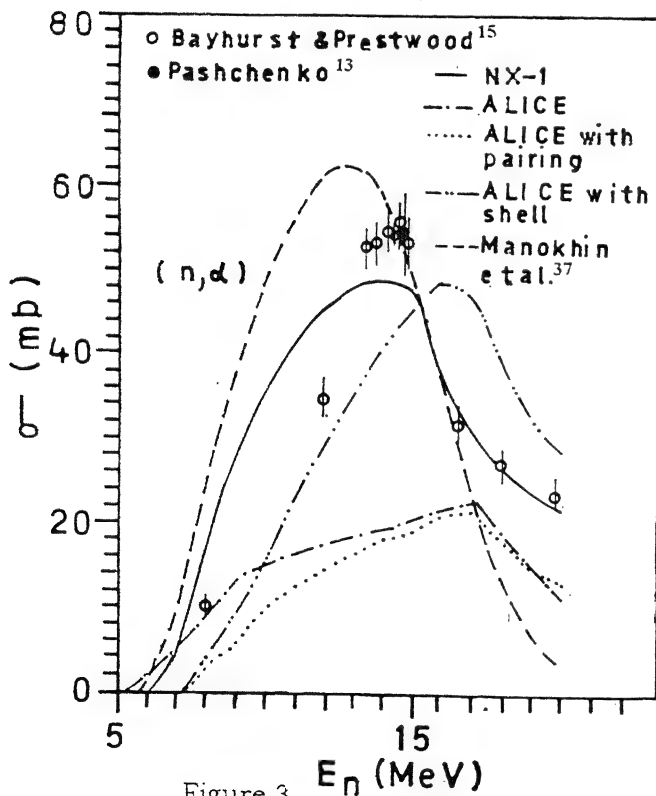
Fig. 1 – $(n, 2n)$ reaction cross-sections of ^{45}Sc. Fig. 2 – (n, p) reaction cross-sections of ^{45}Sc. Fig. 3 – (n, α) reaction cross-sections of ^{45}Sc. Fig. 4 – (n, d), (n, t) and $(n, {}^3He)$ reaction cross-sections of ^{45}Sc.
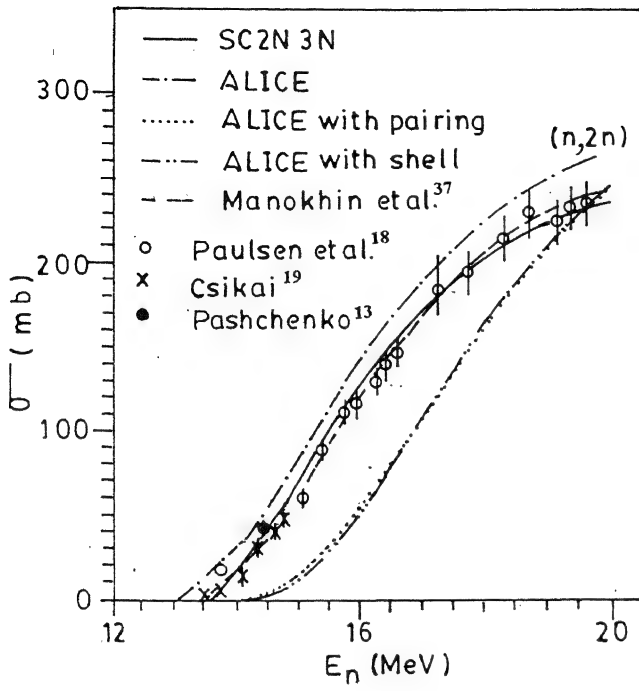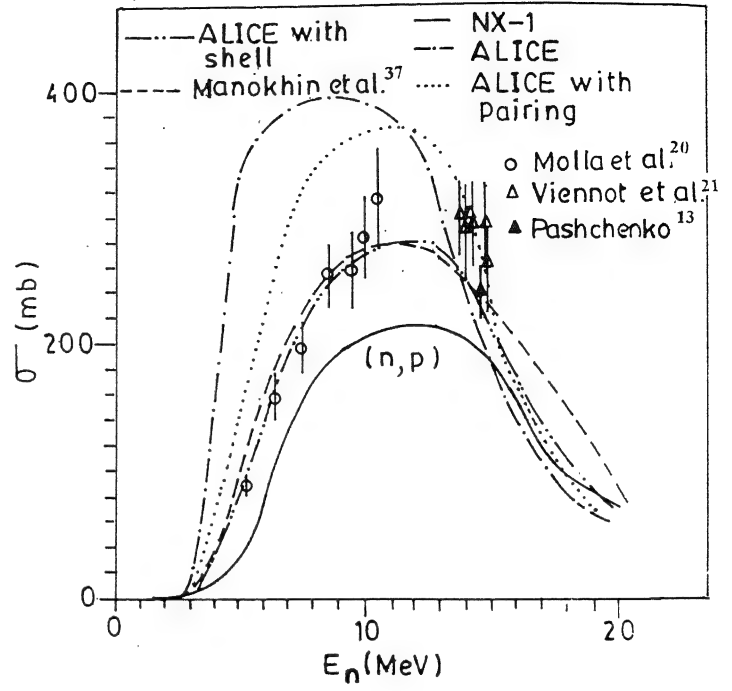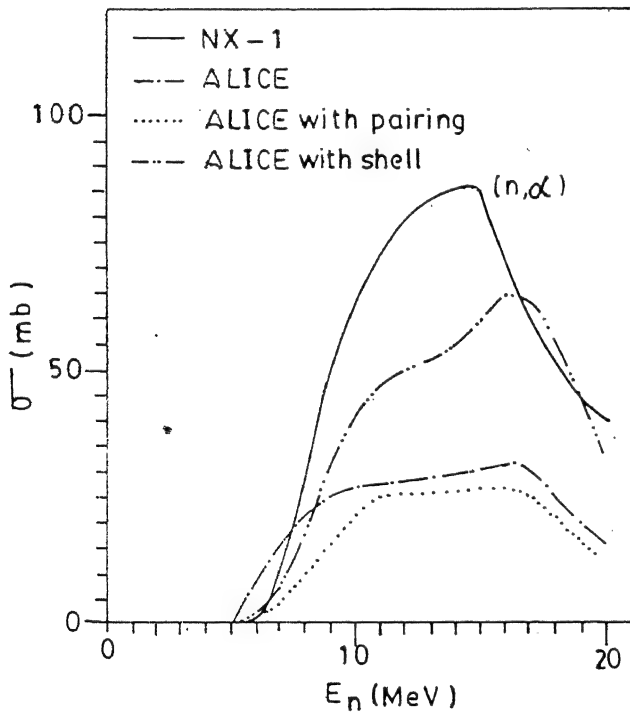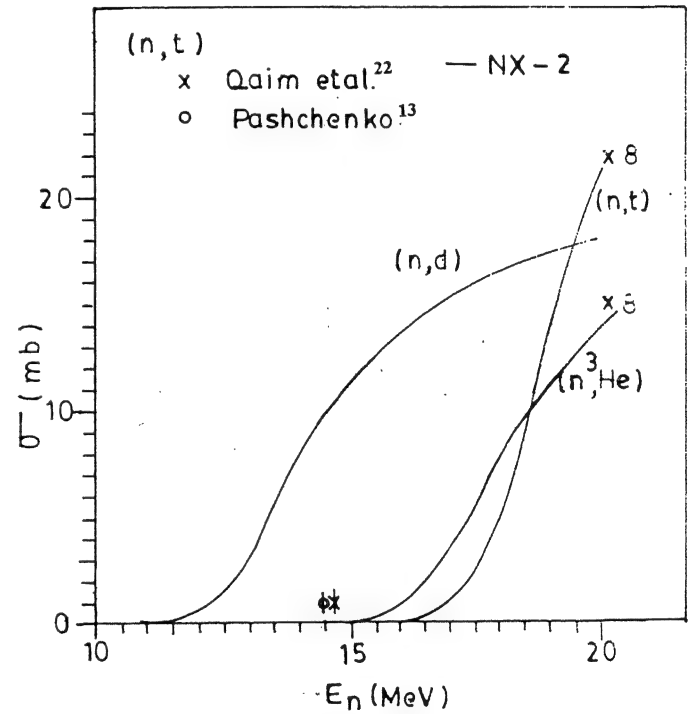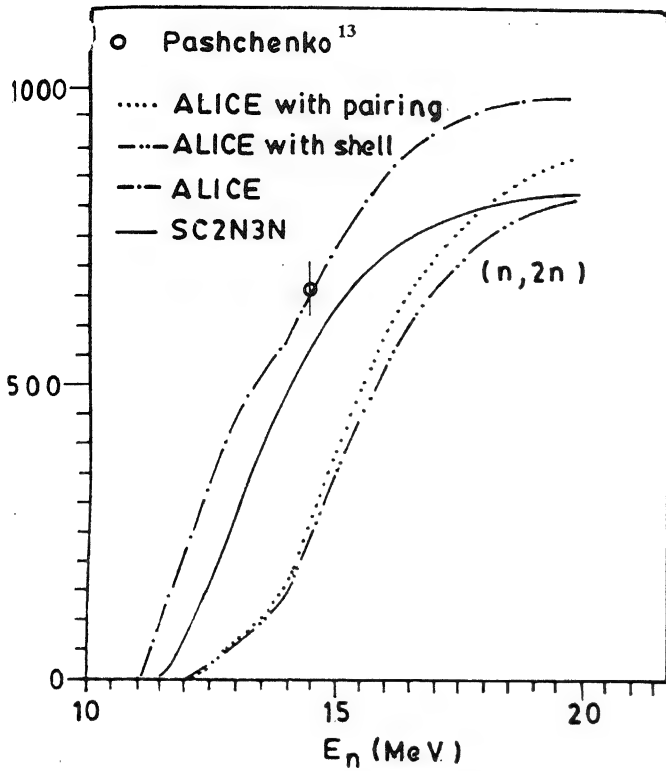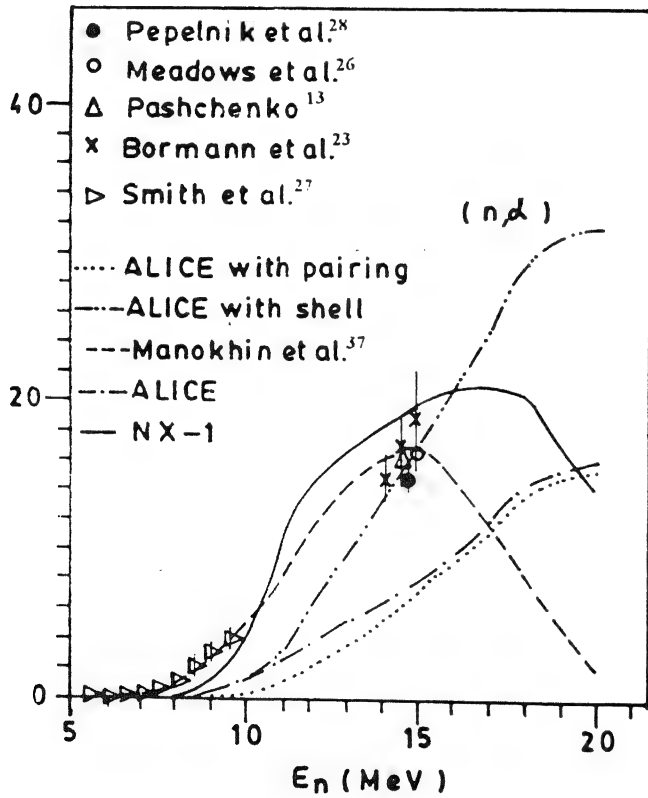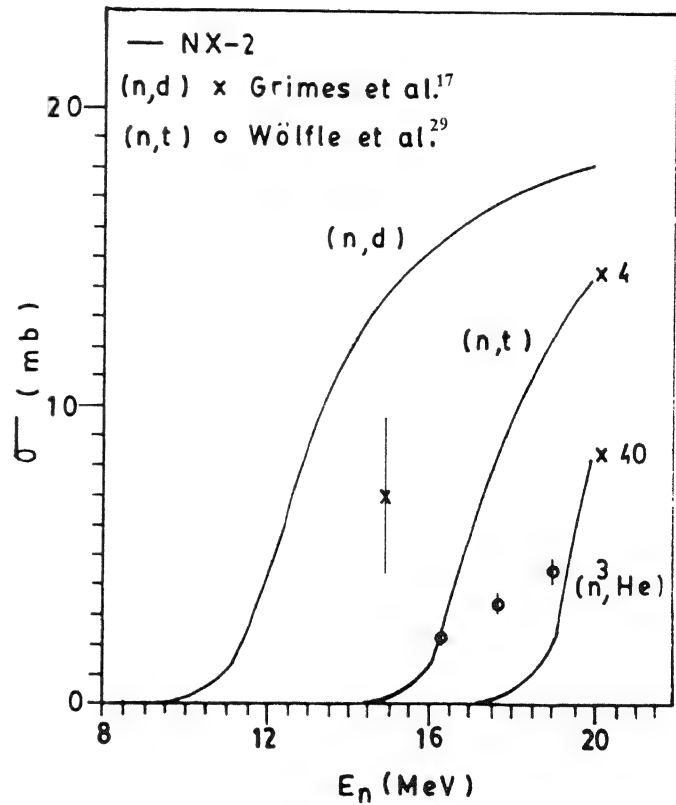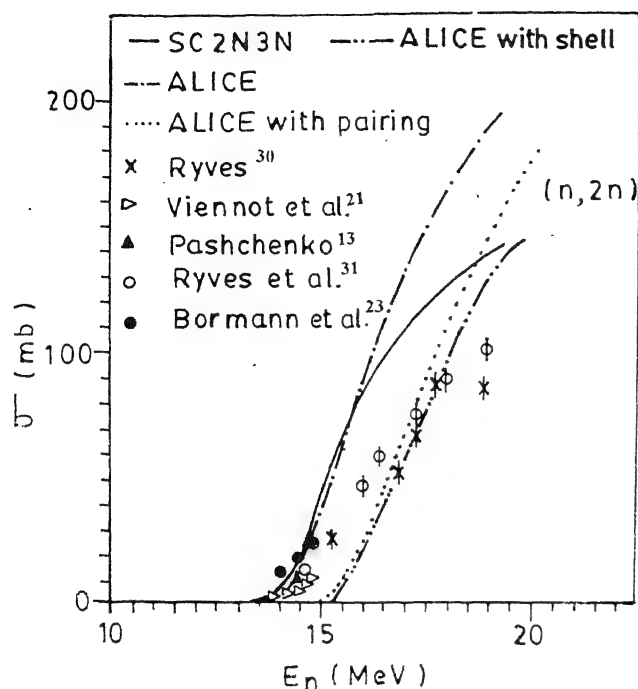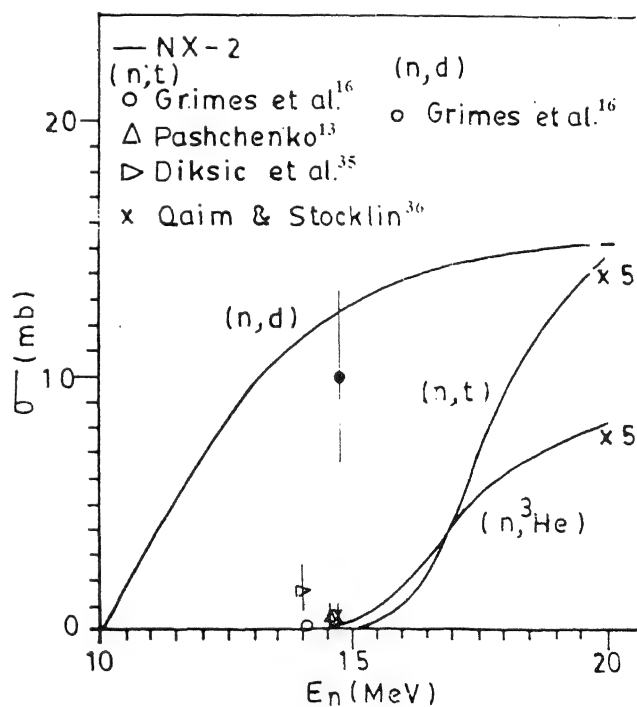
Figure 5

Figure 6

Figure 7

Figure 8

Fig. 5 – (n, 2n) reaction cross-sections of [46]Ti. Fig. 6 – (n, p) reaction. cross-sections of [46]Ti., Fig. 7 – (n, α) reaction cross-sections of [46]Ti. Fig. 8 – (n, d), (n, t) and (n, [3]He) reaction cross-sections of [46]Ti.

Figure 9
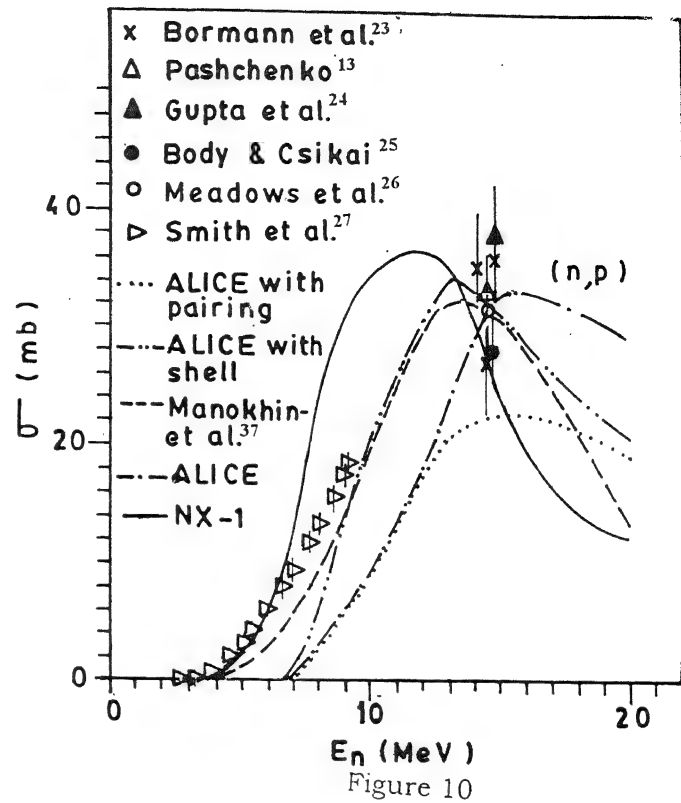
Figure 10

Figure 11

Figure 12

Fig. 9 – $(n, 2n)$ reaction cross-sections of ^{51}V. Fig. 10 – (n, p) reaction., cross-sections of ^{51}V. Fig. 11 – (n, α) reaction cross-sections of ^{51}V. Fig. 12 – (n, d), (n, t) and $(n, ^3$He) reaction cross-sections of ^{51}V.

Figure 13
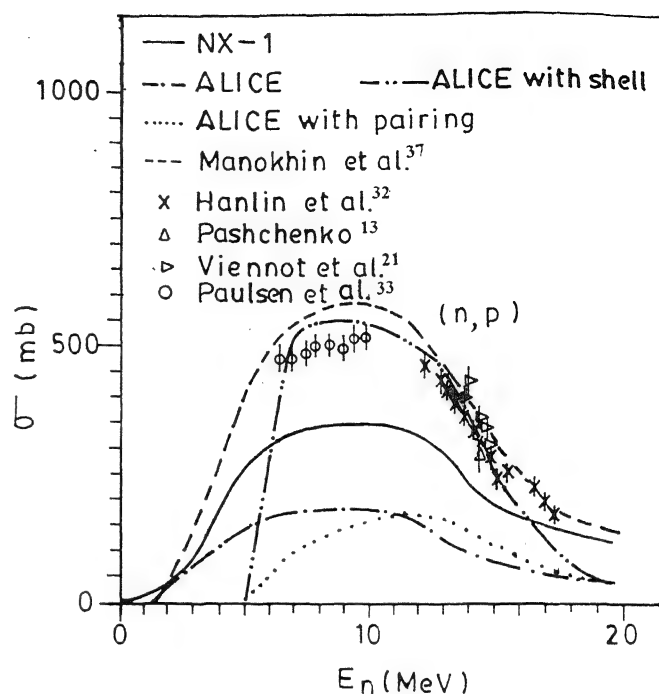
Figure 14
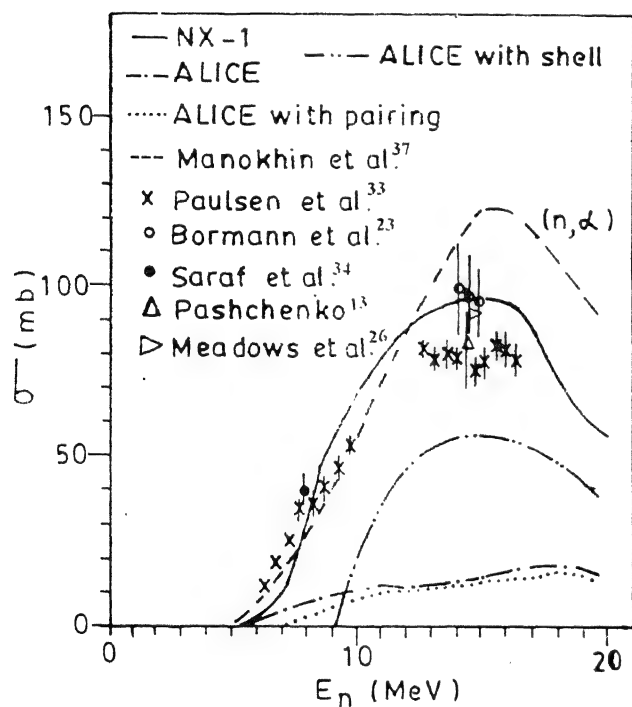
Figure 15

Figure 16

Fig. 13 – $(n, 2n)$ reaction cross-sections of ^{54}Fe. Fig. 14 – (n, p) reaction cross-sections of ^{54}Fe. Fig. 15 – (n, α) reaction cross-sect of ^{54}Fe. Fig. 16 – (n, d), (n, t) and $(n, ^3He)$ reaction cross-sections of ^{54}Fe.

For neutrons, the optical model parameter set due to Wilmore and Hodgson[8] listed in Table 1 is used. The binding energies and Q-values used in the present work were all based on experimental masses. The ALICE code includes experimental masses in block data, so that a simple input parameter results in all Q-values and binding energies being internally generated from experimental mass tables.

The computations of $(n, 2n)$, (n, p), (n, α), (n, d), (n, t) and $(n, {}^3He)$ reaction cross-sections have also been carried out using the systematic codes SC2N3N, NX-1 and NX-2. These contain analytical formula with parameters based on experimental data and derived by using the constant temperature evaporation model for statistical phenomena and the exciton model for precompound part. The detailed formulae for the computation of these cross-sections have been described by Bansal and Mohindra[9]. Here the pre-equilibrium emission is considered to occur only at the state of exciton number $n = 3$. The energy level density of the compound nucleus is taken in the form of constant temperature.

$$\rho\left(A, E\right) \propto \exp\left[E / T\left(A\right)\right] \qquad (10)$$

where E is excitation energy of the compound nucleus and the nuclear temperature $T(A)$ is taken as $T(A) = 13A^{-1/2}$. For these computations the Q-values and separation energies have been taken from the tabulations of Audi et al.[10]

Results and Discussion

The computed excitation functions using different codes have been compared with the available experimental values[11-36] and the results are shown in Fig. (1-16). The evaluated cross-sections of $(n, 2n)$, (n, p) and (n, α) reactions given by Manokhin et al.[37] were also considered for comparison.

It is observed that for the same incident neutron energy the decrease in $(n,$ charged particle$)$ reaction cross-sections has been observed with the increase in mass of the target nuclei, whereas $(n, 2n)$ reaction cross-sections are increasing with increase in the mass of the target nuclei for the same incident neutron energy in case of the isotopes studied. The similar variation was observed by Qaim et al.[38] in

case of (n, t) reaction cross-sections of ${}^{27}Al$, ${}^{59}Co$ and ${}^{93}Nb$. This is due to the fact that for medium and heavy mass nuclei (Z between 15 and 92), as a result of high negative Q-values and the increasing coulomb barrier for emission of charged particles, the $(n,$ charged particle$)$ reaction cross-sections in heavier nuclei are expected to be small.

There are some medium mass nuclei with a small neutron exces as, for example ${}^{46}_{22}Ti$ and ${}^{54}_{26}Fe$ for which, the separation energy of protons is considerably smaller than that of neutrons. In these cases, the emission of protons substantially competes with that of neutrons and therefore these nuclei are characterized by $(n, 2n)$ cross-sections much smaller and (n, p) cross-sections much larger than the values typical for the mass region. The same effect was observed by Pavlik et al.[39] in case of the isotope ${}^{58}Ni$. Due to these effects the calculated $(n, 2n)$ cross-sections of medium mass nuclei, for which the neutron excess is small, sensitively depends on the model parameters, therefore these calculations are of special interest.

In case of ${}^{45}Sc$ (n, p) ${}^{45}Ca$ reaction, the cross-sections obtained using NX-1 code, ALICE code after applying pairing energy correction and the existing evaluations of Manokhin et al.[37] are close to the measured ones, whereas ALICE code applying shell correction gives deviation within 10 to 30%. The excitation functions of (n, p) reaction for the isotopes ${}^{46}Ti$, ${}^{51}V$ and ${}^{54}Fe$ show excellent agreement with the results of ALICE code after applying shell correction and with the evaluation given by Manokhin et al.[37], the deviations being approximately within experimental errors.

The (n, α) reaction cross-sections of all the isotopes considered show fairly good agreement within experimental errors with the results of NX-1 code, ALICE code after shell correction and Manokhin et al.[37] results except in the case of ${}^{54}Fe$ (n, α) ${}^{51}Cr$ reaction for which the ALICE code after shell correction gives lower results.

Acknowledgements

References

1. Sinha, Amar & Garg, S.B. (1981) *Atomkern Energie* **38** : 282.

2. Blann, M. & Vonach, H.K. (1983) *Phys. Rev.* **C28** : 1475.

3. Blann, M. (1991) *Recent Progress and Current Status of Pre-equilibrium Reaction Theories and Computer Code* ALICE, UCRL-JC-10905 Z, LLNL, California, USA.

4. Zhang Zin, Zhou Delin & Cai Dunjiu (1986) *Radiat. Eff.* **96** : 269.

5. Zhang Zin, Zhou Delin & Cai Dunjiu (1987) *The Systematics of (n, 2n) and (n, 3n) Cross-sections,* NEA Data Bank, France, p. 2.

6. Zhao Zhixiang & Zhou Delin (1988) *Nucl. Sci. Engg.* **99** : 367.

7. Zhao Zhixiang & Zhou Delin (1986) *Systematics of Excitation Functions for (n, charged particle) Reactions,* NEA Data Bank, France, p. 4.

8. Wilmore, D. & Hodgson, P.E. (1964) *Nucl. Phys.* **55** : 673.

9. Bansal, S.L. (nee Goyal) & Mohindra, R.K. (1994) *Nucl. Sci. J. (Taiwan)* **31** : 411.

10. Audi, G., Wapstra, A.H. & Thibault, C. (2003) *Nucl. Phys.* **A729** : 337.

11. Frehaut, J. & Mosinski, G. (1975) *Proc. of the 4th Conf. on Nuclear Cross-sections and Technology,* Washington DC, USA, p. 855.

12. Hudson, C.G., Alford, W.L. & Ghorai, S.K. (1978) *Ann. Nucl. Energy* **5** : 589.

13. Pashchenko, A.B. (1991) *Reaction Cross-sections Induced by 14.5 MeV and by Cf-252 and U-235 Fission Spectrum Neutrons, Reports* INDC (CCP)-323/L IAEA Nuclear Data Section, Vienna, Austria.

14. Veeser, L.R., Arthur, E.D. & Young, P.G. (1977) *Phys. Rev.* **C16** : 1792.

15. Bayhurst, B.P. & Prestwood, R.J. (1961) *J. Inorg. Nucl. Chem.* **23** : 173.

16. Grimes, S.M., Haight, R.C., Alvar, K.R., Barschall, H.H. & Borchers, R.R. (1979) *Phys. Rev.* **C19** : 2127.

17. Grimes, S.M., Haight, R.C. & Anderson, J.D. (1978) *Phys. Rev.* **C17** : 508.

18. Paulsen, A., Liskien, H. & Widera, R. (1975) *Atomkern Energie* **26** : 34.

19. Csikai, J. (1982) *Proc. of the Int. Conf. on Nuclear Data for Science and Technology,* Antwerp, Belgium, p. 414.

20. Molla, N.I., Qaim, S.M. & Uhl, M. (1990) *Phys. Rev.* **C42:** 1540.

21. Viennot, M., Berrada, M., Paic, G. & Joly, S. (1991) *Nucl. Sci. Engg.* **108** : 289.

22. Qaim, S.M., Klapdor, H.V. & Reiss, H. (1980) *Phys. Rev.* **C22** : 1371.

23. Bormann, M., Neuert, H. & Scobel, W. (1974) *Handbook on Nuclear Activation Cross-sections, Technical Report Series, No. 156,* IAEA, Vienna, Austria, p. 87.

24. Gupta, J.P., Bhardwaj, H.D. & Prasad, R. (1985) *Pramana* **24** : 637.

25. Body, Z. & Csikai, J. (1987) *Handbook on Nuclear Activation Data, Technical Report Series No. 273,* IAEA, Vienna, Austria, p. 261.

26. Meadows, J.W., Smith, D.L., Bretcher, M.M. & Cox, S.A. (1987) *Ann. Nucl. Energy* **14** : 489.

27. Smith, D.L., Meadows, J.W. & Konno, I. (1984) *Ann. Nucl. Energy* **11** : 623.

28. Pepelnik, R., Anders, B. & Bahal, B.M. (1986) *Radiat. Eff.* **92** : 211.

29. Wolfle, R., Qaim, S.M., Liskien, H. & Widera, R. (1990) *Radiochimica Acta* **50** : 5.

30. Ryves, W. (1978) *Data File EXFOR-20772. 802,* Nuclear Data Section, IAEA, Vienna, Austria.

31. Ryves, T.B., Kolkowski, P. & Zieba, K.J. (1978) *J. Phys. G : Nucl. Phys.* **4** : 1783.

32. Hanlin, Lu, Ji-Zhou, Li, Pei-Guo, Fan & Jian-Zhou, Huang (1982) *Chin. J. Nucl. Phys.* **4** : 272.

33. Paulsen, A., Widera, R., Arnotte, F. & Liskien, H. (1979) *Nucl. Sci. Engg.* **72** : 113.

34. Saraf, S.K., Brient, C.E., Egun, P.M., Grimes, S.M., Mishra, V. & Pedroni, R.S. (1991) *Nucl. Sci. Engg.* **107** : 365.

35. Diksic, M., Strohal, B. & Slaus, I. (1974) *J. Inorg. Nucl. Chem.* **36** : 477.

36. Qaim, S.M. & Stocklin, G.L. (1973) *J. Inorg. Nucl. Chem.* **35** : 19.

37. Manokhin, V.N., Pashchenko, A.B., Plyaskin, V.I., Bychkov, V.M. & Pronyaev, G. (1987) *Activation Cross-sections induced by Fast neutrons, Technical Reports Series No. 273,* IAEA, Vienna, Austria, p. 305.

38. Qaim, S.M., Wolfle, R. & Liskien, H. (1982) *Phys. Rev.* **C25** : 203.

39. Pavlik, A., Winkler, G., Uhl, M., Paulsen, A. & Liskien, H. (1985) *Nucl. Sci. Engg.* **90** : 186.

THE NATIONAL ACADEMY OF SCIENCES, INDIA
5, Lajpatrai Road, New Katra, Allahabad - 211002

Guidelines for the Authors/Contributors for submitting papers

Proceedings of the National Academy of Sciences, India
(Section A – Physical Sciences)

[A) WHAT TO SUBMIT

The following categories of papers are published in the Proceedings of the National Academy of Sciences, India (Section A - Physical Sciences) :

(1)   **Review Articles:** This should be a critical review highlighting the present status and an overview of the past work on any relevant subject of current topical interest. It has to be written in a manner to help either in initiating the work in that particular area or in increasing the comprehension of the current challenges. If such an article is accepted by the Academy for publication, then **Rupees Two Thousand** would be given to the "corresponding author" after the publication of the paper in the Proceedings to meet the contingency expenses. Ordinarily, the Review Article should not exceed 25 printed pages.

(2)   **Original Articles:** This should give new results obtained by the authors and be prepared in the format of the journal. Ordinarily such papers should not be more than 12 printed pages.

(3)   **Special Issues for Conference Proceedings:** Proceedings of National and International Conferences, as a special issue of the journal, can also be brought out with organizers as Guest Editors. At least, one of the Guest Editors should be Fellow of the Academy. Guest Editors shall be responsible for proper refereeing of the papers and for ensuring their high quality.

It is presumed that the articles submitted for publication have not been submitted to any other journal by the authors. Authors shall be liable themselves for such an act.

[B) WHO CAN SUBMIT

(1)   All scientists (Indian or Foreign) can directly send their article for publication. **If there are more than one author, each author should certify that he/she agrees to the submission of the review/research paper.**

(2)   In addition to above, all the Fellows of the National Academy of Sciences, India are also authorized to forward quality papers in their research field for publication in the journals of the Academy. The name of the communicating Fellow would be printed in the paper as "Communicated by .....................F.N.A.Sc".

The communicating Fellow should certify that:

(i)   The forwarded paper is in his/her field of specialization,

(ii)   He/she has read the paper and reviewed it carefully.

        However, if the Editorial Board finds it necessary, it may get the paper reviewed again.

[C] WHOM TO SUBMIT

The papers should be sent to the Managing Editor, Proceedings of the National Academy of Sciences, India (Section A – Physical Sciences); 5 Lajjpat Rai Road, New Katra, Allahabad - 211 002

[D] HOW TO SUBMIT

The authors may submit the papers directly or forwarded through a Fellow of the Academy as prescribed above. It is mandatory to submit "An Electronic Version" as well as "three hard-copies". The text of the manuscript as per format of the journal outlined below, and preferably with scanned figures, should be supplied as a plain ASCII file (Wordstar 5.5 or 7.0 and Microsoft Word for Window 6.0 are also acceptable, but ASCII is preferred). The language of the journal is English.

[E] FORMAT OF THE MANUSCRIPT

(i) Title of the paper should be in **bold** and running (14-font size) through the full page width.

(ii) **Author's name/Affiliations** may also run through the full page width. Names should be in 12 point font-size and **bold** while affiliations should be 8 point font size in *italics*. Please note that if any of the author is a Fellow of the Academy, then he should write F.N.A.Sc. after his name.

(iii) **Abstract** should be typed in 8 point font sizes **"bold"**

(iv) **Keywords** (maximum 5 words/phrases, each separated by slash [/]) should follow the Abstract.

(v) **Contents of the text**

  (a) This is to be typed on A4 page in double space in10 point font size.

  (b) The text of the paper should be arranged into suitable headings like Introduction, Materials and Method, Theory or Model, Results, Discussion, Conclusions/Summary, Acknowledgements, References, etc.

  (c) Please note that the Proceedings are published in "two column format". Therefore, the authors are required to draw the figures tables/equations in such a way that they can be easily reduced to one column width (~ 7.5 cm) at the time of publication. Figures must be original drawings or exceptionally sharp glossy prints drawn with stencil and UNO pen.

  (d) All references should be indicated in the text by superscript Arabic numerals, e.g. 'Mirri[1] while working on...'. The list of references should be arranged in order of their occurrence in the text. References should be given in the following style:

  1. Mirri, M.A. (1982), J. Chem. Phys. 58: 282 (for articles in journals)

  White, M. J. D. (1973) Animal Cytology and Evolution, 3rd Ed., Cambridge University Press, London, p. 320 (for books)

  Osgood, C.F. (1977) in Number Theory and Algebra: ed., Zasserhause, H., Academic Press, New York, p. 10 (for edited books)

  Abbreviations of the names of periodicals should conform to those given in the World list of Scientific Periodicals.

[F] MISCELLANEOUS

(i) All papers will be screened by a strict refereeing procedure. However, the responsibility for the authenticity of the contents lies with the authors.

(ii) If a paper is recommended for revision, a maximum of 2 months would be given to authors for revising the manuscript after which it would be treated as a fresh communication.

(iii) Authors will receive galley proof of their paper from the Academy's Editorial Office. They should return the corrected proof within a week of its receipt. If return of the proof is delayed, the proof will be corrected by the Academy, but the responsibility will be entirely that of the author(s).

(iv) No change in the text of the paper will be made after the matter has been composed by the Press. If it is absolutely essential, a postscript may be added.

(v) Reprints: 25 free reprints will be given to the corresponding author for each paper.

[G] SUBSCRIPTION RATE OF THE JOURNALS

Annual Subscription for both Sections (Sec A – Physical Sciences and Sec B – Biological Sciences) : Rs. 500.00; **for each Section** Rs. 250.00; **Single Copy :** Rs. 100.00, **Foreign Subscription :** (a) for one Section: US $100, (b) for both Sections US $200. **(Air Mail charges included in foreign subscription)**

Kind Attention : Fellows and Members of the National Academy of Sciences, India
(Please fill items and return to the Managing Editor – Proceedings of the National Academy of Sciences, India
(Sec A – Physical Sciences; Sec B – Biological Sciences)

The Editorial Boards and Board of Editors of the Journals of the Academy viz. **Proceedings of the National Academy of Sciences, India (Sec A – Physical Sciences), Proceedings of the National Academy of Sciences, India (Sec B– Biological Sciences)** and **National Academy Science Letters,** request its esteemed Fellows and Members to inform their willingness for acting as learned referees for the research papers received for publication in the above Journals. They are also requested to suggest other names of subject experts who may be requested for refereeing as per following proforma.

UPDATED DATA OF REFEREES' PANEL FOR THE JOURNALS OF
THE NATIONAL ACADEMY OF SCIENCES, INDIA

(I) 1. Name, Designation, Affiliation and ....

   Postal Address of the Fellow/Member ....

....

....

   (a) Telephone No. (with area code) ....

   (b) Fax No. (with area code)..

   (c) E-mail Address...

   2. State whether a Fellow or Member...

   3. Subject/Sub-disciplines of your expertise in which you are willing to act as Referee.

Sl. No.	Major Disciplines (Such as Physics etc.)	Sub-discipline alonwith super-speciality	Experimental/Theoretical or both
1.		(i) (a) (b)	
2.		(ii) (a) (b)	
3.		(iii) (a) (b)	

(II) Suggestions regarding additional referees

Sl. No.	Name(s) & Address of those whom you suggest for refereeing	His/Her Major Disciplines (such as Physics etc.)	His/Her Sub-disciplines alongwith any Super-specialities	Experimental/Theoretical or Both
1.			(i) (a) (b)	
2.			(i) (a) (b)	
3.			(i) (a) (b)	

Signature of the Fellow/Member